AIR FORCE INSTITUTE OF TECHNOLOGY

AIR UNIVERSITY
UNITED STATES AIR FORCE

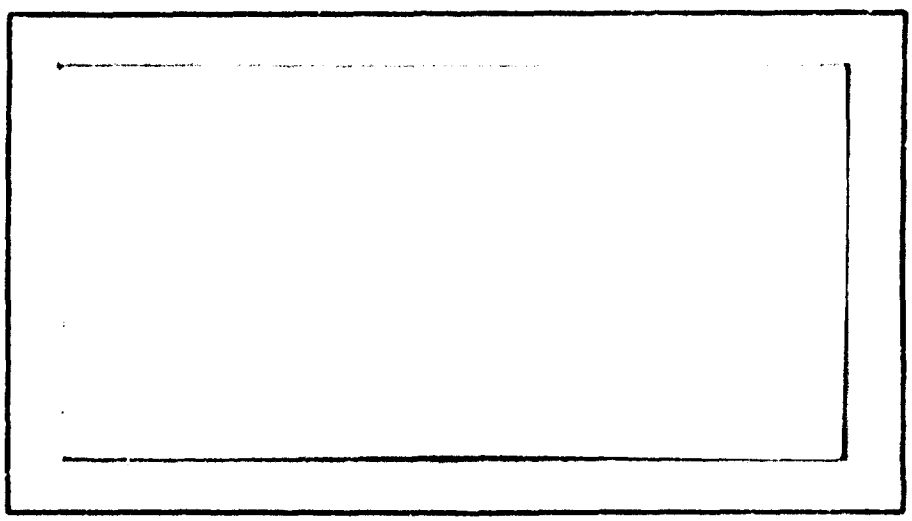

SCHOOL OF ENGINEERING

WRIGHT-PATTERSON AIR FORCE BASE, OHIO

NOTICE TO USERS

Portions of this document have been judged by the NTIS to be of poor reproduction quality and not fully legible. However, in an effort to make as much information as possible available to the public, the NTIS sells this document with the understanding that if the user is not satisfied, the document may be returned for refund.

If you return this document, please include this notice together with the IBM order card (label) to:

National Technical Information Service
U.S. Department of Commerce
Attn: 952.12
Springfield, Virginia 22151

DOCUMENT CONTROL DATA - R & D

(Security classification of title, body of abstract and indexing annotation must be entered when the overall report is classified)

1. ORIGINATING ACTIVITY (Corporate author)	2a. REPORT SECURITY CLASSIFICATION
Air Force Institute of Technology (AFIT-EN) Wright-Patterson AFB, Ohio 45433	Unclassified 2b. GROUP

3. REPORT TITLE

TOWARD A DIFFERENTIAL GAME SOLUTION TO A PRACTICAL TWO AIRCRAFT PURSUIT-EVASION PROBLEM IN THREE-DIMENSIONAL SPACE

4. DESCRIPTIVE NOTES (Type of report and inclusive dates)

MSE Thesis

5. AUTHOR(S) (First name, middle initial, last name)

S.Miles D. Williamson-Noble
Flight Lieutenant, Royal Air Force

6. REPORT DATE	7a. TOTAL NO. OF PAGES	7b. NO. OF REFS
June 1971	115	5

8a. CONTRACT OR GRANT NO.	9a. ORIGINATOR'S REPORT NUMBER(S)
b. PROJECT NO.	GA/EC/71-5
c.	9b. OTHER REPORT NO(S) (Any other numbers that may be assigned this report)
d.	

10. DISTRIBUTION STATEMENT

This document has been approved for public release; distribution unlimited

11. SUPPLEMENTARY NOTES	12. SPONSORING MILITARY ACTIVITY

13. ABSTRACT

A practical two aircraft pursuit-evasion problem in three-dimensional space is posed as a zero sum, perfect information differential game. The purpose of the thesis is to solve this differential game and to obtain optimal or near optimal closed-loop control laws for the two players.

Three models of the aircraft dynamics are used. The first model is primarily a realistic one, and as the state equations are non-linear and highly coupled, it is not possible to obtain optimal closed-loop solutions. The second model is a simplified version of the first. Using this model, the solution is carried further - the costate variables are eliminated from the controls - but closed-loop solutions still cannot be found. The third model used has different controls from the other two, but is roughly similar in nature. Optimal closed-loop controls are obtained for this model. The results obtained from these models show that the three-dimensional problem cannot be considered as a simple extension of the two-dimensional game. The necessary inclusion of the bank angle or a similar control introduces an extra order of complexity into the problem.

As exact optimal closed-loop control laws for the realistic model are not available, the results of the analysis are presented in two ways. Firstly, open-loop minimax solutions for all three models are generated numerically by backward integration from a selection of terminal states. Two-dimensional views of these three-dimensional trajectories are given in both real and relative space. Secondly, pseudo optimal controls for the realistic model are derived, based on the closed-loop controls obtained for the simplest of the three models. These pseudo controls are then used

DOCUMENT CONTROL DATA - R & D

(Security classification of title, body of abstract and indexing annotation must be entered when the overall report is classified)

1. ORIGINATING ACTIVITY *(Corporate author)*	2a. REPORT SECURITY CLASSIFICATION
	2b. GROUP
3. REPORT TITLE	
4. DESCRIPTIVE NOTES *(Type of report and inclusive dates)*	
5. AUTHOR(S) *(First name, middle initial, last name)*	

6. REPORT DATE	7a. TOTAL NO. OF PAGES	7b. NO. OF REFS
8a. CONTRACT OR GRANT NO. b. PROJECT NO. c. d.	9a. ORIGINATOR'S REPORT NUMBER(S) 9b. OTHER REPORT NO(S) *(Any other numbers that may be assigned this report)*	
10. DISTRIBUTION STATEMENT		
11. SUPPLEMENTARY NOTES	12. SPONSORING MILITARY ACTIVITY	

13. ABSTRACT

with the standard dynamics to integrate forward in time from the states reached by backward integration of the realistic open-loop solutions. The pseudo closed-loop solutions give a good approximation to the open-loop solutions for the nominal model under almost all the conditions tested.

DD FORM 1 NOV 65 1473

Unclassified

Security Classification

14 KEY WORDS	LINK A		LINK B		LINK C	
	ROLE	WT	ROLE	WT	ROLE	WT
Differential Games						
Pursuit-Evasion						

Unclassified

Security Classification

TOWARD A DIFFERENTIAL GAME SOLUTION TO A PRACTICAL TWO-AIRCRAFT PURSUIT-EVASION PROBLEM IN THREE-DIMENSIONAL SPACE

THESIS

GA/MC/71-5 S.M.D. Williamson-Noble, MA
Flight Lieutenant, RAF

TOWARD A DIFFERENTIAL GAME SOLUTION TO A PRACTICAL TWO-AIRCRAFT PURSUIT-EVASION PROBLEM IN THREE-DIMENSIONAL SPACE

THESIS

Presented to the Faculty of the School of Engineering of

the Air Force Institute of Technology

Air University

in Partial Fulfillment of the

Requirements for the Degree of

Master of Science

by

S.M.D. Williamson-Noble, MA
Flight Lieutenant RAF

Graduate Astronautics

June 1971

Preface

This work represents the outcome of my attempt to solve either exactly or approximately a realistic two aircraft combat encounter viewed as a differential game. The aircraft are permitted to maneuver in three-dimensions, and are not restricted, as has been the case with most previous studies, to planar motion.

The work received its original inspiration and a lot of its guidance from the Doctoral Dissertation and later unpublished studies of Major William L. Othling Jr. of the Air Force Flight Dynamics Laboratory. I should also like to mention Professor Gerald M. Anderson of the Air Force Institute of Technology and Captain Anthony L. Leatham of the Flight Dynamics Laboratory who both gave me freely of their time and advice.

Finally I should like to thank the United States Air Force for allowing me extensive use of its computer facilities in the preparation of this study.

S.M.D. W-N

Contents

Page

Preface ii

List of Figures v

Abstract vii

I. Introduction 1

II. Outline of the Problem 4

Purpose of the Thesis 4
Reason for the Differential Game Approach 5
Necessary Conditions for a Solution 7
Payoff and Termination Criteria 9

III. Aircraft Models 11

The Standard Model 11
The Zero Gravity and Fixed Velocity Model 14
The Spherical Acceleration Vectogram Model 15

IV. Pursuit-Evasion Differential Game - Standard Model 17

Statement of the Problem 17
Necessary Conditions 18
Partial Problem Solution 25
Examination of Open-Loop Solutions 28

V. Pursuit-Evasion Differential Game - Zero Gravity and Fixed Velocity Model 34

Statement of the Problem 34
Necessary Conditions 35
Partial Problem Solution 38
Examination of Open-Loop Solutions 44

VI. Pursuit-Evasion Differential Game - Spherical Acceleration Vectogram Model 48

Statement of the Problem 48
Necessary Conditions 50
Problem Solution 53
Examination of Solutions 60

VII. Development of Pseudo Closed-Loop Minimax Controls for the Standard Model 62

Best Control Approximation 62

Page

Alternative Control Approximations 65
Suggested Algorithm to Determine a Players Controls During an Actual Encounter 66

VIII. Conclusion and Recommendations 69

Conclusions 69
Recommendations 71

Bibliography 73

Appendix A: The Use of the One Player Optimization Techniques in Certain Different Games 74

Appendix B: Some Unsuccessful Approximations to Closed-Loop Minimax Controls for the Standard Model 78

Appendix C: Plots of Some Typical Minimax Trajectories 83

Vita 113

List of Figures

Figure		Page
1	Definition of State Variables	12
2	Definition of Terminal Parameters	29
3	Standard Model, Real Space, Run 1	85
4	Zero Gravity, Fixed Velocity Model, Real Space, Run 1	86
5	Spherical Vectogram Model, Real Space, Run 1	87
6	Standard Model, Relative Space, Run 1	88
7	Zero Gravity, Fixed Velocity Model, Relative Space, Run 1	89
8	Spherical Vectogram Model, Relative Space, Run 1	90
9	Pseudo Controls with Standard Dynamics, Real Space, Run 1	91
10	Standard Model, Real Space, Run 2	92
11	Zero Gravity, Fixed Velocity Model, Real Space, Run 2	93
12	Spherical Vectogram Model, Real Space, Run 2	94
13	Standard Model, Relative Space, Run 2	95
14	Zero Gravity, Fixed Velocity Model, Relative Space, Run 2	96
15	Spherical Vectogram Model, Relative Space, Run 2	97
16	Pseudo Controls with Standard Dynamics, Real Space, Run 2	98
17	Standard Model, Real Space, Run 3	99
18	Zero Gravity, Fixed Velocity Model, Real Space, Run 3	100
19	Spherical Vectogram Model, Real Space, Run 3	101
20	Standard Model, Relative Space, Run 3	102
21	Zero Gravity, Fixed Velocity Model, Relative Space, Run 3	103

Figure		Page
22	Spherical Vectogram Model, Relative Space, Run 3	104
23	Pseudo Controls with Standard Dynamics, Real Space, Run 3	105
24	Standard Model, Real Space, Run 4	106
25	Zero Gravity, Fixed Velocity Model, Real Space Run 4	107
26	Spherical Vectogram Model, Real Space, Run 4	108
27	Standard Model, Relative Space, Run 4	109
28	Zero Gravity, Fixed Velocity Model, Relative Space, Run 4	110
29	Spherical Vectogram Model, Relative Space, Run 4	111
30	Pseudo Controls with Standard Dynamics, Real Space, Run 4	112

Abstract

A practical two aircraft pursuit-evasion problem in three-dimensional space is posed as a zero sum, perfect information differential game. The purpose of the thesis is to solve this differential game and to obtain optimal or near optimal closed-loop control laws for the two players.

Three models of the aircraft dynamics are used. The first model is primarily a realistic one, and as the state equations are non-linear and highly coupled, it is not possible to obtain optimal closed-loop solutions. The second model is a simplified version of the first. Using this model, the solution is carried further - the costate variables are eliminated from the controls - but closed-loop solutions still cannot be found. The third model used has different controls from the other two, but is roughly similar in nature. Optimal closed-loop controls are obtained for this model. The results obtained from these models show that the three-dimensional problem cannot be considered as a simple extension of the two-dimensional game. The necessary inclusion of the bank angle or a similar control introduces an extra order of complexity into the problem.

As exact optimal closed-loop control laws for the realistic model are not available, the results of the analysis are presented in two ways. Firstly, open-loop minimax solutions for all three models are generated numerically by backward integration from a selection of terminal states. Two-dimensional views of these three-dimensional trajectories are given in both real and relative space. Secondly, pseudo optimal controls for the realistic model are derived, based on the closed-loop controls ob-

tained for the simplest of the three models. These pseudo controls are then used with the standard dynamics to integrate forward in time from the states reached by backward integration of the realistic open-loop solutions. The pseudo closed-loop solutions give a good approximation to the open-loop solutions for the realistic model under almost all the conditions tested.

TOWARD A DIFFERENTIAL GAME SOLUTION TO A PRACTICAL TWO-AIRCRAFT PURSUIT-EVASION PROBLEM IN THREE DIMENSIONAL SPACE

I. Introduction

The aerial dogfight is a problem for which no analytically derived optimal maneuvers have yet been found. The knowledge of such maneuvers would be of use both in the design and in the operation of any aircraft that might be involved in aerial combat. In the field of design, the value of some function such as the time to intercept from certain specified initial conditions, subject to optimal maneuvering by both combatants, would provide a good numerical indicator for use in reaching compromises between various aspects of performance. In the field of operations, it might not be practicable to fly optimal trajectories exactly, but a knowledge of them would be helpful in developing and evaluating tactics.

A discussion of the merits and demerits of the various methods which may be used to analyze the dogfight is given in Chapter II. This thesis poses the dogfight as a zero sum, perfect information, pursuit-evasion differential game. The purpose of the thesis is to analyze this problem, and to proceed as far as possible with its solution.

In his doctoral dissertation (Ref 4), Othling considers the dogfight as a differential game where both players are restricted to two-dimensional planar motion. He considers a realistic or standard model of the aircraft dynamics for which he obtains open-loop controls, and then goes on to consider various simplified dynamic models for which he is able to obtain closed-loop solutions. This thesis extends the study to problems in which three-dimensional maneuvering is permitted.

Originally it was felt that the problem in three-dimensions would be similar to that in two-dimensions, and that it would in effect only require an increase in the number of equations to be handled. However, it was found that the necessary inclusion of the direction of the lift vector as one of the controls added considerably to the complexity of the problem.

In order to analyze the problem, three models of the aircraft dynamics are developed. These models are described in Chapter III. The first model is a realistic or standard representation. The second model is a simplified version of the first model, but one which retains the basic nature and controls of the standard. The third model is a more drastically altered representation which is aimed primarily at obtaining a closed-loop solution. In Chapter IV, the differential game using the standard dynamic model is investigated, and the solution carried as far as possible. In Chapter V, the same is done for the second dynamic model. In Chapter VI, the differential game using the most simplified dynamic model is investigated, and closed-loop controls are obtained.

The feasibility of using the closed-loop controls developed for the simplest model as an approximation to closed-loop controls for the standard model is examined in Chapter VII. A possible algorithm for deriving near-optimal controls in a dogfight situation is also suggested in this chapter.

In the course of attempting the solution of the first two dynamic models, the author discovered a theorem which may well be of more general use in problems where the costate differential equations are not directly integrable. This theorem and its proof are given in

Appendix A.

Since it is not expected that the study of the aerial pursuit-evasion problem will cease with this thesis, results which may be of value to other workers on the problem are given in Appendices B and C. These results are certain unsuccessful approximations to the open-loop controls for the standard model, and a series of graphical plots of typical trajectories in real and relative space for all three models. Trajectories obtained by using the synthesized near-optimal controls with the standard dynamics are also shown.

It is felt that this thesis makes a definite contribution towards finding optimal controls for use in aerial encounters. Furthermore it serves to show that the use of simplified models can be of great value in examining realistic problems. Finally, for the first time in the study of realistic differential game problems, results are obtained which begin to look as though they might be of direct applicability.

II. Outline of the Problem

Purpose of the Thesis

The purpose of this thesis is to solve a realistic two aircraft pursuit-evasion differential game, where the players may maneuver freely in three-dimensional space.

The problem is first defined in terms of two aircraft with dynamics which approximate closely those found in real life. A closed-loop solution for this problem could not and probably cannot be found, so a selection of open-loop minimax trajectories is generated numerically, and then examined and compared with other more approximate solutions.

Once the most realistic or "standard" model has been investigated, the aim is to find the aircraft model which is closest in its dynamic representation to the standard and yet able to be solved completely. With this in mind, two models are presented. The first is a fixed velocity, zero gravity version of the standard model; only open-loop solutions for this problem could be found, but the model is as simple as it is possible to get whilst still retaining the basic nature of the standard model. The model for which closed-loop controls could be found is termed the "spherical vectogram model." As the usefulness of this model is limited in so far as it approximates the standard model, only a solution "in the small" (Ref 3:66) is presented. The controls found from this model are used to synthesize pseudo-optimal closed-loop controls for the standard model.

The above steps provide a significant advance in the development of realistic control laws for the two aircraft pursuit-evasion problem. However, there is still much work to do in refining these control laws,

and so the final aim of this thesis is to serve as a background for future workers in the field, and to document some of the unproductive lines of approach to the problem.

Reason for the Differential Game Approach

The reason for choosing the differential game approach to the two aircraft pursuit-evasion problem is that there is no alternative approach which offers the same possibilities.

The concept of energy maneuverability, which has received a lot of attention in recent years, is only of use in putting a prospective combatant in an advantageous position from which to start an engagement, and then in showing the best way in which to perform certain specific predetermined maneuvers. There is no guidance available as to what maneuvers should be performed in order to close with the opponent and effect a kill.

Ordinary optimization techniques are not really applicable as they credit only one player with the intelligence and ability to maneuver other than along a predetermined flight path. This is not to say that ordinary optimization techniques cannot yield useful results, but merely that these results are severely limited in nature.

"Seat of the pants" techniques are probably the best available, but are unlikely to be optimal, and are highly subjective. Furthermore, even if an individual pilot were able to fly optimal trajectories, he would find it most difficult to characterize these maneuvers so that they could be followed by another pilot (human or automatic).

In a differential game both players may maneuver within the limits set by the constraints on their controls. Both players strive to mini-

mize their costs expressed as some integral of the state variables and controls during the progress of the game and some function of the states at termination.

The three greatest drawbacks in approaching a dogfight as a differential game are:

1. During the course of a game the roles of the players are fixed, so that the evader may not become the pursuer nor may the pursuer become the evader.
2. Closed-loop solutions are hard to obtain except with simplified dynamic representations, and open-loop solutions are not in general optimal against non-optimal maneuvers by the other player.
3. Whatever conditions are chosen to determine capture, or the end of a game, are final and unless some provision for it is made in the cost function, there is no consideration of the possibility of the need for a re-engagement.

However, it is felt that these drawbacks are easily outweighed by the results that may be obtained using the differential game approach. It must be stressed that this is the only method for treating an encounter problem where the players have differing aims and are able to use controls which affect the outcome of these aims.

The parameters of a two aircraft pursuit-evasion problem are such that it may be posed as a two-player perfect information, zero-sum differential game. Once the perfect information zero-sum game has been solved, it may be of value to investigate the problem viewed as a non-zero-sum game, and to examine the effects of imperfect information.

However, the first priority is to obtain a solution to the perfect information zero-sum differential game, and it is towards this end that this thesis is directed.

Necessary Conditions for a Solution

Necessary conditions for a saddle-point solution, or set of minimax strategies, to a zero-sum perfect information differential game are given in a number of standard texts (Ref 1:277, Ref 3:67), and are summarized below.

The differential game problem is defined by the dynamic system

$$\dot{\bar{x}} = \bar{f}(\bar{x},\bar{u},\bar{v},t); \qquad \bar{x}(t_0) = \bar{x}_0 \tag{2-1}$$

where $\bar{x}$ is the n-dimensional state vector, $\bar{u}$ is the m-vector pursuer's control and $\bar{v}$ is the p-vector evader's control. $\bar{u}$ and $\bar{v}$ may or may not be subject to constraints. The game has the terminal constraints

$$\Psi(\bar{x}(t_f),t_f) = 0 \tag{2-2}$$

which define an n-dimensional surface in the (n + 1)-dimensional space consisting of the n components of $\bar{x}$ (t_f), and t_f. The game has the performance criterion, or payoff,

$$J = \phi\ (\bar{x}(t_f),t_f) + \int_{t_0}^{t_f} L(\bar{x},\bar{u},\bar{v},t)\ dt \tag{2-3}$$

The aim is to find the controls $\bar{u}^*$ and $\bar{v}^*$ such that

$$J(\bar{u}^*,\bar{v}) \leq J(\bar{u}^*,\bar{v}^*) \leq J(\bar{u},\bar{v}^*) \tag{2-4}$$

If $\bar{u}^*$ and $\bar{v}^*$ can be found, the pair $(\bar{u}^*,\bar{v}^*)$ is called a saddle point of the game and $J(\bar{u}^*,\bar{v}^*)$ is called the value of the game.

The existence of a solution is dependent on the fact that

$$\min_{\bar{u}} \max_{\bar{v}} J(\bar{u},\bar{v}) = \max_{\bar{v}} \min_{\bar{u}} J(\bar{u},\bar{v}) \tag{2-5}$$

A necessary condition for a saddle point solution of the above differential game is that the Hamiltonian defined by

$$H(t,\bar{x},\bar{\lambda},\bar{u},\bar{v}) = \bar{\lambda}^T \bar{f} + L \tag{2-6}$$

must be minimized over the set of admissible $\bar{u}$ and maximized over the set of admissible $\bar{v}$ and that

$$H^* = \max_{\bar{v}} \min_{\bar{u}} H = \min_{\bar{u}} \max_{\bar{v}} H \tag{2-7}$$

$\bar{\lambda}$ is the n-dimensional costate vector, and the costate differential equations are

$$\dot{\bar{\lambda}} = -H_{\bar{x}} \tag{2-8}$$

the transversality conditions are given by

$$H(t_f) = -\phi_t(t_f); \quad \bar{\lambda}(t_f) = \phi_{\bar{x}}(t_f) \tag{2-9}$$

where $\Phi(x(t_f),t_f) = \phi + \nu\,\Psi$ (2-10)

and ν = arbitrary constant

If t does not appear explicitly in either H or the control constraints, then H is constant.

It was previously stated that the optimal solution to the differential game problem is the pair of controls $(\bar{u}^*,\bar{v}^*)$ which provides a saddle point of J. If the pair $(\bar{u}^*,\bar{v}^*)$ is given as $(\bar{u}^*(t),\bar{v}^*(t))$,

one speaks of an open-loop solution. If the controls are expressed as functions of the instantaneous state and time

$$\bar{u}^* = \bar{k}_u(\bar{x},t) \tag{2-11}$$

$$\bar{v}^* = \bar{k}_v(\bar{x},t) \tag{2-12}$$

one has what is known as a feedback or closed-loop control law.

Payoff and Termination Criteria

The basic type of encounter for which the approach outlined in this thesis is most appropriate is one between two fighter aircraft. The armament of such aircraft would normally be either air-to-air missiles, or cannons, or both. It was decided to use as terminal surface a typical launch envelope for a next-generation short-range missile. One such missile might have a maximum target range of 5000 ft and a minimum target range of 1500 ft at launch. The missile could be fired while maneuvering at high load factors (e.g., up to 8g) and the target should lie within approximately 120° of the attacking aircraft's velocity vector at the instant of firing. To simplify the problem the terminal surface considered as equivalent to this is taken as a sphere of radius R = 5000 ft centered at the pursuer. Because of the large arc of fire, the loss of realism by not considering the angular restrictions is small, as, with the roles of the aircraft fixed, there will be very few minimax trajectories in which the evader flies into the capture region from behind. The terminal surface may thus be written as

$$\Psi \equiv (x_E-x_p)\Big|^2_{t=t_f} + (y_E-y_p)\Big|^2_{t=t_f} + (z_E-z_p)\Big|^2_{t=t_f} - R^2 = 0 \tag{2-13}$$

where in this problem R = 5000 ft.

The payoff is taken as time to capture, expressed for the purposes of this thesis as

$$J = \int_{t_0}^{t_f} dt \tag{2-14}$$

Payoffs which include the relative energies of the two players at termination as well as the time to capture may be useful later, but for the present the aim is to find a solution to the realistic problem without unnecessary complications.

III. Aircraft Models

The purpose of this chapter is to derive and justify the state differential equations used in the three models presented in this thesis.

The Standard Model

The aim of this model is to give as realistic a representation of the aircraft dynamics as possible without undue complications of the equations of motion. With this in mind, the following assumptions are made:

1. The aircraft are considered to be point masses.
2. The earth is flat and the acceleration of gravity is constant.
3. The thrust of each aircraft is constant and tangent to its flight path.
4. The weight of each aircraft is constant.
5. Lift and drag forces are respectively normal and tangent to the flight path.

The aircraft equations of motion may then be written as

$$\dot{x} = V \cos\gamma \cos\chi \tag{3-1}$$

$$\dot{y} = V \cos\gamma \sin\chi \tag{3-2}$$

$$\dot{z} = V \sin\gamma \tag{3-3}$$

$$\dot{V} = \frac{g}{W} [T - D - W \sin\gamma] \tag{3-4}$$

$$\dot{\gamma} = \frac{g}{VW} [L \cos\mu - W \cos\gamma] \tag{3-5}$$

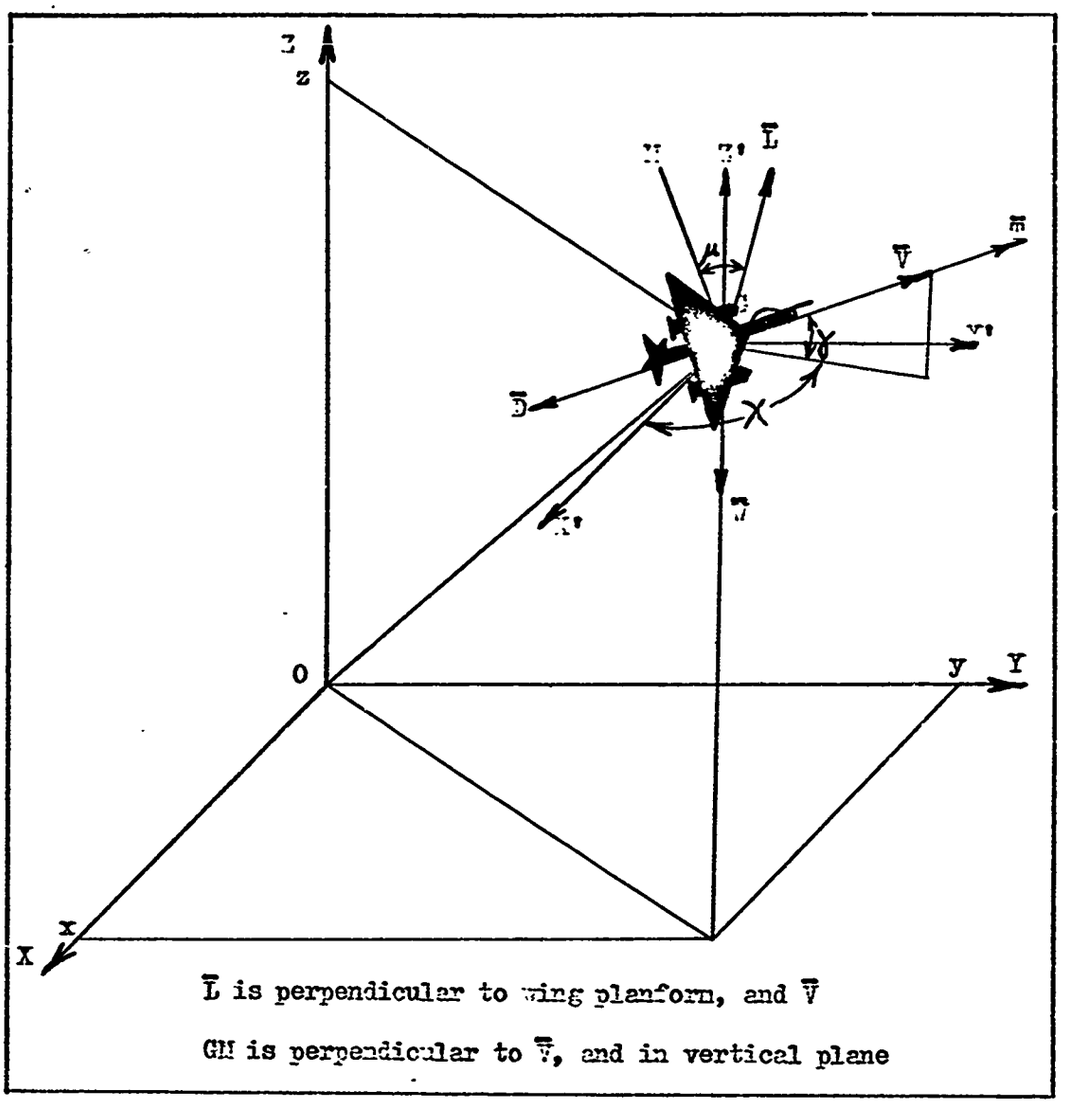

Figure 1. Definition of State Variables

$$\dot{\chi} = \frac{g}{VW \cos \gamma} [L \sin \mu] \tag{3-6}$$

The state variables are defined in Fig. 1. x,y,z are the coordinates of the aircraft's center of mass with respect to a set of inertial axes. V is the aircraft's velocity. γ is the flight path inclination, and χ the aircraft heading angle. T is the thrust, D the drag, W the weight and L the lift of the aircraft. μ is the roll angle of the aircraft about its velocity vector, and is under the pilot's control.

The aerodynamic forces are defined by

$$D = \tfrac{1}{2} \rho V^2 A C_D, \quad L = \tfrac{1}{2} \rho V^2 A C_L \tag{3-7}$$

where ρ is the air density, A a reference area, C_D the drag coefficient and C_L the lift coefficient.

The following further assumptions are now made:

1. The air density ρ is considered to be constant throughout the airspace used in the encounter.
2. The pilot of each aircraft has direct control over the lift coefficient C_L.
3. The aircraft have parabolic drag polars so that

$$C_D = k_O + k_I C_L^2 \tag{3-8}$$

where k_O is the zero-lift drag coefficient and k_I the induced drag factor.

For notational simplicity it is convenient to define the constants

$$k_T = Tg/W \tag{3-9}$$

$$k_D = \rho A g/2W \tag{3-10}$$

It is also convenient to consider that μ is restricted to the range $-\pi/2 \leq \mu \leq \pi/2$, and that C_L may be positive or negative. Limits on maneuverability are set by constraining C_L such that

$$C_{L_{min}} \leq C_L \leq C_{L_{max}} \tag{3-11}$$

Since inverted flight is possible it is sensible to set

$$C_{L_{min}} = - C_{L_{max}} \tag{3-12}$$

which is equivalent to

$$|C_L| \leq C_{L_{max}} \tag{3-13}$$

The aircraft equations of motion are now

$$\dot{x} = V \cos \gamma \cos \chi \tag{3-14}$$

$$\dot{y} = V \cos \gamma \sin \chi \tag{3-15}$$

$$\dot{z} = V \sin \gamma \tag{3-16}$$

$$\dot{V} = k_T - k_D (k_O + k_I C_L^2) V^2 - g \sin \gamma \tag{3-17}$$

$$\dot{\gamma} = k_D V C_L \cos \mu - g \cos \gamma / V \tag{3-18}$$

$$\dot{\chi} = k_D V C_L \sin \mu / \cos \gamma \tag{3-19}$$

The Zero Gravity and Fixed Velocity-Model

The aim of this model is essentially to simplify the standard model as much as possible without losing the basic nature of the model.

The gravitational force on the aircraft is neglected since it may be argued that it is present only as an acceleration which affects both players equally.

Each aircraft is assumed to have a velocity fixed in magnitude. This may be justified on the basis that fighter aircraft often operate close to the velocity that is the maximum allowable with external stores. Changes in the magnitude of each aircraft's velocity are therefore small.

With these two additional assumptions, the aircraft equations of motion are

$$\dot{x} = V \cos\gamma \cos\chi \tag{3-20}$$

$$\dot{y} = V \cos\gamma \sin\chi \tag{3-21}$$

$$\dot{z} = V \sin\gamma \tag{3-22}$$

$$\dot{\gamma} = k_D V C_L \cos\mu \tag{3-23}$$

$$\dot{\chi} = k_D V C_L \sin\mu / \cos\gamma \tag{3-24}$$

The Spherical Acceleration Vectogram Model

The purpose of this model is to yield a differential game which can be solved in closed form, and yet has dynamics that are not too unrealistic. A model that satisfies these requirements is one in which each aircraft is considered to be in dynamic equilibrium except for a maneuvering force of constant magnitude which the pilot may apply in any direction at will.

The dynamic equations of this model are

$$\dot{x} = V_x \tag{3-25}$$

$$\dot{y} = V_y \tag{3-26}$$

$$\dot{z} = V_z \tag{3-27}$$

$$\dot{V}_x = F\ell_1 \tag{3-28}$$

$$\dot{V}_y = F\ell_2 \tag{3-29}$$

$$\dot{V}_z = F\ell_3 \tag{3-30}$$

where V_x, V_y, V_z are the components of the aircraft's velocity in the x,y,z directions. F is the specific excess force and is constant in magnitude. ℓ_1, ℓ_2, ℓ_3 are the direction cosines of the maneuvering force and are the player's controls.

IV. Pursuit-Evasion Differential Game - Standard Model

The purpose of this chapter is to solve a differential game problem using the aircraft dynamics derived in Chapter III for the standard aircraft model. The author was unable to solve the game completely, and so closed-loop controls are not found. For the benefit of any future workers on this problem, the details of the partial solution are given, and there is a brief discussion of computer generated open-loop solutions.

Statement of the Problem

The problem is to determine a saddle point of

$$J(t_f) = \int_{t_0}^{t_f} dt \tag{4-1}$$

subject to

$$\dot{x}_P = V_P \cos \gamma_P \cos \chi_P \tag{4-2}$$

$$\dot{y}_P = V_P \cos \gamma_P \sin \chi_P \tag{4-3}$$

$$\dot{z}_P = V_P \sin \gamma_P \tag{4-4}$$

$$\dot{V}_P = k_{TP} - k_{DP} (k_{OP} + k_{IP} C_{LP}^2) V_P^2 - g \sin \gamma_P \tag{4-5}$$

$$\dot{\gamma}_P = k_{DP} V_P C_{LP} \cos \mu_P - g \cos \gamma_P / V_P \tag{4-6}$$

$$\dot{\chi}_P = k_{DP} V_P C_{LP} \sin \mu_P / \cos \gamma_P \tag{4-7}$$

and

$$\dot{x}_E = V_E \cos \gamma_E \cos \chi_E \tag{4-8}$$

$$\dot{y}_E = V_E \cos \gamma_E \sin \chi_E \tag{4-9}$$

$$\dot{z}_E = V_E \sin \gamma_E \tag{4-10}$$

$$\dot{V}_E = k_{TE} - k_{DE} (k_{OE} + k_{IE} C_{LE}^2) V_E^2 - g \sin \gamma_E \tag{4-11}$$

$$\dot{\gamma}_E = k_{DE} V_E C_{LE} \cos \mu_E - g \cos \gamma_E / V_E \tag{4-12}$$

$$\dot{\chi}_E = k_{DE} V_E C_{LE} \sin \mu_E / \cos \gamma_E \tag{4-13}$$

with a terminal surface given by

$$\Psi \equiv (x_p - x_E)\Big|_{t=t_f}^2 + (y_p - y_E)\Big|_{t=t_f}^2 + (z_p - z_E)\Big|_{t=t_f}^2 - R^2 = 0 \tag{4-14}$$

The subscripts P and E refer to the pursuer and the evader respectively. The pursuer's controls are C_{LP} and μ_p, and the evader's controls are C_{LE} and μ_E. The controls are subject to the constraints

$$|C_{LP}| \leq C_{LP_{max}} \tag{4-15}$$

$$|C_{LE}| \leq C_{LE_{max}} \tag{4-16}$$

and for convenience it is considered that

$$-\pi/2 \leq \mu_p \leq \pi/2 \tag{4-17}$$

$$-\pi/2 \leq \mu_E \leq \pi/2 \tag{4-18}$$

All the above state variables and constants are defined in Chapter III.

Necessary Conditions

Applying the necessary conditions for a saddle point solution, the

Hamiltonian H is given by

$$H = 1 + \lambda_{XP} V_P \cos\gamma_P \cos\chi_P + \lambda_{YP} V_P \cos\gamma_P \sin\chi_P + \lambda_{ZP} V_P \sin\gamma_P$$
$$+ \lambda_{VP} [k_{TP} - k_{DP} (k_{OP} + k_{IP} C_{LP}^2) V_P^2 - g \sin\gamma_P]$$
$$+ \lambda_{\gamma P} [k_{DP} V_P C_{LP} \cos\mu_P - g \cos\gamma_P / V_P] + \lambda_{XP} k_{DP} V_P C_{LP} \sin\mu_P / \cos\gamma_P$$
$$+ \lambda_{XE} V_E \cos\gamma_E \cos\chi_E + \lambda_{YE} V_E \cos\gamma_E \sin\chi_E + \lambda_{ZE} V_E \sin\gamma_E$$
$$+ \lambda_{VE} [k_{TE} - k_{DE} (k_{OE} + k_{IE} C_{LE}^2) V_E^2 - g \sin\gamma_E]$$
$$+ \lambda_{\gamma E} [k_{DE} V_E C_{LE} \cos\mu_E - g \cos\gamma_E / V_E]$$
$$+ \lambda_{XE} k_{DE} V_E C_{LE} \sin\mu_E / \cos\gamma_E \qquad (4\text{-}19)$$

The Hamiltonian is to be minimized with respect to the pursuer's controls, and maximized with respect to the evader's controls. As H is not linear in any of the controls, the possibility of singular controls is not investigated.

If C_{LP} is in the interior of its admissible range, then it is necessary that

$$\frac{\partial H}{\partial C_{LP}} = 0 \qquad (4\text{-}20)$$

and

$$\frac{\partial^2 H}{\partial C_{LP}^2} \geq 0 \qquad (4\text{-}21)$$

Applying these conditions,

$$\frac{\partial H}{\partial C_{LP}} = -2 \lambda_{VP} k_{DP} k_{IP} \bar{C}_{LP} V_P^2 + \lambda_{\gamma P} k_{DP} V_P \cos\mu_P$$
$$+ \lambda_{XP} k_{DP} V_P \sin\mu_P / \cos\gamma_P$$
$$= 0 \qquad (4\text{-}22)$$

and

$$\frac{\partial^2 H}{\partial C_{LP}^2} = -2\ \lambda_{VP} k_{DP} k_{IP} V_P^2 \geq 0 \tag{4-23}$$

which gives

$$\bar{C}_{LP} = (\lambda_{\gamma P} \cos \mu_P \cos \gamma_P + \lambda_{\chi P} \sin \mu_P)/2\ \lambda_{VP} k_{IP} V_P \cos \gamma_P \tag{4-24}$$

and, since k_{DP}, k_{IP} and V_P^2 are positive,

$$\lambda_{VP} \leq 0 \tag{4-25}$$

Thus the admissible control C_{LP}^* that minimizes H is

$$C_{LP}^* = \begin{cases} \bar{C}_{LP} \text{ if } |\bar{C}_{LP}| \leq C_{LP_{max}} \text{ and } \lambda_{VP} \leq 0 \\ \pm C_{LP_{max}} \text{ if the above conditions are not met, according to whichever gives the smaller value of H} \end{cases} \tag{4-26}$$

Similarly, if C_{LE} is in the interior of its admissible range, then it is necessary that

$$\frac{\partial H}{\partial C_{LE}} = 0 \tag{4-27}$$

and

$$\frac{\partial^2 H}{\partial C_{LE}^2} \leq 0 \tag{4-28}$$

Applying these conditions,

$$\bar{C}_{LE} = (\lambda_{\gamma E} \cos \mu_E \cos \gamma_E + \lambda_{\chi E} \sin \mu_E)/2\ \lambda_{VE} k_{IE} V_E \cos \gamma_E \tag{4-29}$$

and

$$\lambda_{VE} \geq 0 \tag{4-30}$$

Thus the admissible control C_{LE}^* that maximizes H is

$$C_{LE}^* = \begin{cases} \bar{C}_{LE} \text{ if } |\bar{C}_{LE}| \leq C_{LE_{max}} \text{ and } \lambda_{VE} \geq 0 \\ \pm C_{LE_{max}} \text{ if the above conditions are not met according to whichever gives the smaller value of H} \end{cases} \tag{4-31}$$

It is further necessary that

$$\frac{\partial H}{\partial \mu_P} = 0 \tag{4-32}$$

and

$$\frac{\partial^2 H}{\partial \mu_P^2} \geq 0 \tag{4-33}$$

Applying these conditions,

$$\frac{\partial H}{\partial \mu_P} = -\lambda_{\gamma P} k_{DP} V_P C_{LP} \sin \mu_P + \lambda_{\chi P} k_{DP} V_P C_{LP} \cos \mu_P / \cos \gamma_P = 0 \tag{4-34}$$

and

$$\frac{\partial^2 H}{\partial \mu_P^2} = -\lambda_{\gamma P} k_{DP} V_P C_{LP} \cos \mu_P - \lambda_{\chi P} k_{DP} V_P C_{LP} \sin \mu_P / \cos \gamma_P \geq 0 \tag{4-35}$$

These conditions are satisfied if $C_{LP} = 0$, in which case the value of μ_P has no physical significance. Otherwise the admissible control μ_P^* that minimizes H is given by

$$\sin \mu_P^* = -\lambda_{\chi P} \operatorname{sgn} \left[C_{LP} \cos \gamma_P \right] \Big/ \sqrt{\lambda_{\chi P}^2 + \lambda_{\gamma P}^2 \cos^2 \gamma_P} \tag{4-36}$$

$$\cos \mu_P^* = -\lambda_{\chi P} \cos \gamma_P \operatorname{sgn} \left[C_{LP} \cos \gamma_P \right] \Big/ \sqrt{\lambda_{\chi P}^2 + \lambda_{\gamma P}^2 \cos^2 \gamma_P} \tag{4-37}$$

It is also necessary that

$$\frac{\partial H}{\partial \mu_E} = 0 \tag{4-38}$$

and

$$\frac{\partial^2 H}{\partial \mu_E^2} \leq 0 \tag{4-39}$$

Applying these conditions, the admissible control μ_E^* that maximizes H is given by

$$\sin \mu_E^* = \lambda_{\chi E} \operatorname{sgn} \left[C_{LE} \cos \gamma_E \right] \Big/ \sqrt{\lambda_{\chi E}^2 + \lambda_{\gamma E}^2 \cos^2 \gamma_E} \tag{4-40}$$

$$\cos \mu_E^* = \lambda_{\gamma E} \cos \gamma_E \operatorname{sgn} \left[C_{LE} \cos \gamma_E \right] \Big/ \sqrt{\lambda_{\chi E}^2 + \lambda_{\gamma E}^2 \cos^2 \gamma_E} \tag{4-41}$$

If both of the pursuer's controls are on the interior of their admissible sets it is further necessary that the matrix

$$\begin{bmatrix} \dfrac{\partial^2 H}{\partial C_{LP}^2} & \dfrac{\partial^2 H}{\partial C_{LP} \partial \mu_P} \\ \dfrac{\partial^2 H}{\partial \mu_P \partial C_{LP}} & \dfrac{\partial^2 H}{\partial \mu_P^2} \end{bmatrix}$$

is non-negative definite. In order to examine this, it is noted that

$$\frac{\partial^2 H}{\partial C_{LP} \partial \mu_P} = -\lambda_{\gamma P} k_{DP} V_P \sin \mu_P + \lambda_{\chi P} k_{DP} V_P \cos \mu_P / \cos \gamma_P$$

$$= \frac{\partial H}{\partial \mu_P} / C_{LP} \tag{4-42}$$

But

$$\frac{\partial H}{\partial \mu_P} = 0 \tag{4-43}$$

so that

$$\frac{\partial^2 H}{\partial \mu_P \partial C_{LP}} = \frac{\partial^2 H}{\partial C_{LP} \partial \mu_P} = 0 \tag{4-44}$$

and thus satisfaction of the individual necessary conditions on C_{LP} and μ_P ensures that the above matrix is non-negative definite. A similar proof holds for the evader's controls.

The costate equations are

$$\dot{\lambda}_{XP} = -\frac{\partial H}{\partial x_P} = 0 \tag{4-45}$$

$$\dot{\lambda}_{YP} = -\frac{\partial H}{\partial y_P} = 0 \tag{4-46}$$

$$\dot{\lambda}_{ZP} = -\frac{\partial H}{\partial z_P} = 0 \tag{4-47}$$

$$\begin{aligned}\dot{\lambda}_{VP} = -\frac{\partial H}{\partial V_P} = &-\lambda_{XP} \cos\gamma_P \cos\chi_P - \lambda_{YP} \cos\gamma_P \sin\chi_P \\ &-\lambda_{ZP} \sin\gamma_P + 2\lambda_{VP} k_{DP} (k_{OP} + k_{IP} C_{LP}^2) V_P \\ &-\lambda_{\gamma P} g \cos\gamma_P / V_P^2 - \lambda_{\gamma P} k_{DP} C_{LP} \cos\mu_P \\ &-\lambda_{\chi P} k_{DP} C_{LP} \sin\mu_P / \cos\gamma_P\end{aligned} \tag{4-48}$$

$$\begin{aligned}\dot{\lambda}_{\gamma P} = \frac{-\partial H}{\partial \gamma_P} = &\lambda_{XP} V_P \sin\gamma_P \cos\chi_P + \lambda_{YP} V_P \sin\gamma_P \sin\chi_P \\ &-\lambda_{ZP} V_P \cos\gamma_P + \lambda_{VP} g \cos\gamma_P - \lambda_{\gamma P} g \sin\gamma_P / V_P \\ &-\lambda_{\chi P} k_{DP} V_P C_{LP} \sin\mu_P \sin\gamma_P / \cos^2\gamma_P\end{aligned} \tag{4-49}$$

$$\dot{\lambda}_{\chi P} = \frac{-\partial H}{\partial \chi_P} = \lambda_{XP} V_P \cos\gamma_P \sin\chi_P - \lambda_{YP} V_P \cos\gamma_P \cos\chi_P \tag{4-50}$$

$$\dot{\lambda}_{XE} = \frac{-\partial H}{\partial x_E} = 0 \tag{4-51}$$

$$\dot{\lambda}_{YE} = \frac{-\partial H}{\partial y_E} = 0 \tag{4-52}$$

$$\dot{\lambda}_{ZE} = \frac{-\partial H}{\partial z_E} = 0 \tag{4-53}$$

$$\begin{aligned}\dot{\lambda}_{VE} = \frac{-\partial H}{\partial V_E} = &-\lambda_{XE} \cos \gamma_E \cos \chi_E - \lambda_{YE} \cos \gamma_E \sin \chi_E \\ &-\lambda_{ZE} \sin \gamma_E + 2\lambda_{VE} k_{DE} (k_{OE} + k_{IE} C_{LE}^2) V_E \\ &-\lambda_{\gamma E} k_{DE} C_{LE} \cos \mu_E - \lambda_{\gamma E} g \cos \gamma_E / V_E^2 \\ &-\lambda_{\chi E} k_{DE} C_{LE} \sin \mu_E / \cos \gamma_E\end{aligned} \tag{4-54}$$

$$\begin{aligned}\dot{\lambda}_{\gamma E} = \frac{-\partial H}{\partial \gamma_E} = &\lambda_{XE} V_E \sin \gamma_E \cos \chi_E + \lambda_{YE} V_E \sin \gamma_E \sin \chi_E \\ &-\lambda_{ZE} V_E \cos \gamma_E + \lambda_{VE} g \cos \gamma_E - \lambda_{\gamma E} g \sin \gamma_E / V_E \\ &-\lambda_{\chi E} k_{DE} V_E C_{LE} \sin \mu_E \sin \gamma_E / \cos^2 \gamma_E\end{aligned} \tag{4-55}$$

$$\dot{\lambda}_{\chi E} = \frac{-\partial H}{\partial \chi_E} = \lambda_{XE} V_E \cos \gamma_E \sin \chi_E - \lambda_{YE} V_E \cos \gamma_E \cos \chi_E \tag{4-56}$$

The transversality conditions give

$$H(t_f) = H(t) = 0 \tag{4-57}$$

$$\lambda_{XP}(t_f) = 2\nu \, (x_p - x_E)\Big|_{t=t_f} = -\lambda_{XE}(t_f) \tag{4-58}$$

$$\lambda_{YP}(t_f) = 2\nu \, (y_p - y_E)\Big|_{t=t_f} = -\lambda_{YE}(t_f) \tag{4-59}$$

$$\lambda_{ZP}(t_f) = 2\nu \, (z_p - z_E)\Big|_{t=t_f} = -\lambda_{ZE}(t_f) \tag{4-60}$$

$$\lambda_{VP}(t_f) = 0 = \lambda_{VE}(t_f) \tag{4-61}$$

$$\lambda_{\gamma P}(t_f) = 0 = \lambda_{\gamma E}(t_f) \tag{4-62}$$

$$\lambda_{\chi P}(t_f) = 0 = \lambda_{\chi E}(t_f) \tag{4-63}$$

where ν is an arbitrary constant.

Partial Problem Solution

In order to evaluate ν, the terminal values of the state and co-state variables are substituted into H, to give

$$\begin{aligned} H(t_f) = 1 &+ 2\nu\,[(x_p-x_E)\,V_p \cos\gamma_p \cos\chi_p]\Big|_{t=t_f} \\ &+ 2\nu\,[(y_p-y_E)\,V_p \cos\gamma_p \sin\chi_p]\Big|_{t=t_f} \\ &+ 2\nu\,[(z_p-z_E)\,V_p \sin\gamma_p]\Big|_{t=t_f} \\ &- 2\nu\,[(x_p-x_E)\,V_E \cos\gamma_E \cos\chi_E]\Big|_{t=t_f} \\ &- 2\nu\,[(y_p-y_E)\,V_E \cos\gamma_E \sin\chi_E]\Big|_{t=t_f} \\ &- 2\nu\,[(z_p-z_E)\,V_E \sin\gamma_E]\Big|_{t=t_f} \\ &= 0 \end{aligned} \tag{4-67}$$

and hence

$$\begin{aligned} 2\nu = 1/\{ &(x_p-x_E)(V_E \cos\gamma_E \cos\chi_E - V_p \cos\gamma_p \cos\chi_p) \\ &+ (y_p-y_E)(V_E \cos\gamma_E \sin\chi_E - V_p \cos\gamma_p \sin\chi_p) \\ &+ (z_p-z_E)(V_E \sin\gamma_E - V_p \sin\gamma_p)\}\Big|_{t=t_f} \end{aligned} \tag{4-68}$$

or more simply

$$2\nu = -1/\{(x_E-x_p)(\dot{x}_E-\dot{x}_p) + (y_E-y_p)(\dot{y}_E-\dot{y}_p) + (z_E-z_p)(\dot{z}_E-\dot{z}_p)\}\Big|_{t=t_f} \tag{4-69}$$

Integration of Eqs (4-45), (4-46), (4-47), (4-51), (4-52) and (4-53) gives

$$\lambda_{XP}(t) = \lambda_{XP}(t_f) \tag{4-70}$$

$$\lambda_{YP}(t) = \lambda_{YP}(t_f) \tag{4-71}$$

$$\lambda_{ZP}(t) = \lambda_{ZP}(t_f) \tag{4-72}$$

$$\lambda_{XE}(t) = \lambda_{XE}(t_f) \tag{4-73}$$

$$\lambda_{YE}(t) = \lambda_{YE}(t_f) \tag{4-74}$$

$$\lambda_{ZE}(t) = \lambda_{ZE}(t_f) \tag{4-75}$$

Eq (4-50) may be written as

$$\dot{\lambda}_{\chi P} = \lambda_{XP}\,\dot{y}_P - \lambda_{YP}\,\dot{x}_P \tag{4-76}$$

which may be integrated to give

$$\lambda_{\chi P}(t) = \lambda_{XP}(t_f)\,[y_p(t) - y_p(t_f)] - \lambda_{YP}(t_f)\,[x_p(t) - x_p(t_f)] \tag{4-77}$$

Similarly

$$\lambda_{\chi E}(t) = \lambda_{XE}(t_f)\,[y_E(t) - y_E(t_f)] - \lambda_{YE}(t_f)\,[x_E(t) - x_E(t_f)] \tag{4-78}$$

One further relationship may be obtained by using the fact that the part of the Hamiltonian which contains only the pursuer's states remains constant (see Appendix A for details), or

$$[\lambda_{XP}\dot{x}_P + \lambda_{YP}\dot{y}_P + \lambda_{ZP}\dot{z}_P + \lambda_{VP}\dot{V}_P + \lambda_{\gamma P}\dot{\gamma}_P + \lambda_{\chi P}\dot{\chi}_P]\Big|_t$$

$$= [\lambda_{XP}\dot{x}_P + \lambda_{YP}\dot{y}_P + \lambda_{ZP}\dot{z}_P]\Big|_{t=t_f} \tag{4-79}$$

which gives

$$\lambda_{VP}(t)\ [k_{TP} - k_{DP}\ (k_{OP} + k_{IP}C_{LP}^2)\ V_P^2 - g \sin \gamma_P]\Big|_t$$

$$+ \lambda_{\gamma P}(t)\ [k_{DP}V_P C_{LP} \cos \mu_P - g \cos \gamma_P / V_P]\Big|_t$$

$$= \lambda_{XP}(t_f)\ [V_P \cos \gamma_P \cos \chi_P\Big|_{t=t_f} - V_P \cos \gamma_P \cos \chi_P\Big|_t]$$

$$+ \lambda_{YP}(t_f)\ [V_P \cos \gamma_P \sin \chi_P\Big|_{t=t_f} - V_P \cos \gamma_P \sin \chi_P\Big|_t]$$

$$+ \lambda_{ZP}(t_f)\ [V_P \sin \gamma_P\Big|_{t=t_f} - V_P \sin \gamma_P\Big|_t] \tag{4-80}$$

Similarly

$$\lambda_{VE}(t)\ [k_{TE} - k_{DE}\ (k_{OE} + k_{IE}C_{LE}^2)\ V_E^2 - g \sin \gamma_E]\Big|_t$$

$$+ \lambda_{\gamma E}(t)\ [k_{DE}V_E C_{LE} \cos \mu_E - g \cos \gamma_E / V_E]\Big|_t$$

$$= \lambda_{XE}(t_f)\ [V_E \cos \gamma_E \cos \chi_E\Big|_{t=t_f} - V_E \cos \gamma_E \cos \chi_E\Big|_t]$$

$$+ \lambda_{YE}(t_f)\ [V_E \cos \gamma_E \sin \chi_E\Big|_{t=t_f} - V_E \cos \gamma_E \sin \chi_E\Big|_t]$$

$$+ \lambda_{ZE}(t_f)\ [V_E \sin \gamma_E\Big|_{t=t_f} - V_E \sin \gamma_E\Big|_t] \tag{4-81}$$

The author was unable to find a method of integrating Eqs (4-48), (4-49), (4-54) and (4-55) other than numerically.

Examination of Open-Loop Solutions

At this stage the coordinate axes are still free to be located anywhere in space. In order to examine the minimum number of parameters required to define the terminal states, it is convenient to locate the origin of the coordinate axes at the terminal position of the pursuer. The direction of the z-axis is fixed by the local gravity, but the x-axis may be rotated about the z-axis until the direction of the pursuer's velocity vector at termination lies in the xz-plane. There are then seven parameters required to define the terminal values of the state variables. The seven parameters S_1 to S_7 are shown in Fig. 2. S_1 and S_2 give the magnitude and direction of the pursuer's velocity; S_3 and S_4 give the position of the evader relative to the pursuer; S_5, S_6 and S_7 give the magnitude and direction of the evader's velocity.

In terms of these parameters the values of the state variables at termination are given by

$$x_p(t_f) = 0 \tag{4-82}$$

$$y_p(t_f) = 0 \tag{4-83}$$

$$z_p(t_f) = 0 \tag{4-84}$$

$$V_p(t_f) = S_1 \tag{4-85}$$

$$\gamma_p(t_f) = S_2 \tag{4-86}$$

$$\chi_p(t_f) = 0 \tag{4-87}$$

$$x_E(t_f) = R \cos S_3 \cos S_4 \tag{4-88}$$

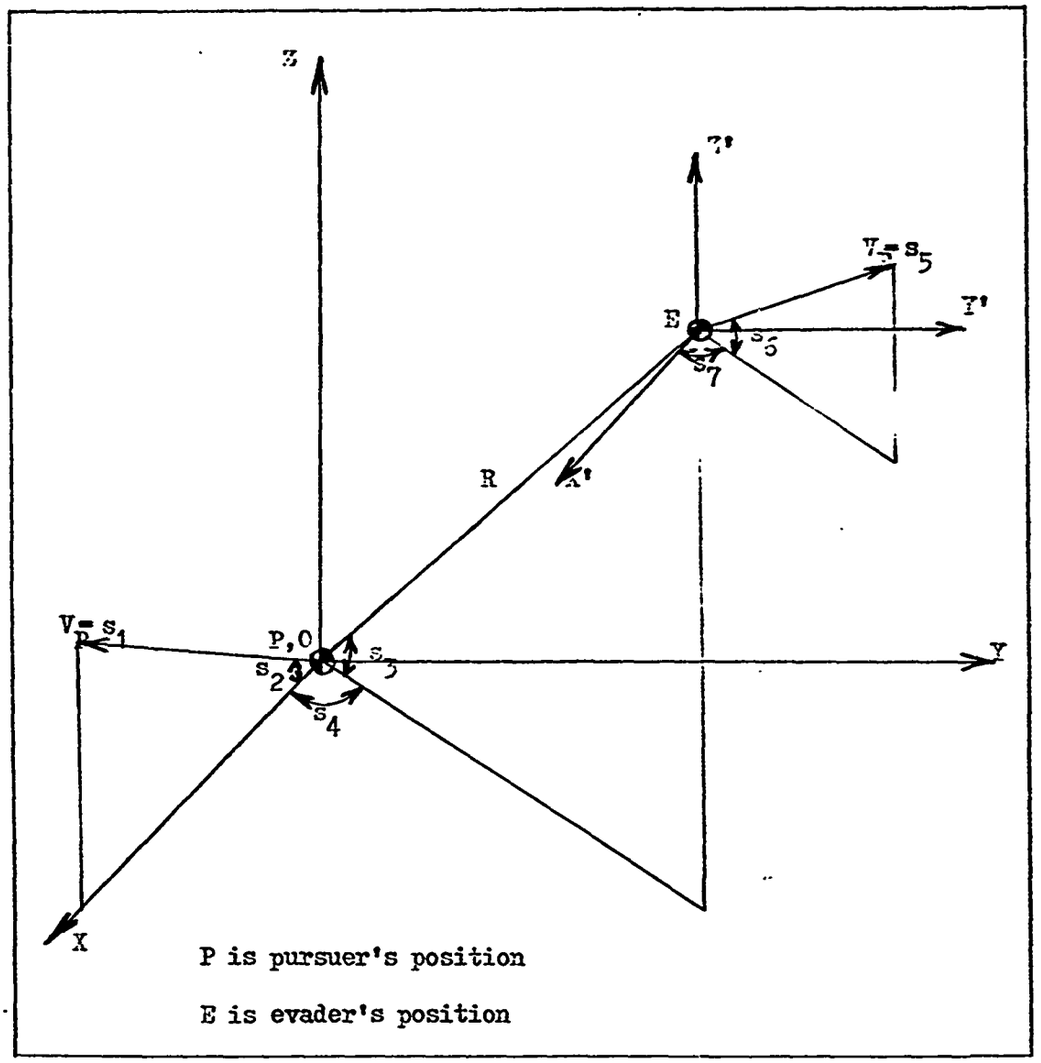

Figure 2. Definition of Terminal Parameters

$$y_E(t_f) = R \cos S_3 \sin S_4 \tag{4-89}$$

$$z_E(t_f) = R \sin S_3 \tag{4-90}$$

$$V_E(t_f) = S_5 \tag{4-91}$$

$$\gamma_E(t_f) = S_6 \tag{4-92}$$

$$x_E(t_f) = S_7 \tag{4-93}$$

A requirement for the useable part of the terminal surface (Ref 3:83) is that

$$\min_{C_{LP},\, \mu_P} \max_{C_{LE},\, \mu_E} \dot{r} \leq 0 \tag{4-94}$$

where $\dot{r} = \frac{dr}{dt}$ (4-95)

and $r^2 = (x_E-x_p)^2 + (y_E-y_p)^2 + (z_E-z_p)^2$ (4-96)

However, the instantaneous value of $\dot{r}$ is independent of either the pursuer's or the evader's controls, and so the above condition merely states that the pursuer must be closing on the evader at termination. In terms of the terminal parameters, the boundary of the useable part is given by

$$S_5[\sin S_3 \sin S_6 + \cos S_3 \cos S_6 \cos (S_7-S_4)]$$

$$= S_1[\sin S_2 \sin S_3 + \cos S_2 \cos S_3 \cos S_4] \tag{4-97}$$

As the author has been unable to solve the problem for closed-loop control laws, the next step is to examine a number of open loop

minimax trajectories integrated backwards in time from the terminal surface. This does not constitute a solution of the problem, as with seven terminal parameters it is quite impractical to map all of free space. However, the solutions obtained are of use in examining the validity of simplified models, and in determining the sensitivity of the solutions to the individual terminal parameters.

Projections of four typical trajectories are shown in Appendix C. The projections were plotted using the three-dimensional Calcomp routine (Ref 2:1 et seq). The trajectories are shown both in real space, and in relative space where the origin is fixed at the pursuer.

Examination of a large number of trajectories by the author revealed no discernible pattern in the values of the bank angles. Moving forward in time, the coefficients of lift remained at their maxima (either positive or negative) unless a tail-chase situation was being approached, when they reduced smoothly and monotonically towards zero. The pursuer's and the evader's lift controls did not in general move away from their limits at the same instant. In-plane approximations to the solution are not considered valid, as even a small out of plane component at termination indicated large out of plane maneuvers had been performed. Trajectories terminating with angular parameters in the order of 1 radian away from the tail-chase configuration could only be integrated backwards in time for a few seconds (typically about 5 sec) before the aircraft velocities became unrealistically large.

It had been hoped as an alternative approach to fit artifically generated closed-loop controls to these trajectories by a least squares fit. A number of possible control laws were fitted to one

trajectory (see Appendix B for details) and then tested on other trajectories. Unfortunately, although it was possible to fit some of the trial functions to any one of the open-loop solutions with an error in the synthesized controls of less than 1%, the approximation became very poor (typical error 100%) when the terminal parameters were altered significantly.

Before passing the problem to the computer for solution, it should be noticed that the lift and bank angle controls are at present undefined at $t = t_f$. Applying L'Hospital's rule

$$\bar{C}_{LP}(t_f) = \lim_{t \to t_f} \{(\lambda_{\gamma P} \cos \mu_P \cos \gamma_P + \lambda_{\chi P} \sin \mu_P)/2\lambda_{VP} k_{IP} V_P \cos \gamma_P\}$$

$$= [(\dot{\lambda}_{\gamma P} \cos \mu_P \cos \gamma_P + \dot{\lambda}_{\chi P} \sin \mu_P)/2\dot{\lambda}_{VP} k_{IP} V_P \cos \gamma_P]\Big|_{t=t_f} \tag{4-98}$$

and

$$\tan \mu_P^*(t_f) = \lim_{t \to t_f} \{\lambda_{\chi P}/\lambda_{\gamma P} \cos \gamma_P\}$$

$$= [\dot{\lambda}_{\chi P}/\dot{\lambda}_{\gamma P} \cos \gamma]\Big|_{t=t_f} \tag{4-99}$$

Similarly

$$\bar{C}_{LE}(t_f) = [(\dot{\lambda}_{\gamma E} \cos \mu_E \cos \gamma_E + \dot{\lambda}_{\chi E} \sin \mu_E)/2\dot{\lambda}_{VE} k_{IE} V_E \cos \gamma_E]\Big|_{t=t_f} \tag{4-100}$$

and

$$\tan \mu^*(t_f) = [\dot{\lambda}_{\chi E}/\dot{\lambda}_{\gamma E} \cos \gamma]\Big|_{t=t_f} \tag{4-101}$$

In certain cases, one such being $S_2 = S_3 = S_4 = S_6 = S_7 = 0$, the above

expressions are still undefined since $\dot{\lambda}_x = \dot{\lambda}_y = 0$. This corresponds to the case of terminating with singular controls. The possibility of singular controls was not investigated further, since in the time available it was considered more desirable to continue the search for a solution "in the small" than to investigate the various surfaces. However, if the reader is himself investigating any trajectories terminating near the direct tail-chase he should beware of this problem.

V. Pursuit-Evasion Differential Game-Zero Gravity and Fixed Velocity Model

The purpose of this chapter is to solve a differential game problem using the aircraft dynamics derived in Chapter III for the zero gravity and fixed velocity model. Although this is the most drastically simplified model which can be found that retains the basic nature of the standard model and its controls, the author was still unable to solve for closed-loop controls. It is, however, possible to solve for the controls in terms of the terminal values of the state variables, by eliminating the costate variables from the problem.

Statement of the Problem

The problem is to determine a saddle point of

$$J(t_f) = \int_{t_0}^{t_f} dt \tag{5-1}$$

subject to

$$\dot{x}_P = V_P \cos \gamma_P \cos \chi_P \tag{5-2}$$

$$\dot{y}_P = V_P \cos \gamma_P \sin \chi_P \tag{5-3}$$

$$\dot{z}_P = V_P \sin \gamma_P \tag{5-4}$$

$$\dot{\gamma}_P = k_{DP} V_P C_{LP} \cos \mu_P \tag{5-5}$$

$$\dot{\chi}_P = k_{DP} V_P C_{LP} \sin \mu_P / \cos \gamma_P \tag{5-6}$$

and

$$\dot{x}_E = V_E \cos \gamma_E \cos \chi_E \tag{5-7}$$

$$\dot{y}_E = V_E \cos \gamma_E \sin \chi_E \tag{5-8}$$

$$\dot{z}_E = V_E \sin \gamma_E \tag{5-9}$$

$$\dot{\gamma}_E = k_{DE} V_E C_{LE} \cos \mu_E \tag{5-10}$$

$$\dot{\chi}_E = k_{DE} V_E C_{LE} \sin \mu_E / \cos \gamma_E \tag{5-11}$$

where V_E and V_P are constant, and where the terminal surface is given

$$\Psi \equiv (x_P - x_E)\Big|^2_{t=t_f} + (y_P - y_E)\Big|^2_{t=t_f} + (z_P - z_E)\Big|^2_{t=t_f} - R^2 = 0 \tag{5-12}$$

The subscripts P and E refer to the pursuer and the evader respectively. The pursuer's controls are C_{LP} and μ_P and the evader's controls are C_{LE} and μ_E. The controls are subject to the constraints

$$|C_{LP}| \leq C_{LP_{max}} \tag{5-13}$$

$$|C_{LE}| \leq C_{LE_{max}} \tag{5-14}$$

and as before it is considered that

$$-\pi/2 \leq \mu_P \leq \pi/2 \tag{5-15}$$

$$-\pi/2 \leq \mu_E \leq \pi/2 \tag{5-16}$$

Necessary Conditions

Applying the necessary conditions for a saddle point solution, the Hamiltonian H is given by

$$H = 1 + \lambda_{XP}V_P \cos\gamma_P \cos\chi_P + \lambda_{YP}V_P \cos\gamma_P \sin\chi_P + \lambda_{ZP}V_P \sin\gamma_P$$
$$+ \lambda_{\gamma P}k_{DP}V_P C_{LP} \cos\mu_P + \lambda_{\chi P}k_{DP}V_P C_{LP} \sin\mu_P/\cos\gamma_P$$
$$+ \lambda_{XE}V_E \cos\gamma_E \cos\chi_E + \lambda_{YE}V_E \cos\gamma_E \sin\chi_E + \lambda_{ZE}V_E \sin\gamma_E$$
$$+ \lambda_{\gamma E}k_{DE}V_E C_{LE} \cos\mu_E + \lambda_{\chi E}k_{DE}V_E C_{LE} \sin\mu_E/\cos\gamma_E \qquad (5\text{-}17)$$

The Hamiltonian is to be minimized with respect to the pursuer's controls, and maximized with respect to the evader's controls.

Exactly as in Chapter IV with the standard model, the necessary conditions on μ_P are satisfied if $C_{LP} = 0$, in which case the value of μ_P has no physical significance. Otherwise the admissible control μ_P^* that minimizes H is given by

$$\sin\mu_P^* = -\lambda_{\chi P}\,\mathrm{sgn}\left[C_{LP}\cos\gamma_P\right] \Big/ \sqrt{\lambda_{\chi P}^2 + \lambda_{\gamma P}^2\cos^2\gamma_P} \qquad (5\text{-}18)$$

$$\cos\mu_P^* = -\lambda_{\gamma P}\cos\gamma_P\,\mathrm{sgn}\left[C_{LP}\cos\gamma_P\right] \Big/ \sqrt{\lambda_{\chi P}^2 + \lambda_{\gamma P}^2\cos^2\gamma_P} \qquad (5\text{-}19)$$

with the possibility of a singular control in μ_P if $\lambda_{\gamma P} = \lambda_{\chi P} = 0$ for a finite time. Similarly the necessary conditions on μ_E are satisfied if $C_{LE} = 0$, in which case the value of μ_E has no physical significance. Otherwise the admissible control μ_E^* that maximizes H is given by

$$\sin\mu_E^* = \lambda_{\chi E}\,\mathrm{sgn}\left[C_{LE}\cos\gamma_E\right] \Big/ \sqrt{\lambda_{\chi E}^2 + \lambda_{\gamma E}^2\cos\gamma\,\gamma_E} \qquad (5\text{-}20)$$

$$\cos\mu_E^* = \lambda_{\gamma E}\cos\gamma_E\,\mathrm{sgn}\left[C_{LE}\cos\gamma_E\right] \Big/ \sqrt{\lambda_{\chi E}^2 + \lambda_{\gamma E}^2\cos^2\gamma_E} \qquad (5\text{-}21)$$

with the possibility of a singular control in μ_E if $\lambda_{\gamma E} = \lambda_{\chi E} = 0$ for a finite time.

Both C_{LP} and C_{LE} appear linearly in H, so it is convenient to define switching functions S_P and S_E such that

$$S_P = \lambda_{\gamma P} \cos \mu_P + \lambda_{\chi P} \sin \mu_P / \cos \gamma_P \tag{5-22}$$

and

$$S_E = \lambda_{\gamma E} \cos \mu_E + \lambda_{\chi E} \sin \mu_E / \cos \gamma_E \tag{5-23}$$

The minimax controls C_L are then given by

$$C_{LP}^* = - C_{LP_{max}} \operatorname{sgn} [S_P] \tag{5-24}$$

$$C_{LE}^* = C_{LE_{max}} \operatorname{sgn} [S_E] \tag{5-25}$$

with the possibility of singular controls in C_{LP} and C_{LE} if $S_P = 0$, or $S_E = 0$ for a finite time.

The costate equations are

$$\dot{\lambda}_{XP} = 0 \tag{5-26}$$

$$\dot{\lambda}_{YP} = 0 \tag{5-27}$$

$$\dot{\lambda}_{ZP} = 0 \tag{5-28}$$

$$\dot{\lambda}_{\gamma P} = \lambda_{XP} V_P \sin \gamma_P \cos \chi_P + \lambda_{YP} V_P \sin \gamma_P \sin \chi_P - \lambda_{ZP} V_P \cos \gamma_P - \lambda_{\chi P} k_{DP} V_P C_{LP} \sin \mu_P \sin \gamma_P / \cos^2 \gamma_P \tag{5-29}$$

$$\dot{\lambda}_{\chi P} = \lambda_{XP} V_P \cos \gamma_P \sin \chi_P - \lambda_{YP} V_P \cos \gamma_P \cos \chi_P \tag{5-30}$$

and

$$\dot{\lambda}_{XE} = 0 \tag{5-31}$$

$$\dot{\lambda}_{YE} = 0 \tag{5-32}$$

$$\dot{\lambda}_{ZE} = 0 \tag{5-33}$$

$$\dot{\lambda}_{\gamma E} = \lambda_{XE} V_E \sin \gamma_E \cos \chi_E + \lambda_{YE} V_E \sin \gamma_E \sin \chi_E - \lambda_{ZE} V_E \cos \gamma_E - \lambda_{\chi E} k_{DE} V_E C_{LE} \sin \mu_E \sin \gamma_E / \cos^2 \gamma_E \tag{5-34}$$

$$\dot{\lambda}_{\chi E} = \lambda_{XE} V_E \cos \gamma_E \sin \chi_E - \lambda_{YE} V_E \cos \gamma_E \cos \chi_E \tag{5-35}$$

The transversality conditions give

$$H(t_f) = H(t) = 0 \tag{5-36}$$

$$\lambda_{XP}(t_f) = 2\nu \, (x_p - x_E)\Big|_{t=t_f} = -\lambda_{XE}(t_f) \tag{5-37}$$

$$\lambda_{YP}(t_f) = 2\nu \, (y_p - y_E)\Big|_{t=t_f} = -\lambda_{YE}(t_f) \tag{5-38}$$

$$\lambda_{ZP}(t_f) = 2\nu \, (z_p - z_E)\Big|_{t=t_f} = -\lambda_{ZE}(t_f) \tag{5-39}$$

$$\lambda_{\gamma P}(t_f) = 0 = \lambda_{\gamma E}(t_f) \tag{5-40}$$

$$\lambda_{\chi P}(t_f) = 0 = \lambda_{\chi E}(t_f) \tag{5-41}$$

where ν is an arbitrary constant.

Partial Problem Solution

The possibility of singular controls is first investigated. The necessary condition for a singular control in C_{LP} is that $S_P = 0$ for a finite time, which gives

$$S_P = \lambda_{\gamma P} \cos \mu_P + \lambda_{\chi P} \sin \mu_P / \cos \gamma_P = 0 \tag{5-42}$$

or

$$\tan \mu_P = -\lambda_{\gamma P} \cos \gamma_P / \lambda_{\chi P} \tag{5-43}$$

However, for $C_{LP} \neq 0$, and non-singular μ_P

$$\tan \mu_P = \frac{\lambda_{\chi P}}{\lambda_{\gamma P} \cos \gamma_P} \tag{5-44}$$

which gives

$$\lambda_{\chi P}^2 = -\lambda_{\gamma P}^2 \cos^2 \gamma_P \tag{5-45}$$

This can only be satisfied if $\lambda_{\chi P} = \lambda_{\gamma P} = 0$, since $\cos \gamma_P = 0$ is a point of singularity in the state equation, and so must be discounted.

Now if $\lambda_{\chi P} = \lambda_{\gamma P} = 0$ for a finite time, which it should be noted is also the condition for a singular control in μ_P,

$$\dot{\lambda}_{\chi P} = \lambda_{\chi P} V_P \cos \gamma_P \sin \chi_P - \lambda_{\gamma P} V_P \cos \gamma_P \cos \chi_P = 0 \tag{5-46}$$

or

$$\tan \chi_P = \lambda_{\gamma P} / \lambda_{\chi P} = \text{const.} \tag{5-47}$$

and

$$\dot{\lambda}_{\gamma P} = \lambda_{\chi P} V_P \sin \gamma_P \cos \chi_P + \lambda_{\gamma P} V_P \sin \gamma_P \sin \chi_P - \lambda_{ZP} V_P \cos \gamma_P = 0 \tag{5-48}$$

or

$$\tan \gamma_P = \lambda_{ZP} / \{\lambda_{\chi P} \cos \chi_P + \lambda_{\gamma P} \sin \chi_P\} = \text{const.} \tag{5-49}$$

This means that $\dot{\chi}_P = \dot{\gamma}_P = 0$, and the only way this can be true is if $C_{LP} = 0$.

Thus the only possibility for a singular control in C_{LP} is

$$C_{LP}^* = 0, \quad \mu_P^* \text{ of no significance} \tag{5-50}$$

An identical argument may be used to show that the only possibility for a singular control in C_{LE} is

$$C_{LE}^* = 0, \quad \mu_E^* \text{ of no significance} \tag{5-51}$$

Now in order to solve the costate equations it is necessary to evaluate ν, which must satisfy the following equation:

$$\begin{aligned} H(t_f) = 1 &- 2\nu \left[(x_E - x_p)\, V_p \cos\gamma_p \cos\chi\right]\Big|_{t=t_f} \\ &- 2\nu \left[(y_E - y_p)\, V_p \cos\gamma_p \sin\chi_p\right]\Big|_{t=t_f} - 2\nu \left[(z_E - z_p)\, V_p \sin\gamma_p\right]\Big|_{t=t_f} \\ &+ 2\nu \left[(x_E - x_p)\, V_E \cos\gamma_E \cos\chi_E\right]\Big|_{t=t_f} \\ &+ 2\nu \left[(y_E - y_p)\, V_E \cos\gamma_E \sin\chi_E\right]\Big|_{t=t_f} + 2\nu \left[z_E - z_p)\, V_E \sin\gamma_E\right]\Big|_{t=t_f} \\ &= 0 \end{aligned} \tag{5-52}$$

and hence

$$2\nu = -1/\left\{(x_E - x_p)(\dot{x}_E - \dot{x}_p) + (y_E - y_p)(\dot{y}_E - \dot{y}_p) + (z_E - z_p)(\dot{z}_E - \dot{z}_p)\right\}\Big|_{t=t_f} \tag{5-53}$$

Integration of Eqs (5-26), (5-27), (5-28), (5-31), (5-32) and (5-53) gives

$$\lambda_{XP}(t) = \lambda_{XP}(t_f) \tag{5-54}$$

$$\lambda_{YP}(t) = \lambda_{YP}(t_f) \tag{5-55}$$

$$\lambda_{ZP}(t) = \lambda_{ZP}(t_f) \tag{5-56}$$

$$\lambda_{XE}(t) = \lambda_{XE}(t_f) \tag{5-57}$$

$$\lambda_{YE}(t) = \lambda_{YE}(t_f) \tag{5-58}$$

$$\lambda_{ZE}(t) = \lambda_{ZE}(t_f) \tag{5-59}$$

Eq (5-30) may be rewritten as

$$\dot{\lambda}_{XP} = \lambda_{XP}\dot{y}_P - \lambda_{YP}\dot{x}_P \tag{5-60}$$

which may be integrated to give

$$\lambda_{XP}(t) = \lambda_{XP}(t_f)\ [y_P(t)-y_P(t_f)] - \lambda_{YP}(t_f)\ [x_P(t)-x_P(t_f)] \tag{5-61}$$

Similarly

$$\lambda_{XE}(t) = \lambda_{XE}(t_f)\ [y_E(t)-y_E(t_f)] - \lambda_{YE}(t_f)\ [x_E(t)-x_E(t_f)] \tag{5-62}$$

The remaining costate variables may now be found by using the fact that that part of the Hamiltonian which contains only the pursuer's (evader's) states remains constant (see Appendix A for details), or

$$[\lambda_{XP}\dot{x}_P + \lambda_{YP}\dot{y}_P + \lambda_{ZP}\dot{z}_P + \lambda_{YP}\dot{y}_P + \lambda_{XP}\dot{x}_P]\Big|_t$$

$$= [\lambda_{XP}\dot{x}_P + \lambda_{YP}\dot{y}_P + \lambda_{ZP}\dot{z}_P]\Big|_{t=t_f} \tag{5-63}$$

which gives, on non-singular arcs

$$\lambda_{\gamma p}(t) = \Big[\lambda_{XP}(t_f)\ [\dot{x}_p(t_f)-\dot{x}_p(t)] + \lambda_{YP}(t_f)\ [\dot{y}_p(t_f)-\dot{y}_p(t)]$$
$$+ \lambda_{ZP}(t_f)\ [\dot{z}_p(t_f)-\dot{z}_p(t)] - \lambda_{XP}(t_f)\ [y_p(t)-y_p(t_f)]\ \dot{\chi}_p(t)$$
$$+ \lambda_{YP}(t_f)\ [x_p(t)-x_p(t_f)]\ \dot{\chi}_p(t) \Big] / \dot{\gamma}_p(t) \qquad (5\text{-}64)$$

where all the above terms are known as functions of the current and terminal values of the states, and of the controls. The known values have not been inserted in Eq (5-64) for the benefit of clarity.

Similarly

$$\lambda_{\gamma E}(t) = \Big[\lambda_{XE}(t_f)\ [\dot{x}_E(t_f)-\dot{x}_E(t)] + \lambda_{YE}(t_f)\ [\dot{y}_E(t_f)-\dot{y}_E(t)]$$
$$+ \lambda_{ZE}(t_f)\ [\dot{z}_E(t_f)-\dot{z}_E(t)] - \lambda_{XE}(t_f)\ [y_E(t)-y_E(t_f)]\ \dot{\chi}_E(t)$$
$$+ \lambda_{YE}(t_f)\ [x_E(t)-x_E(t_f)]\ \dot{\chi}_E(t) \Big] / \dot{\gamma}_E(t) \qquad (5\text{-}65)$$

Substitution of these values of the costates into the expression for the bank angles, when not on a singular arc yields

$$\sin \mu_p^* = k_{DP} V_p C_{LP}^* \left[(x_E-x_p)\Big|_{t=t_f} [y_p(t)-y_p(t_f)] - (y_E-y_p)\Big|_{t=t_f} [x_p(t)-x_p(t_f)] \right]$$
$$/ \cos \gamma_p \left[(x_E-x_p)\Big|_{t=t_f} [\dot{x}_p(t_f)-\dot{x}_p(t)] + (y_E-y_p)\Big|_{t=t_f} [\dot{y}_p(t_f)-\dot{y}_p(t)] \right.$$
$$\left. + (z_E-z_p)\Big|_{t=t_f} [z_p(t_f)-z_p(t)] \right] \qquad (5\text{-}66)$$

where $C_{LP}^* = \pm C_{LP_{max}}$, and

$$\sin \mu_E^* = k_{DE} V_E C_{LE}^* \left[(x_E - x_p)\Big|_{t=t_f} [y_E(t) - y_E(t_f)] - (y_E - y_p)\Big|_{t=t_f} [x_E(t) - x_E(t_f)] \right]$$

$$\Big/ \cos \gamma_E \left[(x_E - x_p)\Big|_{t=t_f} [\dot{x}_E(t_f) - \dot{x}_E(t)] + (y_E - y_p)\Big|_{t=t_f} [\dot{y}_E(t_f) - \dot{y}_E(t)] \right.$$

$$\left. + (z_E - z_p)\Big|_{t=t_f} [\dot{z}_E(t_f) - \dot{z}_E(t)] \right] \qquad (5\text{-}67)$$

where $C_{LE}^* = \pm C_{LE_{max}}$.

Now in order to investigate the switching function S_p, on non-singular arcs

$$S_p = \cos \mu_p \, (\lambda_{\gamma p} + \lambda_{\chi p} \tan \mu_p / \cos \gamma_p)$$

$$= \cos \mu_p \, (\lambda_{\gamma p}^2 \cos^2 \gamma_p + \lambda_{\chi p}^2) / \lambda_{\gamma p} \cos^2 \gamma_p \qquad (5\text{-}68)$$

and since $-\pi/2 \leq \mu_p \leq \pi/2$

$$S_p > 0 \text{ if } \lambda_{\gamma p} > 0 \qquad (5\text{-}69)$$

$$S_p < 0 \text{ if } \lambda_{\gamma p} < 0 \qquad (5\text{-}70)$$

where $\lambda_{\gamma p}$ is given by Eq (5-64). Similarly

$$S_E > 0 \text{ if } \lambda_{\gamma E} > 0 \qquad (5\text{-}71)$$

$$S_E < 0 \text{ if } \lambda_{\gamma E} > 0 \qquad (5\text{-}72)$$

where $\lambda_{\gamma E}$ is given by Eq (5-65).

On singular arcs, the condition that that part of the Hamiltonian containing only the pursuer's states should remain constant gives, since $\lambda_{\gamma p} = \lambda_{\chi p} = 0$

$$\lambda_{xp}(t_f)\ [\dot{x}_p(t)-\dot{x}_p(t_f)] + \lambda_{yp}(t_f)\ [\dot{y}_p(t)-\dot{y}_p(t_f)]$$

$$+ \lambda_{zp}(t_f)\ [\dot{z}_p(t)-\dot{z}_p(t_f)] = 0 \qquad (5\text{-}73)$$

or

$$(x_E-x_p)\Big|_{t=t_f}\ [\dot{x}_p(t)-\dot{x}_p(t_f)] + (y_E-y_p)\Big|_{t=t_f}\ [\dot{y}_p(t)-\dot{y}_p(t_f)]$$

$$+ (z_E-z_p)\Big|_{t=t_f}\ [\dot{z}_p(t)-\dot{z}_p(t_f)] = 0 \qquad (5\text{-}74)$$

and, similarly for the evader

$$(x_E-x_p)\Big|_{t=t_f}\ [\dot{x}_E(t)-\dot{x}_E(t_f)] + (y_E-y_p)\Big|_{t=t_f}\ [\dot{y}_E(t)-\dot{y}_E(t_f)]$$

$$+ (z_E-z_p)\Big|_{t=t_f}\ [\dot{z}_E(t)-\dot{z}_E(t_f)] = 0 \qquad (5\text{-}75)$$

Both the pursuer's and the evader's controls and associated switching functions, both on and off singular arcs, have now been expressed in terms of the current and terminal values of the state variables.

Examination of Open Loop Solutions

At first sight it would seem that the fact that the costate variables have been eliminated from the solution of this problem would greatly simplify the mapping of free space. However, closer scrutiny reveals that unless it is possible to integrate the state equations forward in time and so eliminate the values of the states at termination, no great simplification ensues. The author was only able to integrate the state equations forward along the singular arcs, which are of constant velocity vector, and so open-loop solutions for anything other than trajectories composed only of singular arcs must still

be generated by backward numerical integration from the terminal surface.

For comparison with the results of the standard model it is convenient to use the same terminal parameters as in Chapter IV (see Fig. 2). In this case S_1 and S_5 are not terminal parameters but problem parameters. The values of the state variables at termination, and the boundary of the useable part at termination are exactly as given in Eqs (4-82) to (4-97).

On the terminal surface, $S_P = 0$ instantaneously so $C_{LP}^*(t_f)$ is given by

$$C_{LP}^*(t_f) = \begin{cases} C_{LP_{max}} & \dot{S}_P(t_f) > 0 \\ -C_{LP_{max}} & \dot{S}_P(t_f) < 0 \\ 0 & \dot{S}_P(t_f) = 0 \end{cases} \tag{5-76}$$

and similarly

$$C_{LE}^*(t_f) = \begin{cases} C_{LE_{max}} & \dot{S}_E(t_f) < 0 \\ -C_{LE_{max}} & \dot{S}_E(t_f) > 0 \\ 0 & \dot{S}_E(t_f) = 0 \end{cases} \tag{5-77}$$

As with the standard model

$$\tan \mu_P^*(t_f) = [\dot{\lambda}_{\chi P}/\dot{\lambda}_{\gamma P} \cos \gamma_P]\Big|_{t=t_f} \tag{5-78}$$

and

$$\tan \mu_E^*(t_f) = [\dot{\lambda}_{\chi E}/\dot{\lambda}_{\gamma E} \cos \gamma_E]\Big|_{t=t_f} \qquad (5\text{-}79)$$

When comparing the trajectories obtained from this model with those of the standard model, it should be remembered that gravity has been neglected in this case since it affects both players almost equally. Thus the backward trajectories for the zero gravity case should be imagined displaced vertically a distance $\frac{1}{2} g(t_f-t)^2$ when viewed in real space. With this fact in mind, the trajectories obtained from this model and the standard model are in most cases very similar. The exceptions are those trajectories finishing very close to a horizontal tail chase configuration (Figs. 3 and 4). The reason for this is felt to be that in these cases the singular arcs have been very closely approached, and bearing in mind that the integrations were performed backwards in time the trajectories are determined by the perturbations off the singular arc. A small vertical perturbation corresponds to trajectories that are predominatly in a vertical plane, and a small horizontal perturbation corresponds to trajectories that are predominately in a horizontal plane. Thus with the standard model, gravity is sufficient to force most of the near tail chase trajectories into the vertical plane, whereas with the zero gravity model the small terminal parameters and integration errors dictate the direction the trajectories will take.

The author feels that if closed-loop control laws for this model could be found, then going forward in time the trajectories generated by using these control laws with the standard model dynamics would quite closely approximate the trajectories produced by backward inte-

gration of the full standard model. It would not be impossibly difficult for this hypothesis to be checked by the use of a hybrid computer, or for a limited number of cases by using a gradient technique on a digital computer. The advantage of using the zero gravity fixed velocity model in this case is that the number of terminal parameters has been reduced by two from the case of the standard model, so that the effort involved in generating an open-loop solution forward in time is considerably reduced.

VI. Pursuit-Evasion Differential Game-Spherical Acceleration Vectogram Model

The purpose of this chapter is to solve a differential game problem using the aircraft dynamics derived in Chapter III for the spherical acceleration vectogram model. This represents the best model for which the author was able to obtain closed-loop control laws. The derivation of the closed-loop control laws is given, representing a "solution in the small", but no attempt is made to investigate the various surfaces which would represent a "solution in the large". The reason for this is that the solution of this differential game is not an end in itself, but merely a tool with which to attack the solution of the standard model.

Statement of the Problem

The problem is to determine a saddle point of

$$J(t_f) = \int_{t_0}^{t_f} dt \tag{6-1}$$

subject to

$$\dot{x}_p = V_{XP} \tag{6-2}$$

$$\dot{y}_p = V_{YP} \tag{6-3}$$

$$\dot{z}_p = V_{ZP} \tag{6-4}$$

$$\dot{V}_{XP} = F_p \ell_1 \tag{6-5}$$

$$\dot{V}_{YP} = F_p \ell_2 \tag{6-6}$$

$$\dot{V}_{ZP} = F_P \ell_3 \tag{6-7}$$

and

$$\dot{x}_E = V_{XE} \tag{6-8}$$

$$\dot{y}_E = V_{YE} \tag{6-9}$$

$$\dot{z}_E = V_{ZE} \tag{6-10}$$

$$\dot{V}_{XE} = F_E m_1 \tag{6-11}$$

$$\dot{V}_{YE} = F_E m_2 \tag{6-12}$$

$$\dot{V}_{ZE} = F_E m_3 \tag{6-13}$$

where F_P and F_E are the magnitudes of the specific excess thrust and are constant, and ℓ_i and m_i are the direction cosines of the pursuer's and evader's specific excess thrust vectors respectively, and represent the two players' controls.

The controls are subject to the constraints ℓ_i real and

$$\ell_1^2 + \ell_2^2 + \ell_3^2 = 1 \tag{6-14}$$

and m_i real and

$$m_1^2 + m_2^2 + m_3^2 = 1 \tag{6-15}$$

As with the other models, the terminal surface is given by

$$\Psi \equiv (x_P - x_E)\Big|^2_{t=t_f} + (y_P - y_E)\Big|^2_{t=t_f} + (z_P - z_E)\Big|^2_{t=t_f} - R^2 = 0 \tag{6-16}$$

and the subscripts P and E refer to the pursuer and the evader respectively.

Necessary Conditions

Rather than adjoin the control constraints, it is convenient to make the substitutions

$$\ell_3 = \pm\sqrt{1 - \ell_1^2 - \ell_2^2} \tag{6-17}$$

and

$$m_3 = \pm\sqrt{1 - m_1^2 - m_2^2} \tag{6-18}$$

With these substitutions, the Hamiltonian, H, is given by

$$\begin{aligned} H = 1 &+ \lambda_{XP}V_{XP} + \lambda_{YP}V_{YP} + \lambda_{ZP}V_{ZP} + \lambda_{VXP}F_P\ell_1 + \lambda_{VYP}F_P\ell_2 \\ &\pm \lambda_{VZP}F_P\sqrt{1 - \ell_1^2 - \ell_2^2} + \lambda_{XE}V_{XE} + \lambda_{YE}V_{YE} + \lambda_{ZE}V_{ZE} \\ &+ \lambda_{VXE}F_Em_2 + \lambda_{VYE}F_Em_2 \pm \lambda_{VZE}F_E\sqrt{1 - m_1^2 - m_2^2} \end{aligned} \tag{6-19}$$

The Hamiltonian is to be minimized with respect to the pursuer's controls, and maximized with respect to the evader's controls.

Applying the first necessary conditions

$$\begin{aligned} \frac{\partial H}{\partial \ell_1} &= \lambda_{VXP}F_P \mp \lambda_{VZP}F_P\ell_1/\sqrt{1 - \ell_1^2 - \ell_2^2} \\ &= 0 \end{aligned} \tag{6-20}$$

or

$$\lambda_{VXP}^2(1 - \ell_1^2 - \ell_2^2) = \lambda_{VZP}^2\ell_1^2 \tag{6-21}$$

and

$$\frac{\partial H}{\partial \ell_2} = \lambda_{VYP} F_p \mp \lambda_{VZP} F_p \ell_2 / \sqrt{1 - \ell_1^2 - \ell_2^2}$$

$$= 0 \tag{6-22}$$

or

$$\lambda_{VYP}^2 \left(1 - \ell_1^2 - \ell_2^2 \right) = \lambda_{VZP}^2 \ell_2^2 \tag{6-23}$$

Therefore

$$\ell_1^2 / \ell_2^2 = \lambda_{VXP}^2 / \lambda_{VYP}^2 \tag{6-24}$$

and by symmetry

$$\ell_3^2 / \ell_2^2 = \lambda_{VZP}^2 / \lambda_{VYP}^2 \tag{6-25}$$

Substitution into Eq (6-14) gives

$$\ell_1 = \pm \lambda_{VXP} / \sqrt{\lambda_{VXP}^2 + \lambda_{VYP}^2 + \lambda_{VZP}^2} \tag{6-26}$$

and similar expressions may be obtained for ℓ_2, ℓ_3. Applying the second necessary condition

$$\frac{\partial^2 H}{\partial \ell_1^2} \geq 0 \tag{6-27}$$

is merely checking that ℓ_1 minimizes rather than maximizes H. This is more easily established by substituting for ℓ_1, ℓ_2 and ℓ_3 in H, when it is obvious that to minimize H, since $F_p > 0$,

$$\ell_1^* = -\lambda_{VXP} / \sqrt{\lambda_{VXP}^2 + \lambda_{VYP}^2 + \lambda_{VZP}^2} \tag{6-28}$$

$$\ell_2^* = -\lambda_{VYP} / \sqrt{\lambda_{VXP}^2 + \lambda_{VYP}^2 + \lambda_{VZP}^2} \tag{6-29}$$

$$\ell_3^* = -\lambda_{VZP} / \sqrt{\lambda_{VXP}^2 + \lambda_{VYP}^2 + \lambda_{VZP}^2} \tag{6-30}$$

A similar argument may be used to show that

$$m_1^* = + \lambda_{VXE} / \sqrt{\lambda_{VXE}^2 + \lambda_{VYE}^2 + \lambda_{VZE}^2} \tag{6-31}$$

$$m_2^* = + \lambda_{VYE} / \sqrt{\lambda_{VXE}^2 + \lambda_{VYE}^2 + \lambda_{VZE}^2} \tag{6-32}$$

$$m_3^* = + \lambda_{VZE} / \sqrt{\lambda_{VXE}^2 + \lambda_{VYE}^2 + \lambda_{VZE}^2} \tag{6-33}$$

The costate equations are

$$\dot{\lambda}_{XP} = 0 \tag{6-34}$$

$$\dot{\lambda}_{YP} = 0 \tag{6-35}$$

$$\dot{\lambda}_{ZP} = 0 \tag{6-36}$$

$$\dot{\lambda}_{VXP} = -\lambda_{XP} \tag{6-37}$$

$$\dot{\lambda}_{VYP} = -\lambda_{YP} \tag{6-38}$$

$$\dot{\lambda}_{VZP} = -\lambda_{ZP} \tag{6-39}$$

and

$$\dot{\lambda}_{XE} = 0 \tag{6-40}$$

$$\dot{\lambda}_{YE} = 0 \tag{6-41}$$

$$\dot{\lambda}_{ZE} = 0 \tag{6-42}$$

$$\dot{\lambda}_{VXE} = -\lambda_{XE} \tag{6-43}$$

$$\dot{\lambda}_{VYE} = -\lambda_{YE} \tag{6-44}$$

$$\dot{\lambda}_{VZE} = -\lambda_{ZE} \tag{6-45}$$

The transversality conditions give

$$H(t_f) = H(t) = 0 \tag{6-46}$$

$$\lambda_{XP}(t_f) = 2\nu\ (x_p - x_E)\Big|_{t=t_f} = -\lambda_{XE}(t_f) \tag{6-47}$$

$$\lambda_{YP}(t_f) = 2\nu\ (y_p - y_E)\Big|_{t=t_f} = -\lambda_{YE}(t_f) \tag{6-48}$$

$$\lambda_{ZP}(t_f) = 2\nu\ (z_p - z_E)\Big|_{t=t_f} = -\lambda_{ZE}(t_f) \tag{6-49}$$

$$\lambda_{VXP}(t_f) = 0 = \lambda_{VXE}(t_f) \tag{6-50}$$

$$\lambda_{VYP}(t_f) = 0 = \lambda_{VYE}(t_f) \tag{6-51}$$

$$\lambda_{VZP}(t_f) = 0 = \lambda_{VZE}(t_f) \tag{6-52}$$

where ν is a constant which must satisfy the above conditions.

Problem Solution

Integration of the costate differential equations gives

$$\lambda_{XP}(t) = \lambda_{XP}(t_f) = 2\nu\ (x_p - x_E)\Big|_{t=t_f} \tag{6-53}$$

$$\lambda_{YP}(t) = \lambda_{YP}(t_f) = 2\nu\ (y_p - y_E)\Big|_{t=t_f} \tag{6-54}$$

$$\lambda_{ZP}(t) = \lambda_{ZP}(t_f) = 2\nu\ (z_p - z_E)\Big|_{t=t_f} \tag{6-55}$$

$$\lambda_{VXP}(t) = 2\nu\ (x_p - x_E)\Big|_{t=t_f} (t_f - t) \tag{6-56}$$

$$\lambda_{VYP}(t) = 2\nu\ (y_p - y_E)\Big|_{t=t_f} (t_f - t) \tag{6-57}$$

$$\lambda_{VZP}(t) = 2\nu\ (z_p - z_E)\Big|_{t=t_f} (t_f - t) \tag{6-58}$$

and

$$\lambda_{XE}(t) = \lambda_{XE}(t_f) = -2\nu\ (x_p - x_E)\Big|_{t=t_f} \tag{6-59}$$

$$\lambda_{YE}(t) = \lambda_{YE}(t_f) = -2\nu\ (y_p - y_E)\Big|_{t=t_f} \tag{6-60}$$

$$\lambda_{ZE}(t) = \lambda_{ZE}(t_f) = -2\nu\ (z_p - z_E)\Big|_{t=t_f} \tag{6-61}$$

$$\lambda_{VXE}(t) = -2\nu\ (x_p - x_E)\Big|_{t=t_f} (t_f - t) \tag{6-62}$$

$$\lambda_{VYE}(t) = -2\nu\ (y_p - y_E)\Big|_{t=t_f} (t_f - t) \tag{6-63}$$

$$\lambda_{VZE}(t) = -2\nu\ (z_p - z_E)\Big|_{t=t_f} (t_f - t) \tag{6-64}$$

Substitution of the costate variables into the minimax controls gives

$$\ell_1^* = -2\nu\ (x_p-x_E)\Big|_{t=t_f}\ (t_f-t)/|2\nu\ (t_f-t)R| = (x_E-x_p)\Big|_{t=t_f}\ \text{sgn}\ (\nu)/R \tag{6-65}$$

$$\ell_2^* = (y_E-y_p)\Big|_{t=t_f}\ \text{sgn}\ (\nu)/R \tag{6-66}$$

$$\ell_3^* = (z_E-z_p)\Big|_{t=t_f}\ \text{sgn}\ (\nu)/R \tag{6-67}$$

and

$$m_1^* = -2\nu\ (x_p-x_E)\Big|_{t=t_f}\ (t_f-t)/|2\nu\ (t_f-t)R| = (x_E-x_p)\Big|_{t=t_f}\ \text{sgn}\ (\nu)/R \tag{6-68}$$

$$m_2^* = (y_E-y_p)\Big|_{t=t_f}\ \text{sgn}\ (\nu)/R \tag{6-69}$$

$$m_3^* = (z_E-z_p)\Big|_{t=t_f}\ \text{sgn}\ (\nu)/R \tag{6-70}$$

It is interesting to note that the pursuer's and the evader's controls are identical and constant. Further, the ratio of the components of the controls is the same as the ratio of the corresponding relative coordinates at termination.

Now using the fact that $H(t_f) = 0$ gives

$$H(t_f) = 1 + [2\nu\ (x_p-x_E)(V_{XP}-V_{XE})]\Big|_{t=t_f} + [2\nu\ (y_p-y_E)(V_{YP}-V_{YE})]\Big|_{t=t_f} + [2\nu\ (z_p-z_E)(V_{ZP}-V_{ZE})]\Big|_{t=t_f} = 0 \tag{6-71}$$

or

$$2\nu = -1/\{(x_E-x_p)(V_{XE}-V_{XP}) + (y_E-y_p)(V_{YE}-V_{YP}) + (z_E-z_p)(V_{ZE}-V_{ZP})\}\Big|_{t=t_f} \quad (6\text{-}72)$$

Now if $\bar{r}$ is defined as a vector from the pursuer to the evader, and $\hat{i}$, $\hat{j}$, $\hat{k}$ are unit vectors in the x, y, z-directions

$$\bar{r} = (x_E-x_p)\,\hat{i} + (y_E-y_p)\,\hat{j} + (z_E-z_p)\,\hat{k} \quad (6\text{-}73)$$

$$\dot{\bar{r}} = (V_{XE}-V_{XP})\,\hat{i} + (V_{YE}-V_{YP})\,\hat{j} + (V_{ZE}-V_{ZP})\,\hat{k} \quad (6\text{-}74)$$

and from basic dynamics (differeniate $\bar{r}\cdot\bar{r} = r^2$)

$$\dot{r}r = \dot{\bar{r}}\cdot\bar{r} \quad (6\text{-}75)$$

so that

$$\dot{r}(t_f) = \{(V_{XE}-V_{XP})(x_E-x_p) + (V_{YE}-V_{YP})(y_E-y_p) + (V_{ZE}-V_{ZP})(z_E-z_p)\}\Big|_{t=t_f} /R \quad (6\text{-}76)$$

However, for capture to occur it is necessary that $\dot{r}(t_f) < 0$ and so

$$\{(V_{XE}-V_{XP})(x_E-x_p) + (V_{YE}-V_{YP})(y_E-y_p) + (V_{ZE}-V_{ZP})(z_E-z_p)\}\Big|_{t=t_f} < 0 \quad (6\text{-}77)$$

and hence from Eq (6-72)

$$\nu > 0 \quad (6\text{-}78)$$

The minimax controls are thus

$$\ell_1^* = m_1^* = (x_E-x_p)\Big|_{t=t_f} /R \quad (6\text{-}79)$$

$$\ell_2^* = m_2^* = (y_E - y_p)\Big|_{t=t_f} / R \tag{6-80}$$

$$\ell_3^* = n_3^* = (z_E - z_p)\Big|_{t=t_f} / R \tag{6-81}$$

Using these controls, the state equations are integrated backwards in time from t_f, which gives

$$V_{XP}(t) - V_{XP}(t_f) = \frac{F_p}{R} (x_E - x_p)\Big|_{t=t_f} (t - t_f) \tag{6-82}$$

$$V_{YP}(t) - V_{YP}(t_f) = \frac{F_p}{R} (y_E - y_p)\Big|_{t=t_f} (t - t_f) \tag{6-83}$$

$$V_{ZP}(t) - V_{ZP}(t_f) = \frac{F_p}{R} (z_E - z_p)\Big|_{t=t_f} (t - t_f) \tag{6-84}$$

$$x_p(t) - x_p(t_f) = \frac{F_p}{2R} (x_E - x_p)\Big|_{t=t_f} (t - t_f)^2 + V_{XP}(t_f)(t - t_f) \tag{6-85}$$

$$y_p(t) - y_p(t_f) = \frac{F_p}{2R} (y_E - y_p)\Big|_{t=t_f} (t - t_f)^2 + V_{YP}(t_f)(t - t_f) \tag{6-86}$$

$$z_p(t) - z_p(t_f) = \frac{F_p}{2R} (z_E - z_p)\Big|_{t=t_f} (t - t_f)^2 + V_{ZP}(t_f)(t - t_f) \tag{6-87}$$

and similar expressions for the evader. Since this is a perfect information game the values of the state variables are known at time t, and the aim is to eliminate their values at t_f. Substitution of Eq (6-82) into Eq (6-85) yields

$$x_p(t) - x_p(t_f) = \frac{F_p}{2R}(x_E-x_p)\Big|_{t=t_f}(t-t_f)^2 + v_{XP}(t)\ (t-t_f)$$

$$- \frac{F_p}{R}(x_E-x_p)\Big|_{t=t_f}(t-t_f)^2$$

$$= v_{XP}(t)(t-t_f) - \frac{F_p}{2R}(x_E-x_p)\Big|_{t=t_f}(t-t_f)^2 \qquad (6\text{-}88)$$

and similarly for the evader

$$x_E(t) - x_E(t_f) = v_{XE}(t)(t-t_f) - \frac{F_E}{2R}(x_E-x_p)\Big|_{t=t_f}(t-t_f)^2 \qquad (6\text{-}89)$$

Subtracting Eq (6-89) from Eq (6-88)

$$(x_E-x_p)\Big|_{t=t_f}[1 + (t_f-t)^2\ (F_p-F_E)/2R] = (x_E-x_p) + (V_{XE}-V_{XP})(t_f-t)$$

(6-90)

and similarly

$$(y_E-y_p)\Big|_{t=t_f}[1 + (t_f-t)^2\ (F_p-F_E)/2R] = (y_E-y_p) + (V_{YE}-V_{YP})(t_f-t)$$

(6-91)

$$(z_E-z_p)\Big|_{t=t_f}[1 + (t_f-t)^2\ (F_p-F_E)/2R] = (z_E-z_p) + (V_{ZE}-V_{ZP})(t_f-t)$$

(6-92)

Squaring and adding Eqs (6-90), (6-91), (6-92)

$$R^2\ [1 + (t_f-t)^2\ (F_p-F_E)/2R]^2 = [(x_E-x_p) + (V_{XE}-V_{XP})(t_f-t)]^2$$

$$+ [(y_E-y_p) + (V_{YE}-V_{YP})(t_f-t)]^2 + [(z_E-z_p) + (V_{ZE}-V_{ZP})/(t_f-t)]^2$$

(6-93)

or

$$(t_f-t)^4 \frac{(F_P-F_E)^2}{4} + (t_f-t)^2 [(F_P-F_E) R - (V_{XE}-V_{XP})^2 - (V_{YE}-V_{YP})^2 - (V_{ZE}-V_{ZP})^2] - 2 (t_f-t) [(x_E-x_p)(V_{XE}-V_{XP}) + (y_E-y_p)(V_{YE}-V_{YP}) + (z_E-z_p)(V_{ZE}-V_{ZP})] + R^2 - (x_E-x_p)^2 - (y_E-y_p)^2 - (z_E-z_p)^2 = 0 \quad (6-94)$$

This may be more conveniently expressed using the notation of Eqs (6-73), (6-74) and (6-75) as

$$(t_f-t)^4 \frac{(F_P-F_E)^2}{4} + (t_f-t)^2 [(F_P-F_E) R - \dot{\bar{r}}\cdot\dot{\bar{r}}] - 2 (t_f-t) r\dot{r} + (R^2-r^2) = 0 \quad (6-95)$$

This is a quartic which may be solved at any time t to give (t_f-t) which is the only unknown in the equation. This value of (t_f-t), normally the smallest positive root of the quartic, may then be used to evaluate the controls at time t, which, using Eqs (6-90), (6-91) and (6-92) are

$$\ell_1^* = m_1^* = [(x_E-x_p) + (V_{XE}-V_{XP})(t_f-t)]/[R + \tfrac{1}{2} (F_P-F_E)(t_f-t)^2] \quad (6-96)$$

$$\ell_2^* = m_2^* = [(y_E-y_p) + (V_{YE}-V_{YP})(t_f-t)]/[R + \tfrac{1}{2} (F_P-F_E)(t_f-t)^2] \quad (6-97)$$

$$\ell_3^* = m_3^* = [(z_E-z_p) + (V_{ZE}-V_{ZP})(t_f-t)]/[R + \tfrac{1}{2} (F_P-F_E)(t_f-t)^2] \quad (6-98)$$

Thus open-loop controls are found by solving for (t_f-t) from Eq (6-95)

at some initial time t_0, evaluating ℓ_1^*, ℓ_2^*, ℓ_3^*, m_1^*, m_2^* and m_3^* from Eqs (6-96), (6-97) and (6-98) and keeping them constant. Since continuously updatable open-loop solutions are equivalent to closed-loop solutions, closed-loop controls are found by solving for (t_f-t) continuously and using this value to determine the direction cosines at each instant.

Examination of Solutions

In order to compare the minimax solutions for this model with those of the standard model, runs were made backwards in time for the same terminal states as were used for the open-loop standard model solutions. The magnitude of the specific excess thrust for each player was made equal to that player's maximum specific lift force at termination, so that

$$F_P = k_{DP} [V_P(t_f)]^2 C_{LP_{max}} = k_{DP} S_1^2 C_{LP_{max}} \quad (6\text{-}99)$$

and

$$F_E = k_{DE} [V_E(t_f)]^2 C_{LE_{max}} = k_{DE} S_5^2 C_{LE_{max}} \quad (6\text{-}100)$$

Some typical runs are shown in Appendix C. At first sight it would appear that there is little similarity between the solution to the spherical vectogram model and the solutions to the standard model. However, subject to two restrictions the solutions to the two models show enough similarity to indicate that the model should be of use. The first restriction is that gravity has been ignored, so that as with the zero gravity, fixed velocity model solutions, the trajectories should be considered as being displaced a distance $\frac{1}{2} g(t_f-t)^2$ verti-

cally when viewed in real space. The second restriction is that there is no constraint to stop the player's velocities dropping to unrealistically low values. This is most obvious in Fig. 5 where both players fly out and back along the same line in space, and actually come to rest at one point.

Notwithstanding the above restrictions, the solutions to this spherical vectogram model display to a significant degree some of the general characteristics of the standard solutions. Since in addition this is the only model for which closed-loop control laws could be found and which did display any similarity at all with the standard model, the solution to this spherical vectogram model is used as a basis for formulating near-optimal controls for the standard model.

Finally, it is interesting to note that the above solution not only extends some previous two-dimensional work (Ref 5:1463) into three-dimensions, but also provides equivalent closed-loop controls which were not obtained for the two-dimensional study.

VII. Development of Pseudo Closed-Loop Minimax Controls for the Standard Model

The purpose of this chapter is to derive an approximation to the closed-loop control laws for the standard model based on the solution obtained in Chapter VI to the spherical acceleration vectogram model.

Best Control Approximation

The most successful method the author has found is to solve Eqs (6-95), (6-96), (6-97) and (6-98) at every instant in time. This yields the controls ℓ_1, ℓ_2, ℓ_3, m_1, m_2, m_3 that would be optimal if the dynamics were in fact those of the spherical acceleration vectogram model. Denoting either player's specific excess force as a vector $\bar{F}$, one may think of its component normal to $\bar{V}$ as being equivalent to the specific lift $g\bar{L}/W$. Thus μ is chosen so that

$$\bar{L}\cdot(\bar{F} \times \bar{V}) = 0 \qquad (7\text{-}1)$$

and C_L is chosen so that

$$\left[\frac{\bar{F}\cdot\bar{V}}{V}\right]^2 + \left[\frac{gL}{W}\right]^2 = F^2 \qquad (7\text{-}2)$$

Substituting the values of $\bar{L}$, $\bar{F}$, and $\bar{V}$ into Eq (7-1), gives for the pursuer

$$\begin{aligned}(-\cos\mu_p \sin\gamma_p \cos\chi_p - \sin\mu_p \sin\chi_p)\ (\ell_2 V_{ZP} - \ell_3 V_{YP}) \\ + (-\cos\mu_p \sin\gamma_p \sin\chi_p + \sin\mu_p \cos\chi_p)\ (-\ell_1 V_{ZP} + \ell_3 V_{XP}) \\ + (\cos\mu_p \cos\gamma_p)\ (\ell_1 V_{YP} - \ell_2 V_{XP}) = 0 \qquad (7\text{-}3)\end{aligned}$$

or more simply

$$\tan \mu_P = \Big[(\ell_2 V_{ZP} - \ell_3 V_{YP}) \sin \gamma_P \cos \chi_P + (\ell_3 V_{XP} - \ell_1 V_{ZP}) \sin \gamma_P \sin \chi_P - (\ell_1 V_{YP} - \ell_2 V_{XP}) \cos \gamma_P \Big] \Big/ \Big[(\ell_3 V_{XP} - \ell_1 V_{ZP}) \cos \chi_P - (\ell_2 V_{ZP} - \ell_3 V_{YP}) \sin \chi_P \Big] \tag{7-4}$$

and similarly for the evader

$$\tan \mu_E = \Big[(m_2 V_{ZE} - m_3 V_{YE}) \sin \gamma_E \cos \chi_E + (m_3 V_{XE} - m_1 V_{ZE}) \sin \gamma_E \sin \chi_E - (m_1 V_{YE} - m_2 V_{XE}) \cos \gamma_E \Big] \Big/ \Big[(m_3 V_{XE} - m_1 V_{ZE}) \cos \chi_E - (m_2 V_{ZE} - m_3 V_{YE}) \sin \chi_E \Big] \tag{7-5}$$

If F is chosen so that at any instant

$$F = k_D V^2 C_{L_{max}} \tag{7-6}$$

then Eq (7-2) becomes, for the pursuer,

$$(\ell_1 V_{XP} + \ell_2 V_{YP} + \ell_3 V_{ZP})^2 / V_P^2 + (C_{LP}/C_{LP_{max}})^2 = 1 \tag{7-7}$$

or

$$C_{LP} = \pm C_{LP_{max}} [1 - (\ell_1 V_{XP} + \ell_2 V_{YP} + \ell_3 V_{ZP})^2 / V_P^2]^{\frac{1}{2}} \tag{7-8}$$

Similarly, for the evader,

$$C_{LE} = \pm C_{LE_{max}} [1 - (m_1 V_{XE} + m_2 V_{YE} + m_3 V_{ZE})^2 / V_E^2]^{\frac{1}{2}} \tag{7-9}$$

The signs of C_{LP} and C_{LE} are chosen so as to make $\bar{L}$ act in the same direction along the three axes as $\bar{F}$. Thus for the pursuer's x-component, it is necessary that ℓ_1 and C_{LP} $(-\cos \mu_P \sin \gamma_P \cos \chi_P - \sin \mu_P \sin \chi_P)$ are both positive or both negative. Similarly for the evader's

x-component, it is necessary that m_1 and C_{LE} ($-\cos \mu_E \sin \gamma_E \cos \chi_E - \sin \mu_E \sin \chi_E$) have the same sign.

Using these pseudo controls, the standard dynamics may be integrated forwards a small time Δt. The pseudo controls are then evaluated again and the process repeated until such time as capture occurs or is obviously not going to.

Calcomp plots of four such runs forward in time from the states reached after 10 seconds backward integration of minimax solutions to the standard model are shown in Figs. 9, 16, 23 and 30. The Value of the game for each of these runs should be 10.0 secs. The actual Values obtained were

Run 1	Value = 10.0 secs
Run 2	Value = 6.0 secs
Run 3	Value = 10.0 secs
Run 4	Value = 10.1 secs

Considering Runs 1 and 4 first, the agreement between the approximate forward solutions and the open-loop backward solutions is remarkably good. The two runs are very different in nature and yet in both cases the approximate trajectories follow very closely the open-loop trajectories. Furthermore, the Value for both approximate runs is very close to the standard Value of 10.0 secs. The roots of $(t_f - t)$ evaluated at each instant for the approximate model are generally rather lower than the true time to capture (typically 6 secs instead of 10 secs), so they cannot be used as an instantaneous estimate of the Value of a game. However, the controls based on these roots closely approximate the open-loop controls.

At first sight the results in Run 3 appear as good as those for Runs 1 and 4, but there is one qualification. For all practical purposes, the pursuer may be assumed to capture the evader at 10.0 secs after starting, but he is in fact still 5014 ft from the evader (R = 5000 ft), and starts to move away again after this time of closest approach. This moving away again is first forecast from the solution of Eq (6-95) for (t_f-t). At 9.0 secs after t_0 the smallest positive root of the quartic takes a discontinuous jump from 1.11 secs to 104.20 secs. This corresponds to a change from the quartic having three real positive roots to its having only one. Examination of Eq (6-95) shows that it always has at least one real positive root, but whether or not it has three depends on the sign and magnitude of the coefficients of $(t_f-t)^2$ and (t_f-t).

In Run 2, the general form of the approximate and the open-loop trajectories is the same. However, capture occurs after only 6.0 secs. The reason for this is that at the start of the game in the approximate forward solution, the evader thinks he can escape on the first pass since the value obtained for (t_f-t) is 46.89 secs. The evader thus does not turn quite sharply enough (C_{LE} = 0.70 instead of C_{LE} = 0.75) and so flies into the pursuer. Then at 0.6 secs after t_0, the evader finds that the value of (t_f-t) jumps from 48.04 secs to 6.83 secs, and capture is inevitable.

It should be stressed that the four runs presented and compared above were not chosen so as to show the approximate controls to any particular advantage or disadvantage. The runs were chosen so as to be typical of different types of open-loop solutions, or to show the

effect of velocity variations on the trajectories.

It thus seems that these pseudo optimal controls are a good approximation except where the solution of Eq (6-95) yields only one real positive root. A deeper investigation of this equation and an attempt at a solution of the game of kind for the spherical acceleration vectogram model might yield a better understanding of the precise conditions under which the pseudo control approximation is valid.

Alternative Control Approximations

In an attempt to improve the approximation of the above model, two variations were tried. However, the effect of both variations was found to be generally detrimental.

The first variation tried was to use the values of μ as calculated before, but to use the results of the zero gravity, fixed velocity model in calculating C_L. The lift coefficient was then set to $+C_{L_{max}}$, 0, or $-C_{L_{max}}$. The result of this was to make the trajectories in space for Runs 1 and 4 look slightly better, but change the Values obtained to 10.8 and 8.7 secs respectively. The change in the Values was due to the slower velocities because of the greater induced drag. In Runs 2 and 3 capture failed to occur.

The second variation tried was to modify F_P and F_E so as to give some influence to the differences in potential energy. This was effected by setting

$$F_P = k_{DP} C_{LP_{max}} [V_P^2 - g (z_E - z_P)] \tag{7-10}$$

and

$$F_E = k_{DE} C_{LE_{max}} [V_E^2 + g (z_E - z_P)] \tag{7-11}$$

This is equivalent to basing F on the total energy rather than just the kinetic energy. Using this model the Values obtained for Runs 1 and 4 were 10.0 and 7.6 secs respectively. Again capture failed to occur in Runs 2 and 3.

Suggested Algorithm to Determine a Player's Controls During an Actual Encounter

It seems that the pseudo closed-loop controls developed in Eqs (7-4), (7-5), (7-8) and (7-9) are a good approximation to the optimal closed-loop controls in most circumstances.

The following algorithm, which could be used by the pursuer in an encounter, seems reasonable, but has not yet been tested:

1. Using energy maneuverability considerations fly in such a way as to arrive in the general vicinity of the evader with as large a velocity as possible.
2. Once positioned, set $F_P = k_{DP}\, C_{LP_{max}}\, V_P^2$ and $F_E = k_{DE}\, C_{LE_{max}}\, V_E^2$.
3. Solve Eq (6-95) for the smallest positive root of $(t_f - t)$.
4. Use this value of $(t_f - t)$ in Eqs (6-96), (6-97) and (6-98) to find ℓ_1, ℓ_2, ℓ_3.
5. Evaluate C_{LP} and μ_P using Eqs (7-8) and (7-4).
6. Use these controls for a short time interval, and then return to Step 2 to evaluate new controls.

An algorithm that the evader could use might be:

1. Using energy maneuverability considerations fly in such a way as to avoid for as long as possible arriving in the general vicinity of the pursuer with a velocity disadvantage.

2. As soon as Step 1 fails, or if it becomes obvious that the pursuer has started some form of terminal guidance, set $F_P = k_{DP}\, C_{LP_{max}}\, V_P^2$ and $F_E = k_{DE}\, C_{LE_{max}}\, V_E^2$.
3. Solve Eq (6-95) for the smallest positive root of $(t_f - t)$.
4. Use this value of $(t_f - t)$ in Eqs (6-96), (6-97) and (6-98) to find π_1, π_2, π_3.
5. Evaluate C_{LE} and μ_E using Eqs (7-9) and (7-5).
6. Use these controls for a short time interval, and then return to Step 2 to evaluate new controls.

A knowledge of a solution to the game of kind (Ref 3:8) as well as solutions to the game of degree would also provide both players with valuable information about regions in space that they should avoid or aim for in their preliminary maneuvering. Limitations of both space and time have precluded any investigation of the game of kind as part of this study.

VIII. Conclusions and Recommendations

Conclusions

A realistic two aircraft combat encounter has been posed as a zero sum, perfect information differential game. In analyzing the problem, three models of the aircraft dynamics have been used. These three models were the standard model; the zero gravity, fixed velocity model; and the spherical acceleration vectogram model.

For the standard model, the author obtained open-loop solutions, but was unable to find closed-loop control laws. In order to investigate the nature of the open-loop solutions, a number of them were generated numerically and the trajectories plotted. The controls used in this model were the lift coefficient and the bank angle. The expressions for these controls contained the current values of both the state and costate variables. Examination of a number of numerical solutions showed that the value of each player's lift coefficient would remain at its maximum (either positive or negative) unless a direct tail-chase situation was being approached in which case the coefficient would reduce smoothly and monotonically towards zero. The author was unable to characterize or detect any pattern in the behavior of the bank angle. The only real conclusion formed was that two-dimensional planar assumptions were completely invalid because most trajectories observed showed violent out of plane maneuvers.

For the zero gravity, fixed velocity model, the author again obtained open-loop solutions. As with the standard model, closed-loop control laws could not be found; but in this case it was possible to eliminate the costate variables from the solutions and express the

controls as functions of the current and terminal values of the state variables alone. This provides a considerable simplification in the solution of the two point boundary value problem. Open-loop solutions for this model were generated numerically and plotted for comparison with the standard model. Subject to the limitations of the vertical displacement in space because of the absence of gravity, and the sensitivity of solutions produced by backward integration to initial small disturbances, the solutions to this model showed good agreement with those obtained for the standard model.

For the spherical acceleration vectogram model, the author was able to obtain closed-loop control laws. The controls used in this model were, however, no longer the lift coefficient and the bank angle, but the direction cosines of a specific excess thrust instead. For purposes of comparison with the standard model, a number of open-loop solutions for this model were generated numerically and the trajectories plotted. The solutions were subject to the same limitations as were those for the zero gravity, fixed velocity model, and in addition had the more serious limitation that the aircraft velocities could drop to unrealistically low values. This meant that impossibly sharp turns could be executed. Notwithstanding these limitations, this model is the closest dynamic representation for which closed-loop solutions have been found. Further, the solutions show sufficient similarity to the standard model solutions to indicate that the model should be of considerable value in formulating approximate closed-loop controls for the standard model.

Finally, approximate closed-loop controls for the standard model were produced from the spherical acceleration vectogram model solution.

A number of methods of finding equivalent controls were tried, and each method was tested by integrating the standard dynamics forward in time using these approximate controls. The integrations were started from the states reached by backward integration of open-loop solutions to the standard model. Thus the accuracy of the approximation could be determined from the closeness with which the pseudo optimal trajectories followed the true optimal trajectories. The most effective of the approximations gave good agreement under almost all the conditions tested. However, it is felt that caution should be exercised when considering problems where there is a large altitude difference between the players, since the model makes no allowance for potential energy advantages. Apart from this restriction, the author feels that the approximate controls given in Chapter VII could form the basis for some very good approximations to optimal controls for use in dogfight situations.

Recommendations

The author's main recommendation is that the study of this problem should continue. This thesis has laid the groundwork for obtaining practical approximate solutions to the three-dimensional pursuit-evasion problem, and has shown that such solutions do exist.

The author feels that two further approaches to the problem should be tried. These are:

1. The use of a hybrid computer to investigate the possibility of rapidly obtaining open-loop solutions to either the standard or the zero gravity, fixed velocity model. If these solutions could be obtained rapidly enough, then con-

tinuously updated (or equivalent closed-loop) solutions might be practicable.

2. An investigation of the game of kind for the spherical vectogram model, with particular attention to the number and form of solutions obtained from Eq (6-95).

Bibliography

1. Bryson, A.E. and Y.C. Ho. Applied Optimal Control. Waltham, Massachusetts: Blaisdell Publishing Company, 1969.

2. Calcomp Manual. Three-D, A Perspective Drawing Software System. Anaheim: California Computer Products, Inc. 1968.

3. Isaacs, R. Differential Games. New York: John Wiley and Sons, Inc., 1965.

4. Othling, W.L. Application of Differential Game Theory to Pursuit-Evasion Problems of Two Aircraft. Doctoral Dissertation, DS/MC/67-1 Wright-Patterson Air Force Base, Ohio: Air Force Institute of Technology.

5. Wong, R.E. "Some Aerospace Differential Games." Journal of Spacecraft and Rockets. Volume 4: Number 11:1460 (November 1967).

Appendix A

The Use of One Player Optimization Techniques in Certain Differential Games

In both Chapters IV and V use was made of the fact that that part of the Hamiltonian containing only the pursuer's (evader's) state variables and controls remains constant. The circumstances under which this is true and a proof of the theorem are given in this appendix.

One of the difficulties in obtaining solutions to realistic differential games is in integrating the costate differential equations. Hence, it is felt that the theorem given below may be of great use in that it avoids the need for integration of at least one of the costate equations.

Theorem

Consider a zero-sum perfect information differential game with a payoff of time to capture, or a function of the states at termination, or a combination of both. If the state equations can be written so that the pursuer's (evader's) state variables are independent of both the evader's (pursuer's) state variables and controls; time does not appear explicitly in the Hamiltonian; and all the control constraints are time invariant, then for solutions in the small that part of the Hamiltonian that consists of the terms containing only the pursuer's (evader's) state and costate variables, and the pursuer's (evader's) controls remains constant along minimax trajectories.

Proof

If the pursuer's evader's state equations are independent, it is possible to express the dynamics of a differential game as

$$\dot{\bar{x}}_p = \bar{f}_p\ (\bar{x}_p, \bar{u}, t) \tag{A-1}$$

$$\dot{\bar{x}}_E = \bar{f}_E\ (\bar{x}_E, \bar{v}, t) \tag{A-2}$$

The theorem is restricted to payoffs of the form

$$J = \phi\ (\bar{x}(t_f), t_f) + \int_{t_0}^{t_f} C\ dt \tag{A-3}$$

where C is constant.

The Hamiltonian is then

$$H = \bar{\lambda}^T \bar{f} + C = \bar{\lambda}_p^T \bar{f} + \bar{\lambda}_E^T \bar{f} + C \tag{A-4}$$

Denote that part of the Hamiltonian that consists of the terms containing only the pursuer's state and costate variables and the pursuer's controls as H_p. Then

$$H_p = \bar{\lambda}_p^T \bar{f}_p = \bar{f}_p^T \bar{\lambda}_p \tag{A-5}$$

and

$$\frac{dH_p}{dt} = \frac{\partial H_p{}^T}{\partial \bar{\lambda}_p} \cdot \frac{d\bar{\lambda}_p}{dt} + \frac{\partial H_p}{\partial \bar{x}_p} \cdot \frac{d\bar{x}_p}{dt} + \frac{\partial H_p}{\partial \bar{u}} \cdot \frac{d\bar{u}}{dt} + \frac{\partial H_p}{\partial t} \cdot \frac{dt}{dt} \tag{A-6}$$

Now if t does not appear explicitly in H, it cannot appear explicitly in H_p, so

$$\frac{\partial H_p}{\partial t} = 0 \tag{A-7}$$

Since the Hamiltonian is being evaluated along a minimax trajectory described in the small, either the ith component of the control vector

is internal, in which case

$$\frac{\partial H}{\partial u_i} = \frac{\partial H_p}{\partial u_i} = 0 \tag{A-8}$$

or the control is on the limit, which is time invariant, and so

$$\frac{du_i}{dt} = 0 \tag{A-9}$$

Using Eqs (A-8), (A-9) on each component of the control vector gives

$$\frac{\partial H_p^T}{\partial \bar{u}} \cdot \frac{d\bar{u}}{dt} = 0 \tag{A-10}$$

Now the necessary conditions give

$$\begin{bmatrix} \dot{\bar{\lambda}}_p \\ \dot{\bar{\lambda}}_E \end{bmatrix} = \dot{\bar{\lambda}} = - H_{\bar{x}} = - \begin{bmatrix} \frac{\partial H_p}{\partial \bar{x}_p} \\ \frac{\partial H_E}{\partial \bar{x}_E} \end{bmatrix} \tag{A-11}$$

Substitution of Eqs (A-7), (A-10) and (A-11) into Eq (A-6) gives

$$\frac{dH_p}{dt} = - \frac{\partial H_p^T}{\partial \bar{\lambda}} \cdot \frac{\partial H_p}{\partial \bar{x}_p} + \frac{\partial H_p^T}{\partial \bar{x}_p} \cdot \frac{d\bar{x}_p}{dt}$$

$$= - \bar{f}_p^T \cdot \frac{\partial H_p}{\partial \bar{x}_p} + \frac{\partial H_p^T}{\partial \bar{x}_p} \cdot \bar{f}_p = 0 \tag{A-12}$$

and so

$$H_p = \text{constant} \tag{A-13}$$

An exactly similar argument may be used to show that

$$H_E = \text{constant} \tag{A-14}$$

It has thus been shown that along a minimax trajectory, and subject to the restrictions specified in the theorem, H_p and H_p remain constant.

Appendix B

Some Unsuccessful Approximations to Closed-Loop Minimax Controls for the Standard Model

There are two basic approaches which may be taken in attempting to find approximate closed-loop controls for a differential game which would otherwise be insoluble. The first and most usual of these methods is that of using an approximate model of the true dynamics, and solving the differential game based on this model. This was done in the main body of this report. The other method has the possibility of a truer representation but is less certain of success, and is highly dependent on intuition and luck. This method consists of somehow formulating a proposed control law and then comparing it with numerically evaluated open-loop solutions of the standard model.

In his study of possible approaches to the solution of the standard model, the author tried a number of these artifically generated control laws. Although some of them could be fitted closely to any one trajectory, any significant change in the terminal conditions meant the fit could no longer be considered satisfactory. All but two of the artificial control laws tried were generated by constructing a polynomial from terms that it would appear to be reasonable for the particular control being investigated to depend on. The constants in the polynomial were generated using a least squares fit to a particular open-loop solution. This approximate closed-loop control was then compared with the controls generated by other open-loop solutions. The reason for using a polynomial was that in the absence of any definite reason for using other functions, it was the most convenient form to use in a least squares fit, and most of the common trigonometric and

exponential functions can be approximated by sufficient terms of a polynomial.

One of the exceptions to the above method of formulating trial controls was an analytically derived control law based on the principle that the pursuer (evader) would want to use those controls that would tend at every instant to minimize (maximize) the rate of change of the distance between the two players. The other exception was to consider that at each instant in time the game was about to terminate, and evaluate the controls as though on a terminal surface.

Before listing the trial controls that the author tried, it is convenient to define the following variables:

$\hat{k}$ is a unit vector in the z-direction

$\bar{r}$ is the radius vector from P to E

r is the magnitude of $\bar{r}$

$\dot{r}$ is the rate of change of r

$\bar{V}_P$ is the pursuer's velocity vector

$\bar{V}_{rel}$ is the velocity of E relative to P

$\bar{r}_n$ is the component of $\bar{r}$ normal to $\bar{V}_P$

$\bar{V}_n$ is the component of $\bar{V}_{rel}$ normal to $\bar{V}_P$

g_0 is a reference gravitational acceleration.

Since C_L and μ are both non-dimensional, it seemed logical to non-dimensionalize those terms being used in the various polynomial fits.

The polynomials that were tried in an attempt to synthesize C_{LP} were fitted to $\bar{C}_{LP}$ rather than C_{LP}*. The trial polynomials were

1. $$C_{LP} = \left[A_1 + A_2 \left|\frac{\bar{r}_n}{r}\right| + A_3 \left(\frac{z_E - z_P}{r}\right) + A_4 \left|\frac{\bar{V}_n}{r}\right| \right] \text{sgn } (z_E - z_P) \qquad \text{(B-1)}$$

$$2.\quad C_{LP} = A_1 \frac{g}{g_0 \cos \gamma_p} + \left[A_2 \frac{|\bar{r}_n|}{r} + A_3 \frac{|\bar{V}_n|}{r} \right] \operatorname{sgn} (z_E - z_p) \tag{B-2}$$

$$3.\quad C_{LP} = A_1 \frac{g}{g_0 \cos \gamma_p} + \left[A_2 \frac{|\bar{r}_n|}{r} + A_3 \frac{\bar{r}_n \cdot \bar{V}_n}{r V_p} + A_4 \frac{|\bar{V}_n \times \bar{r}_n|}{r V_p} \right] \operatorname{sgn} (z_E - z_p - r \sin \gamma_p) \tag{B-3}$$

$$4.\quad |C_{LP}| = A_1 \frac{|\bar{r}_n|}{r} + A_2 \frac{\bar{r}_n \cdot \bar{V}_n}{r V_p} + A_3 \frac{|\bar{V}_n \times \bar{r}_n|}{r V_p} \tag{B-4}$$

$$5.\quad |C_{LP}| = A_1 \frac{|\bar{r}_n|}{R} + A_2 \frac{\bar{r}_n \cdot \bar{V}_n}{R V_p} + A_3 \frac{|\bar{V}_n \times \bar{r}_n|}{R V_p} \tag{B-5}$$

where the A_i are arbitrary constants. The fit to the magnitude of C_{LP} could be kept within about 10% with all of the above provided the terminal conditions were not varied too much. The greatest difficulty encountered was in trying to match the switching function which determines the sign of C_{LP}. None of the switching functions used in the above controls was even close to determining the correct sign on C_{LP}.

The polynomials that were used in a trial fit for μ_p were

$$1.\quad \mu_p = A_1 \tan^{-1} \left[\frac{y_E}{x_E} \right] + A_2 \tan^{-1} \left[\frac{y_p}{x_p} \right] + A_3 \chi_E + A_4 \chi_F \tag{B-6}$$

$$2.\quad \mu_p = A_1 \sin^{-1} \left[\frac{\bar{r}_n \cdot (\hat{k} \times \bar{V}_p)}{V_p |\bar{r}_n|} \right] + A_2 (\chi_E - \chi_p) \tag{B-7}$$

$$3.\quad \tan \mu_p = A_1 \frac{y_E}{x_E \cos \gamma_p} + A_2 \frac{y_p}{x_p \cos \gamma_p} + A_3 \tan (\chi_E - \chi_p) \tag{B-8}$$

$$4.\quad \tan \mu_p = A_1 f_1 + A_2 f_2 + A_3 f_1 f_2 + A_4 f_1^3 + A_5 f_2^3 \tag{B-9}$$

$$\text{where } f_1 = \sqrt{(x_E-x_P)^2 + (y_E-y_P)^2}\ \text{sgn}\left[\tan^{-1}\left|\frac{y_E}{x_E}\right| - \chi_P\right] \Big/ (z_E-z_P)\cos\gamma_P \tag{B-10}$$

$$f_2 = \sqrt{(V_{XE}-V_{XP})^2 + (V_{YE}-V_{YP})^2}\ \text{sgn}\,[\chi_E-\chi_P] / (V_{ZE}-V_{ZP})\cos\gamma_P \tag{B-11}$$

None of the above expressions for μ_p even approximated the correct values on trajectories other than those used in evaluating the A_i.

In evaluating the controls that minimize (maximize) $\dot{r}$ at any instant it should be noted that

$$\dot{r} = (\bar{V}_E\cdot\bar{r} - \bar{V}_P\cdot\bar{r})/r \tag{B-12}$$

does not explicitly contain the controls. However, the controls appear explicitly in $\ddot{r}$. Thus to minimize the value of $\dot{r}$ an instant later the pursuer must minimize $\ddot{r}$. Using the standard model dynamics, and setting

$$\frac{\partial\ddot{r}}{\partial\mu_p} = 0, \quad \frac{\partial^2\ddot{r}}{\partial\mu_p^2} \geq 0$$

$$\frac{\partial\ddot{r}}{\partial C_{LP}} = 0, \quad \frac{\partial^2\ddot{r}}{\partial C_{LP}^2} \geq 0$$

gives

$$\tan \mu_p = [(x_E-x_p) \sin \chi_p - (y_E-y_p) \cos \chi_p]/$$
$$[(x_E-x_p) \sin \gamma_p \cos \chi_p + (y_E-y_p) \sin \gamma_p \sin \chi_p$$
$$- (z_E-z_p) \cos \gamma_p] \qquad \text{(B-13)}$$

and

$$\bar{C}_{LP} = - [(x_E-x_p)(\cos \mu_p \sin \gamma_p \cos \chi_p + \sin \mu_p \sin \chi_p)$$
$$+ (y_E-y_p)(\cos \mu_p \sin \gamma_p \sin \chi_p - \sin \mu_p \cos \chi_p)$$
$$- (z_E-z_p) \cos \mu_p \cos \gamma_p]/$$

$$2k_{IP}[(x_E-x_p) \cos \gamma_p \cos \chi_p + (y_E-y_p) \cos \gamma_p \sin \chi_p$$
$$+ (z_E-z_p) \sin \gamma_p] \qquad \text{(B-14)}$$

Similar expressions may be obtained for the evader's controls.

The above expressions were evaluated at a number of points on the open-loop minimax trajectories for the standard model and compared with the open-loop controls. This comparison showed that the above expressions and the actual controls bore little or no resemblance to each other. An error in the value of μ_p of 120° was not unusual and neither the sign nor the magnitude of C_{LP} were in agreement.

The method of considering each instant in time as corresponding to termination meant that by continuously updating the transversality conditions the controls could be evaluated. Agreement with the open-loop minimax controls was no better than using the method of minimizing $\dot{r}$. The two methods are in fact probably equivalent to each other.

Appendix C

Plots of Some Typical Minimax Trajectories

This appendix contains plots of the minimax trajectories for all three models integrated backwards in time for 10 seconds starting from four different terminal states. The plots are shown with the trajectories in both real and relative space. Additionally there are four plots forward in time in real space obtained using the pseudo controls developed in Chapter VII with the standard dynamics. These last four trajectories were obtained using as starting values of the state variables values obtained at the end of 10 seconds backward integration of the standard model.

The plots were obtained using the Three-D Calcomp routine (Ref 2:1 et seq). The values of the terminal parameters used for the four different runs were chosen to be typical of different classes of solutions to the standard model, and not so as to show any of the models to particular advantage or disadvantage.

For the plots in real space, the origin of the axes is at the point where the pursuer is located at termination. In order to give a better feel for the orientation of the trajectories in space, a ground track is plotted as well as the actual trajectory, and vertical shading is provided between the two. The vertical shading lines are given at intervals of 0.4 seconds. The Calcomp routine rescales the axes for each plot; so, in order to give an idea of this scale, each axis is drawn between the maximum and minimum values of that coordinate used in the trajectories. These maximum and minimum values are shown at the top of each plot, where the numbers correspond to feet in actual

space.

The plots in relative space show the path of the evader relative to the pursuer. The position of the pursuer at every instant is taken as the origin of the axes. The other details of these relative space plots are the same as for the plots in real space.

In order to simplify comparisons between the models for a particular set of terminal parameters, the plots are grouped according to parameters used, or "Run", and not according to model.

The aircraft performance parameters used in obtaining the plots are

$$k_{TP} = k_{TE} = 13.416 \tag{C-1}$$

$$k_{DP} = k_{DE} = 0.0002 \tag{C-2}$$

$$k_{OP} = k_{OE} = 0.04 \tag{C-3}$$

$$k_{IP} = k_{IE} = 0.2 \tag{C-4}$$

STANDARD MODEL-REAL SPACE

S1 1200.0 YMX 5100.0 VMX 300.0 TMX 300.0
S2 0.001 YMN -10500.0 VMN 0.0 TMN -6000.0
S3 0.001
S4 0.001
S5 1100.0
S6 -0.001
S7 -0.001

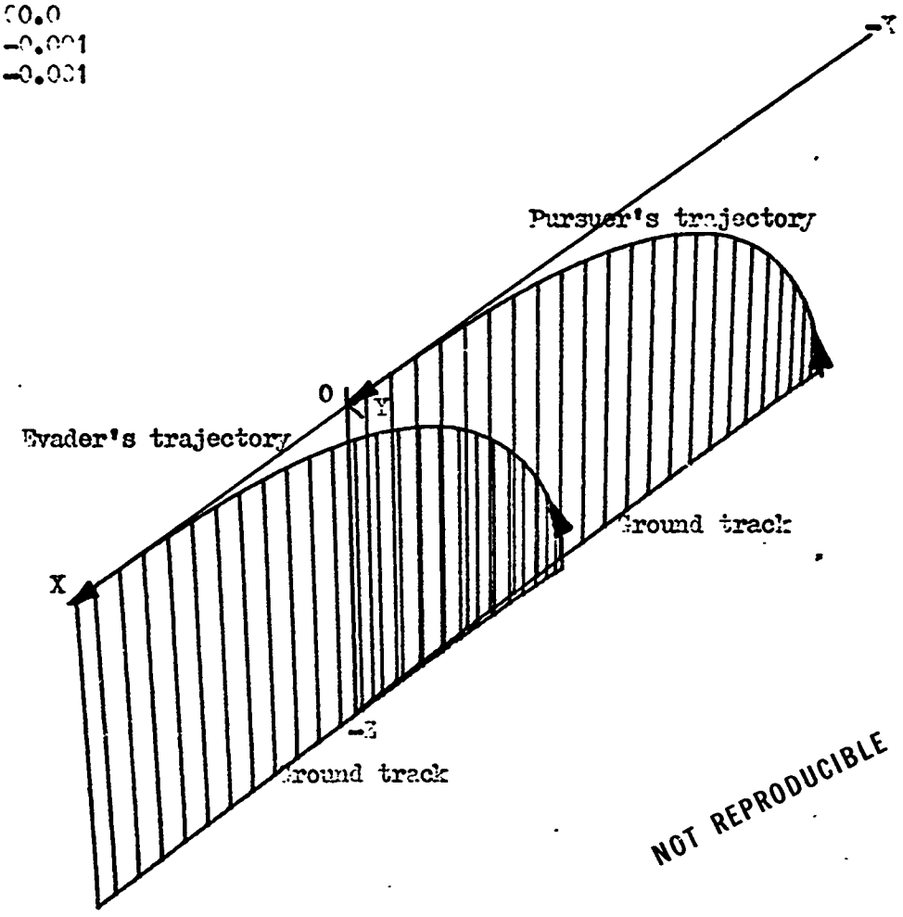

Figure 3. Standard Model, Real Space, Run 1

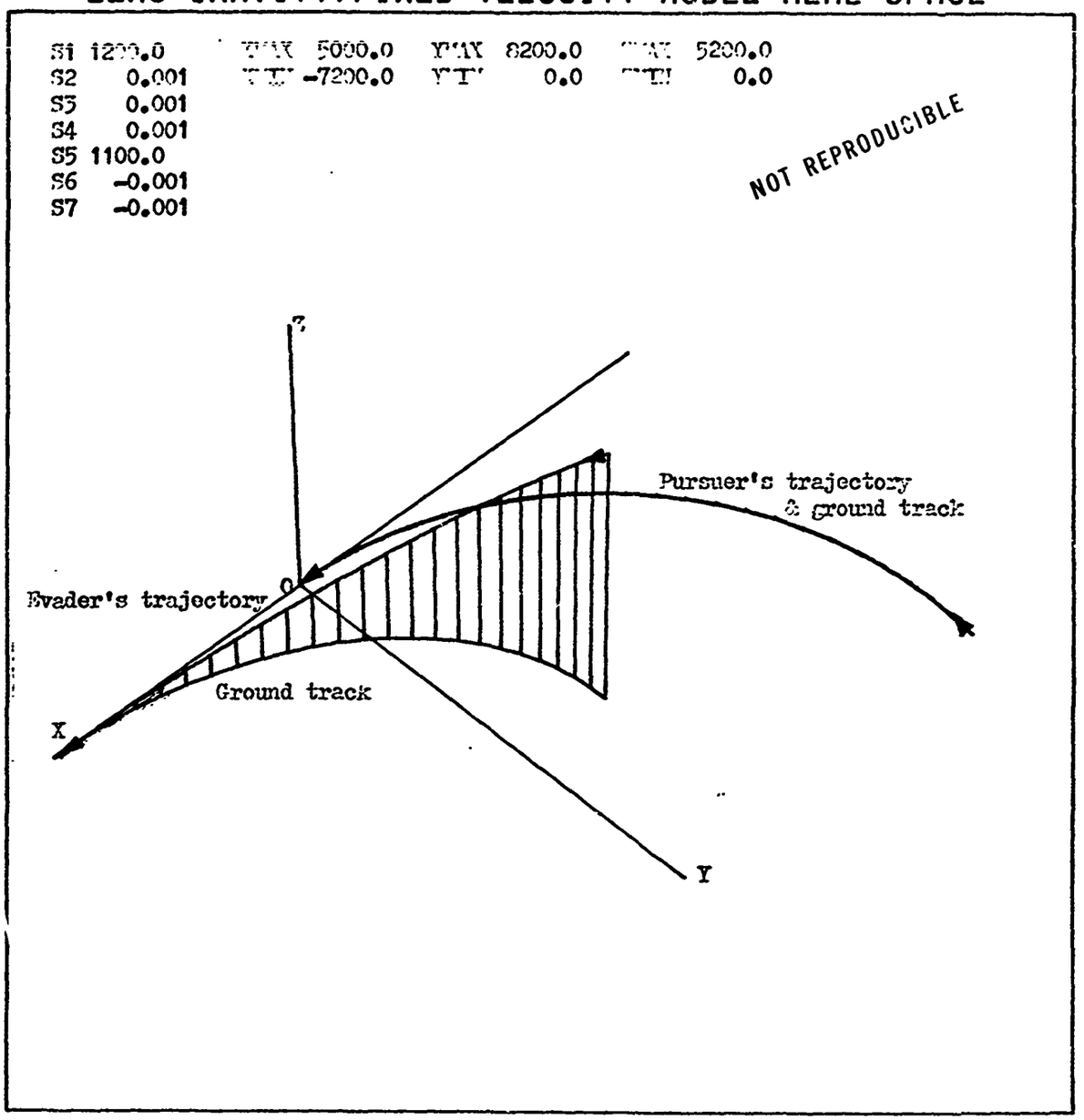

Figure 4. Zero Gravity, Fixed Velocity Model, Real Space, Run 1

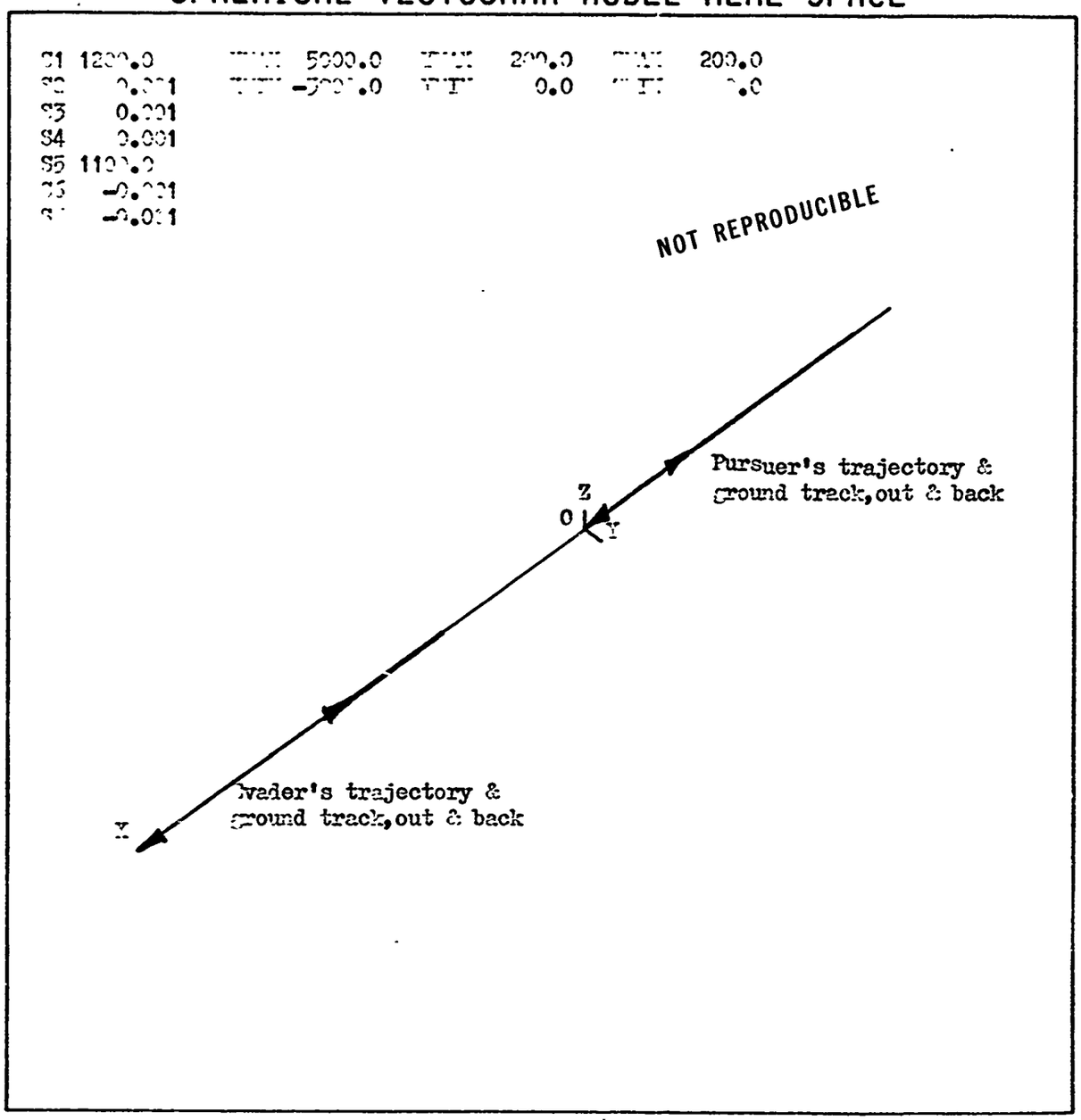

Figure 5. Spherical Vectogram Model, Real Space, Run 1

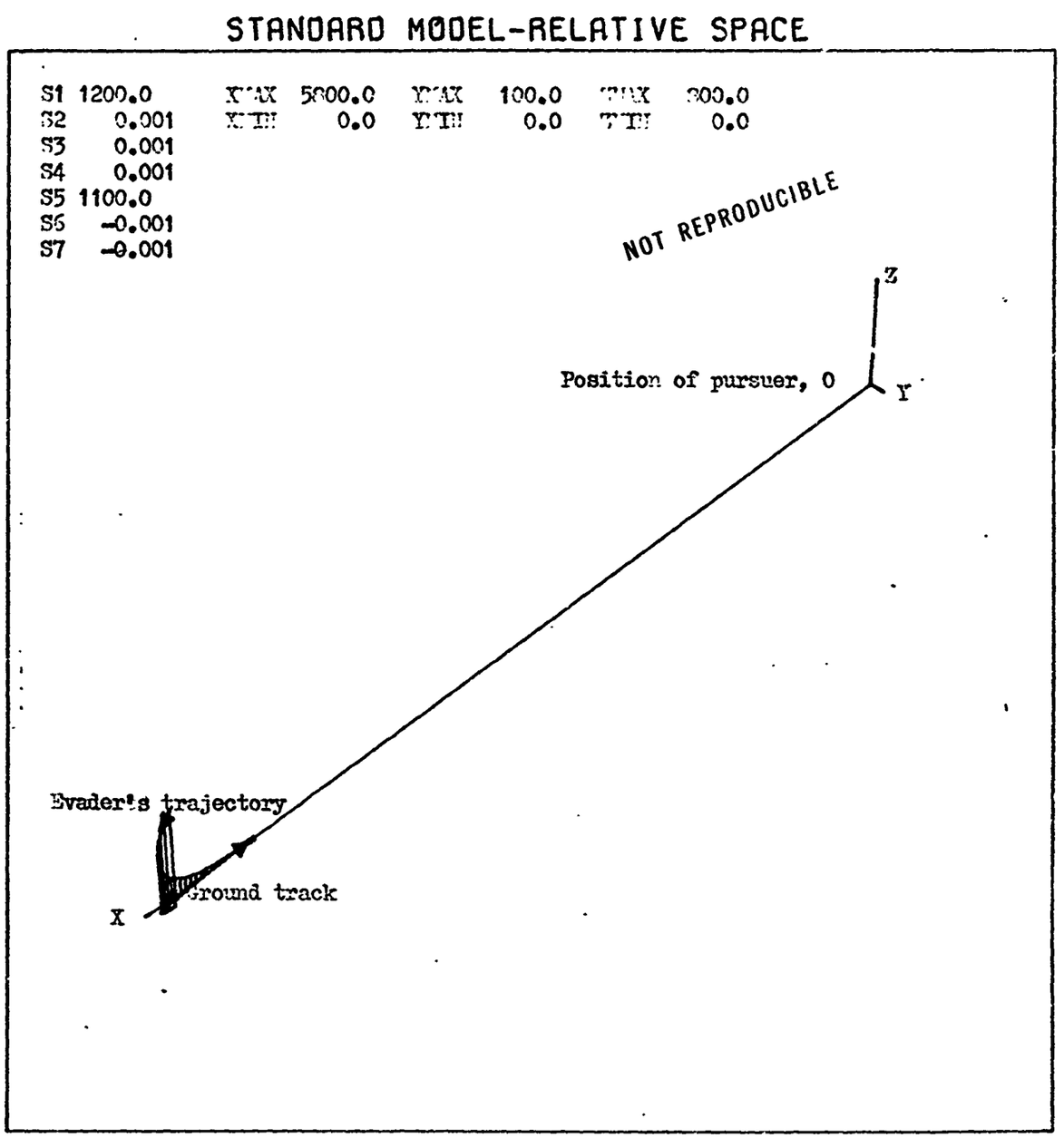

Figure 6. Standard Model, Relative Space, Run 1

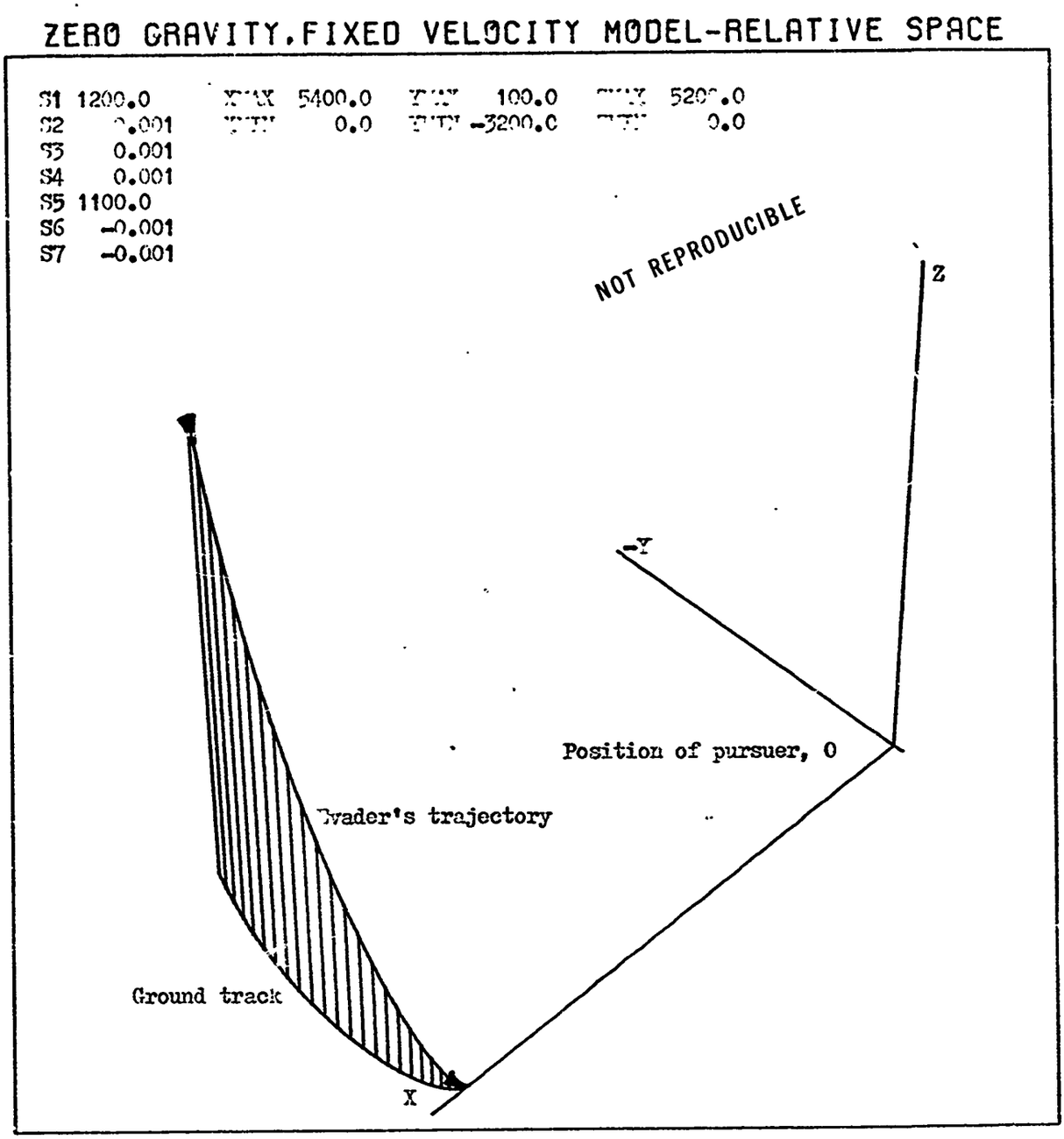

Figure 7. Zero Gravity, Fixed Velocity Model, Relative Space, Run 1

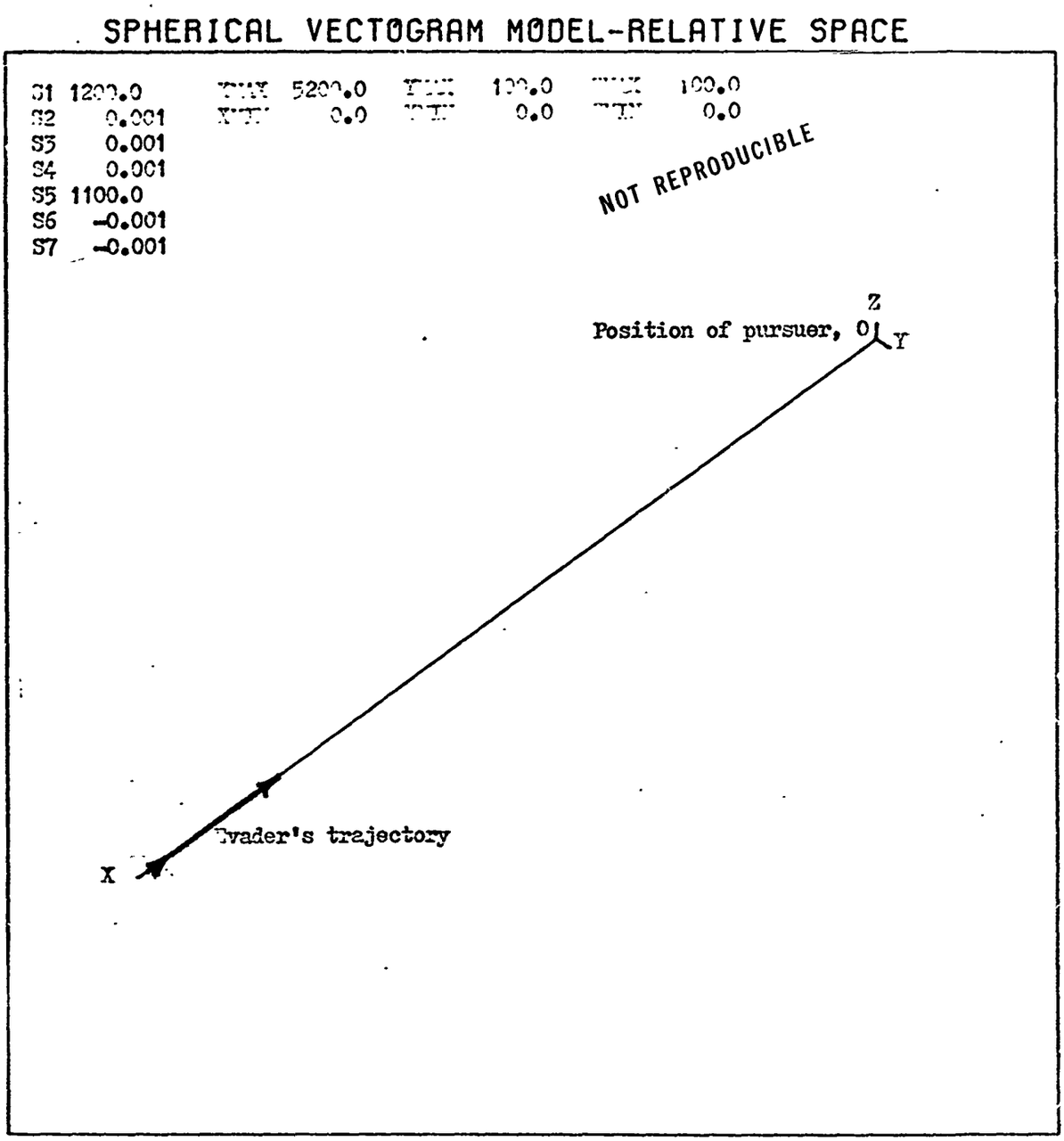

Figure 8. Spherical Vectogram Model, Relative Space, Run 1

STANDARD DYNAMICS, SYNTHESIZED CONTROLS-REAL SPACE

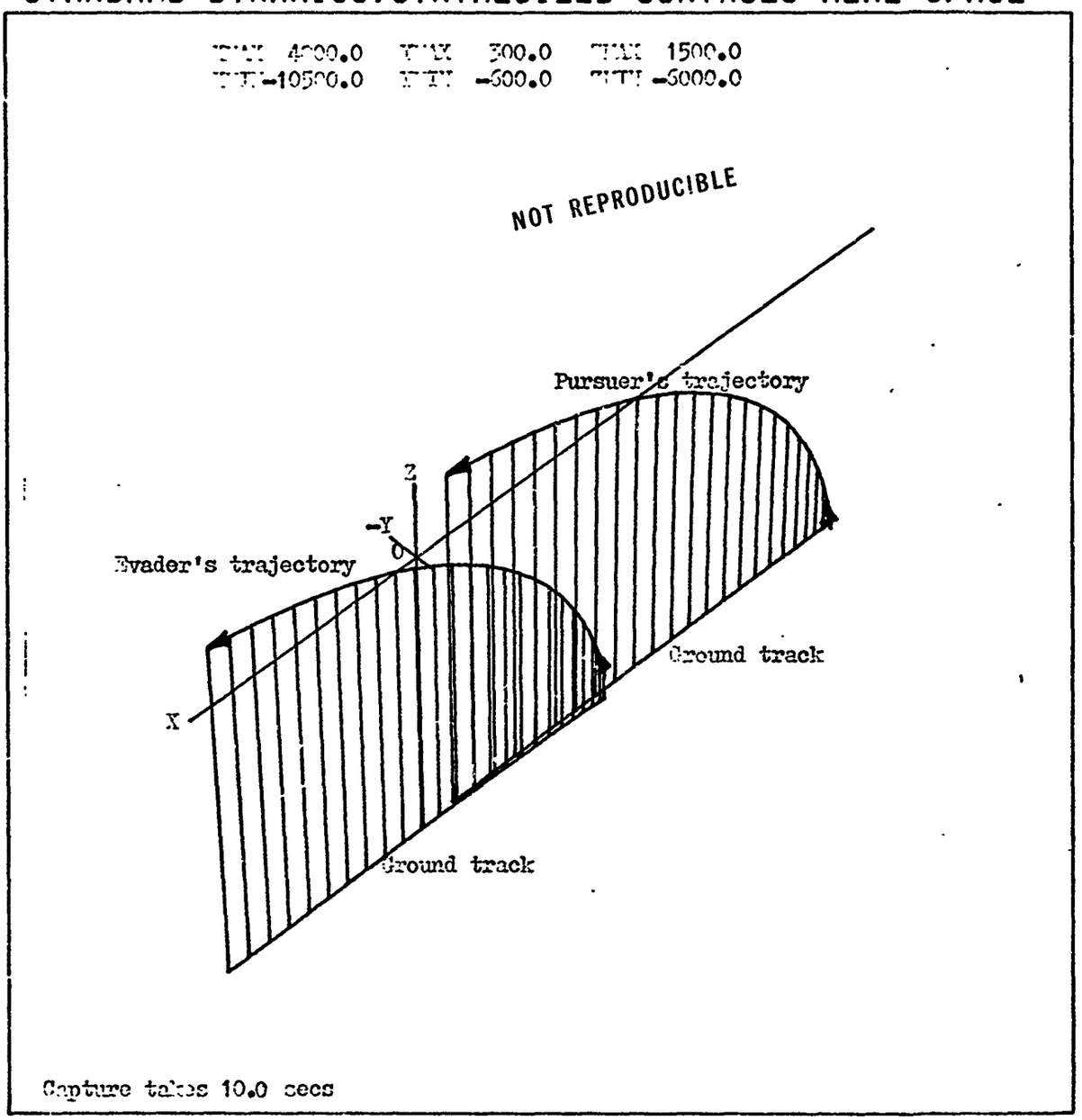

Figure 9. Pseudo Controls with Standard Dynamics, Real Space, Run 1

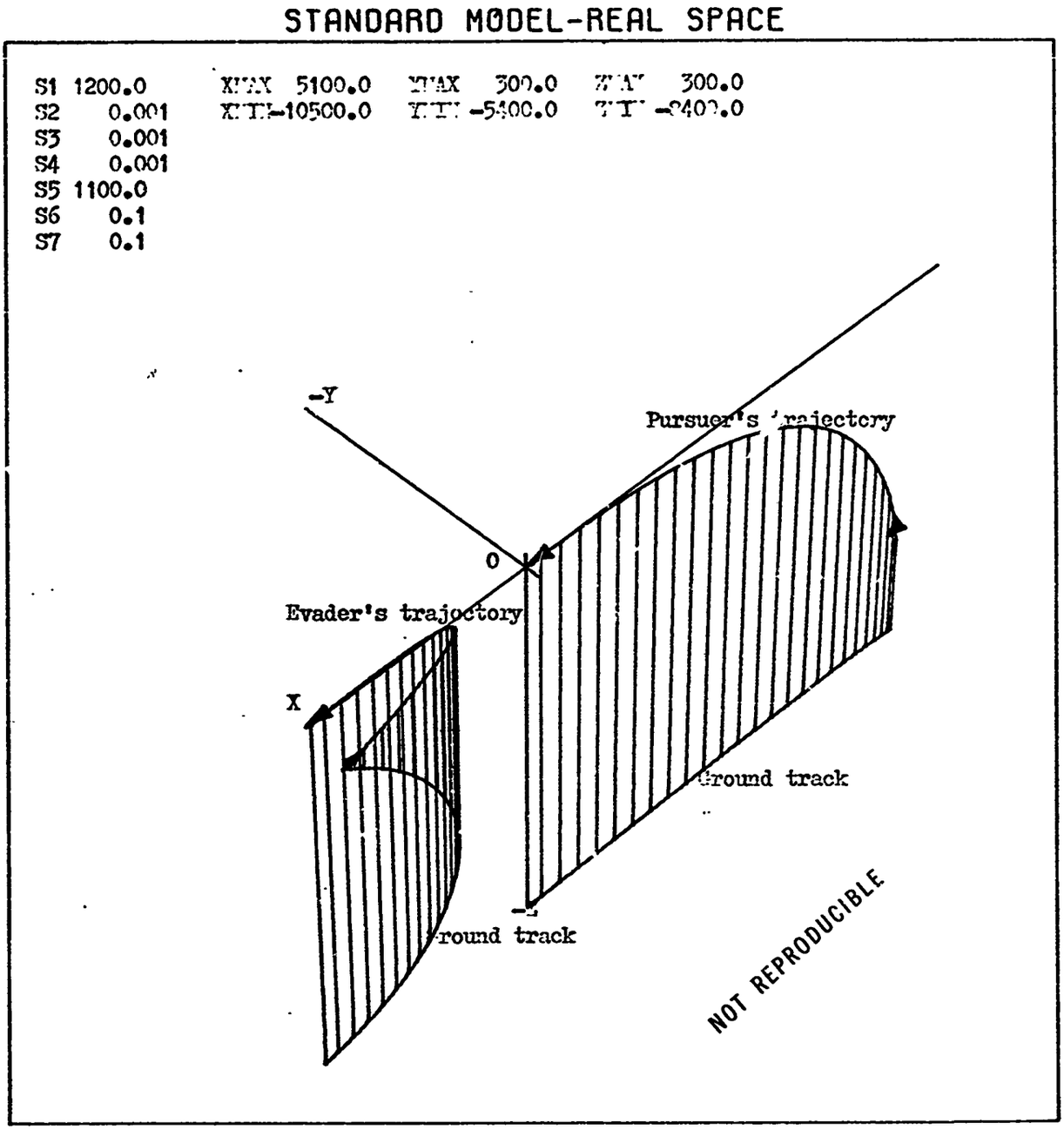

Figure 10. Standard Model, Real Space, Run 2

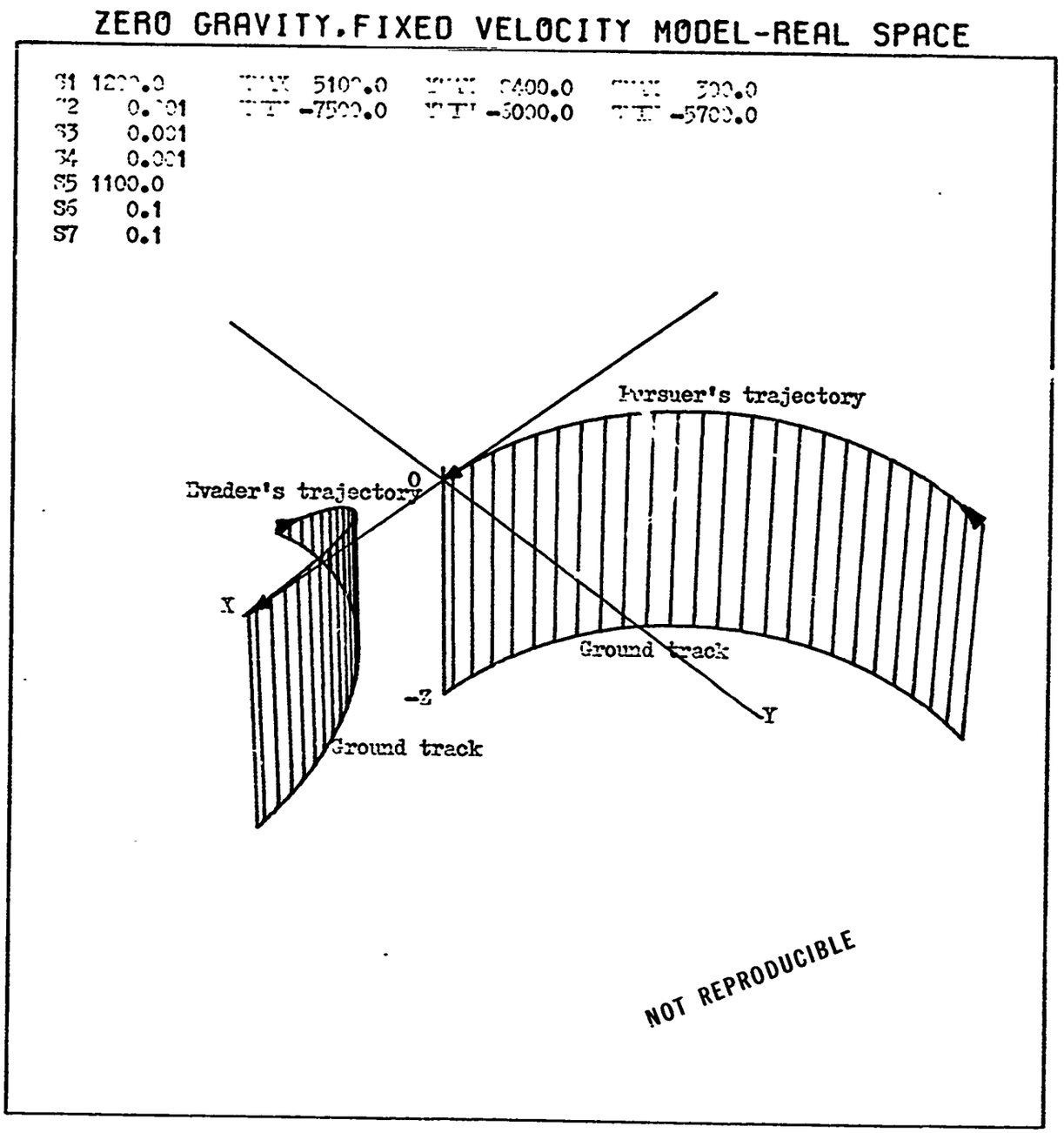

Figure 11. Zero Gravity, Fixed Velocity Model, Real Space, Run 2

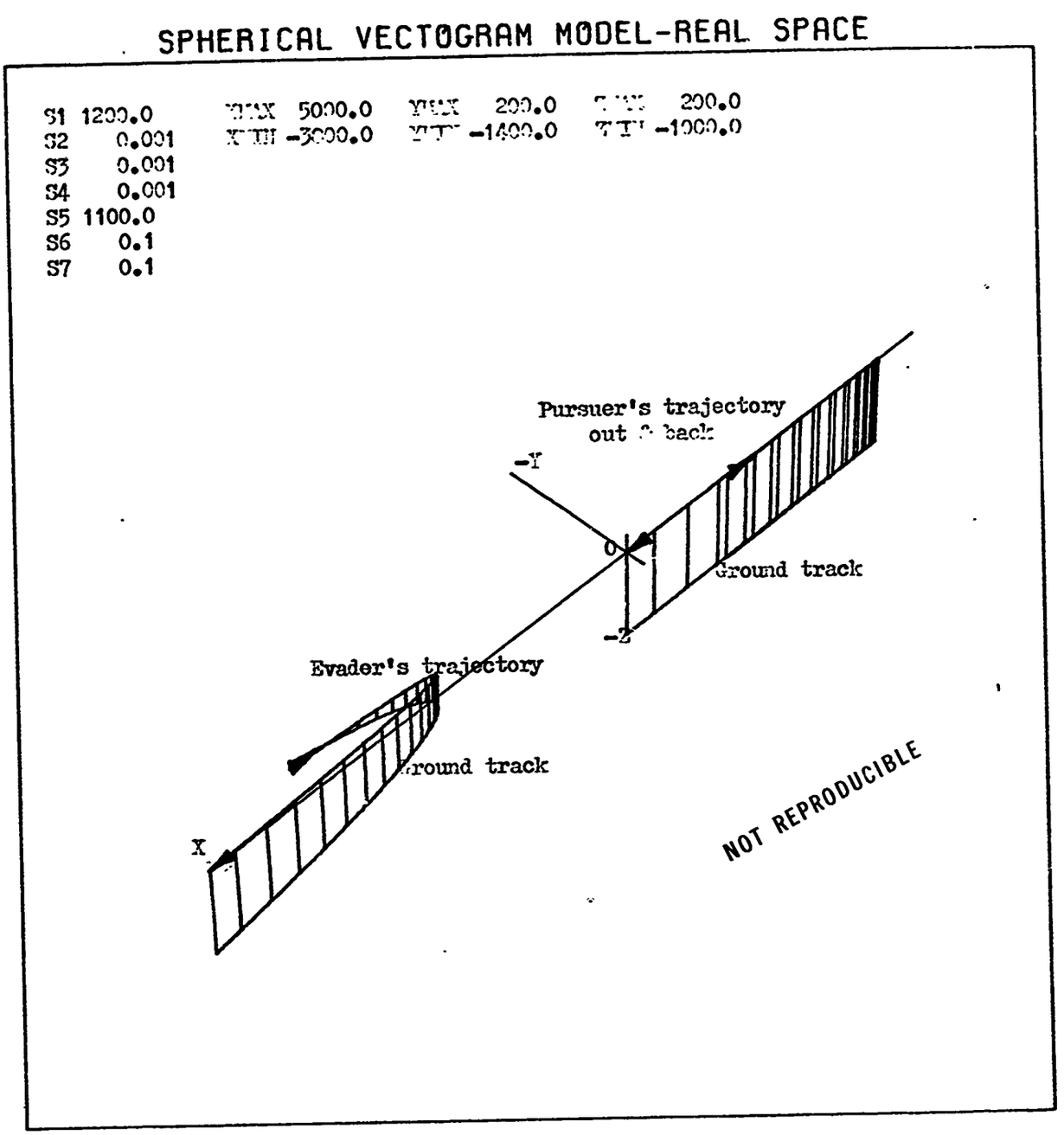

Figure 12. Spherical Vectogram Model, Real Space, Run 2

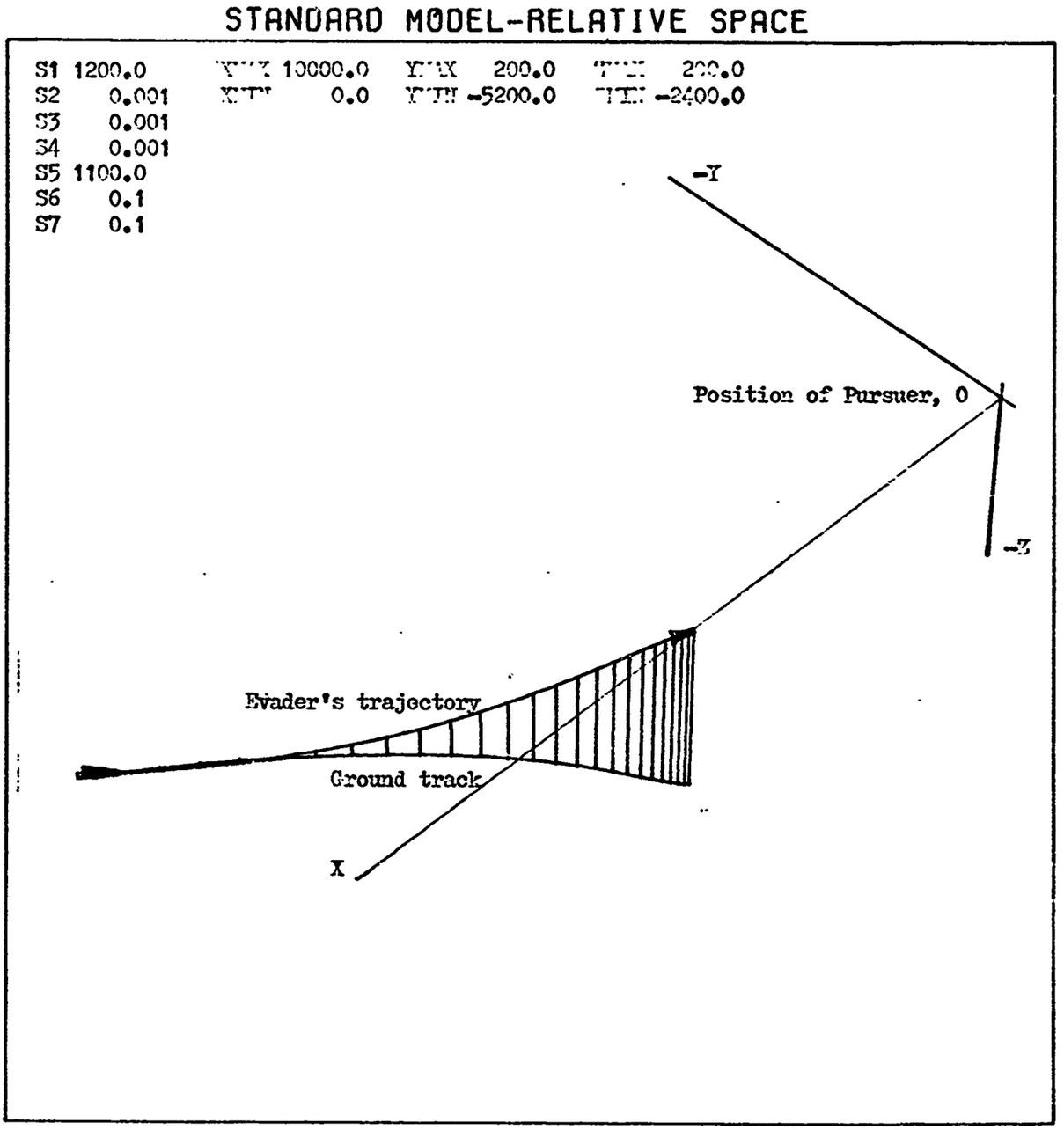

Figure 13. Standard Model, Relative Space, Run 2

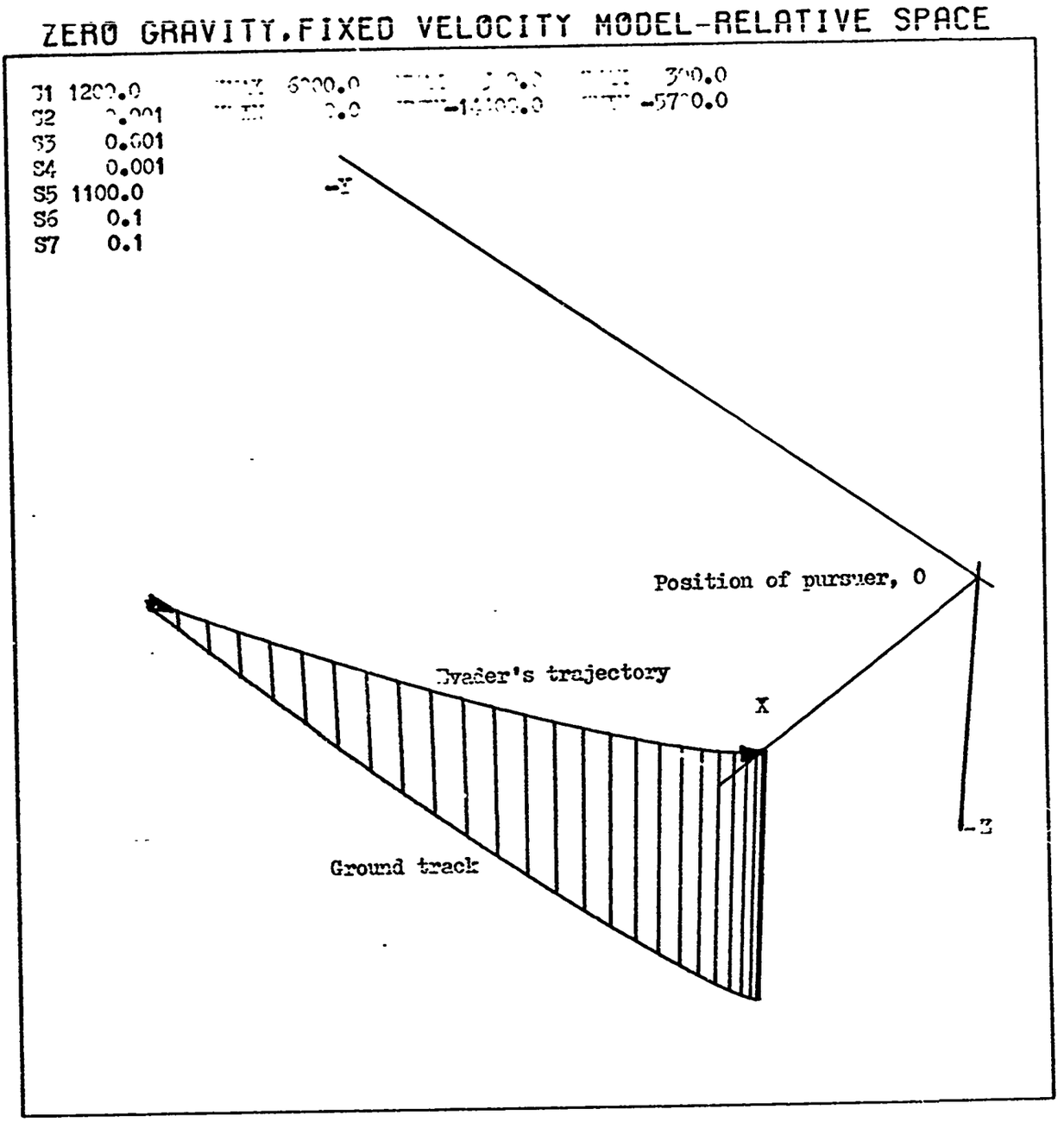

Figure 14. Zero Gravity, Fixed Velocity Model, Relative Space, Run 2

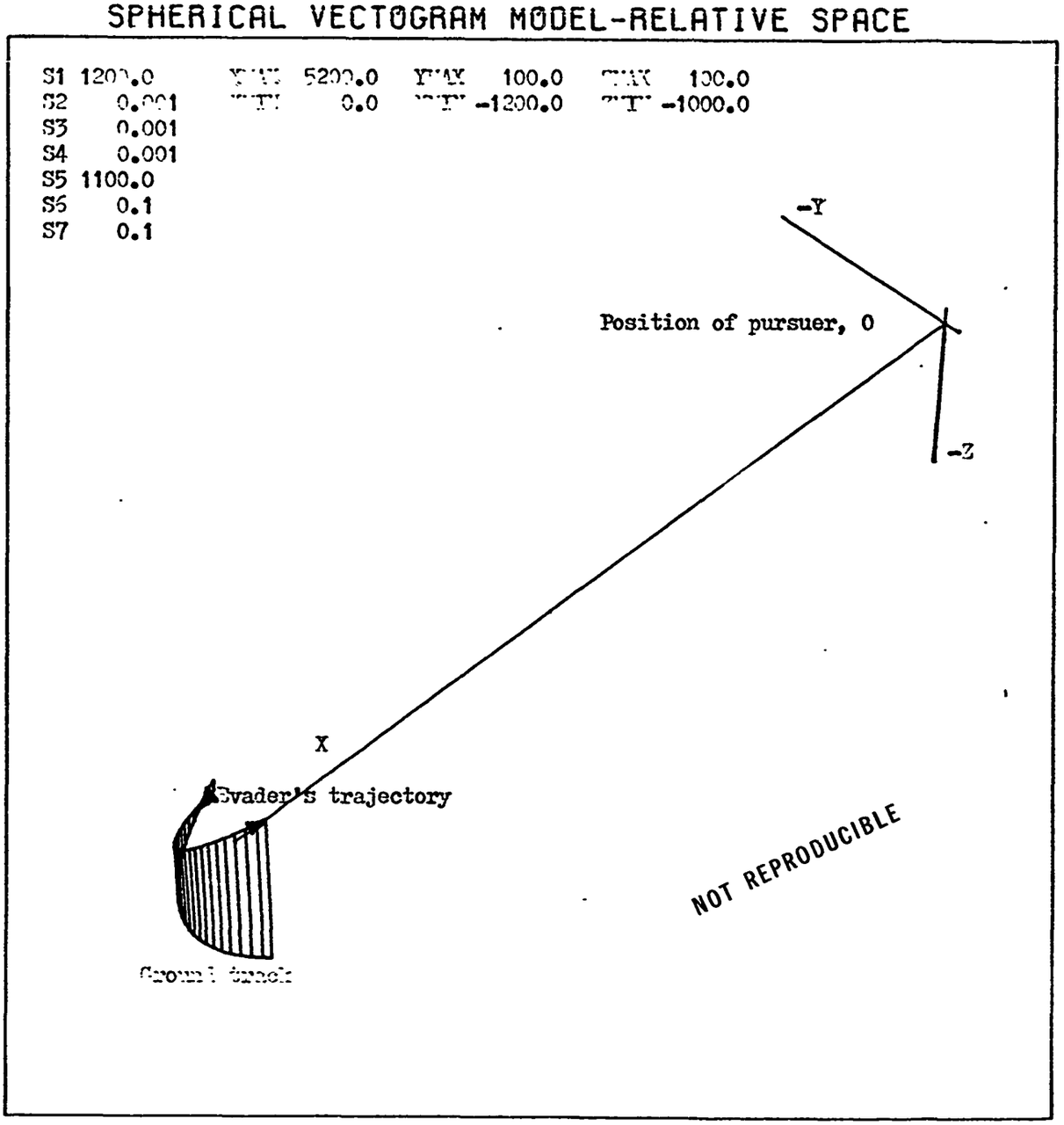

Figure 15. Spherical Vectogram Model, Relative Space, Run 2

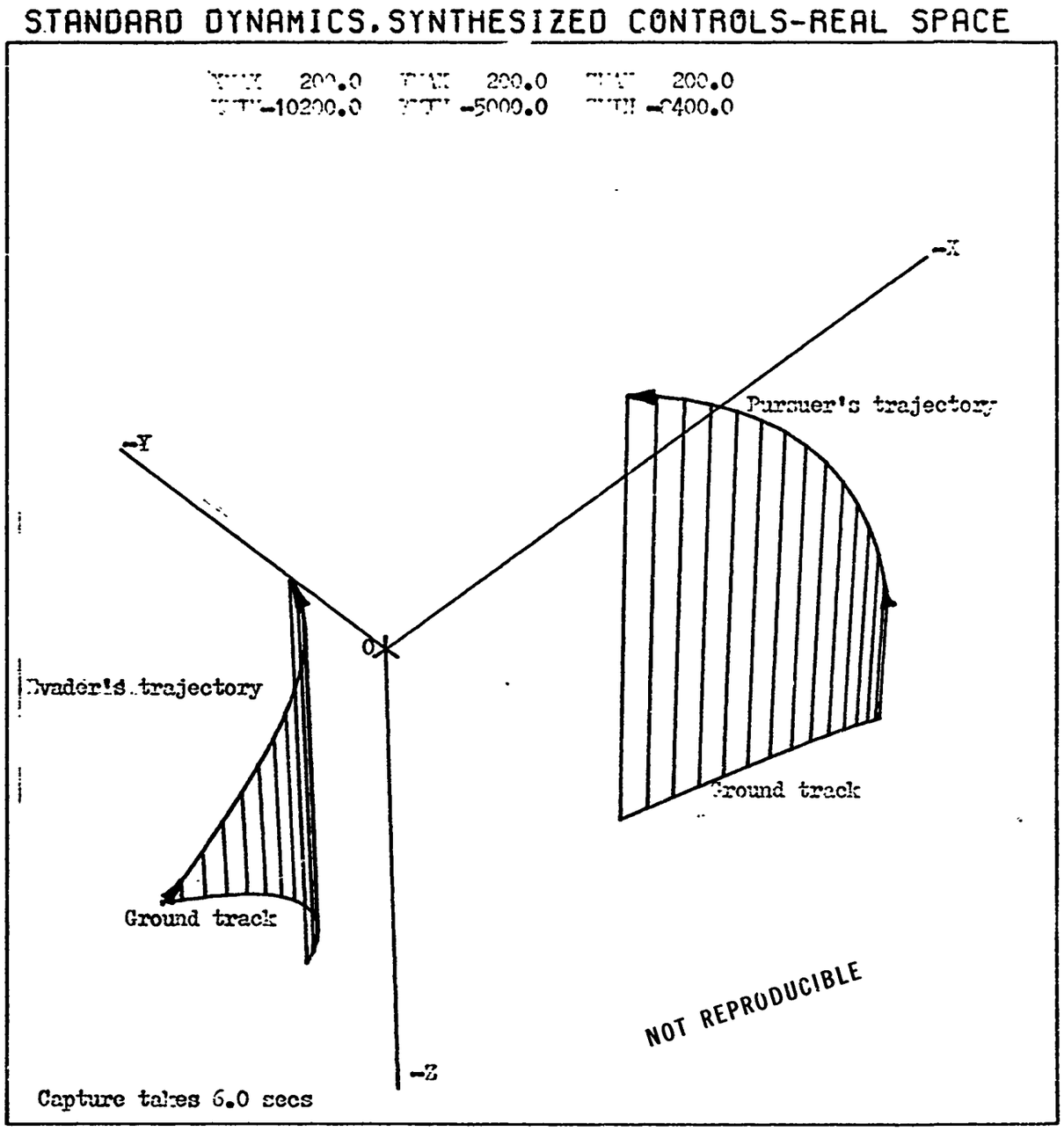

Figure 16. Pseudo Controls with Standard Dynamics, Real Space, Run 2

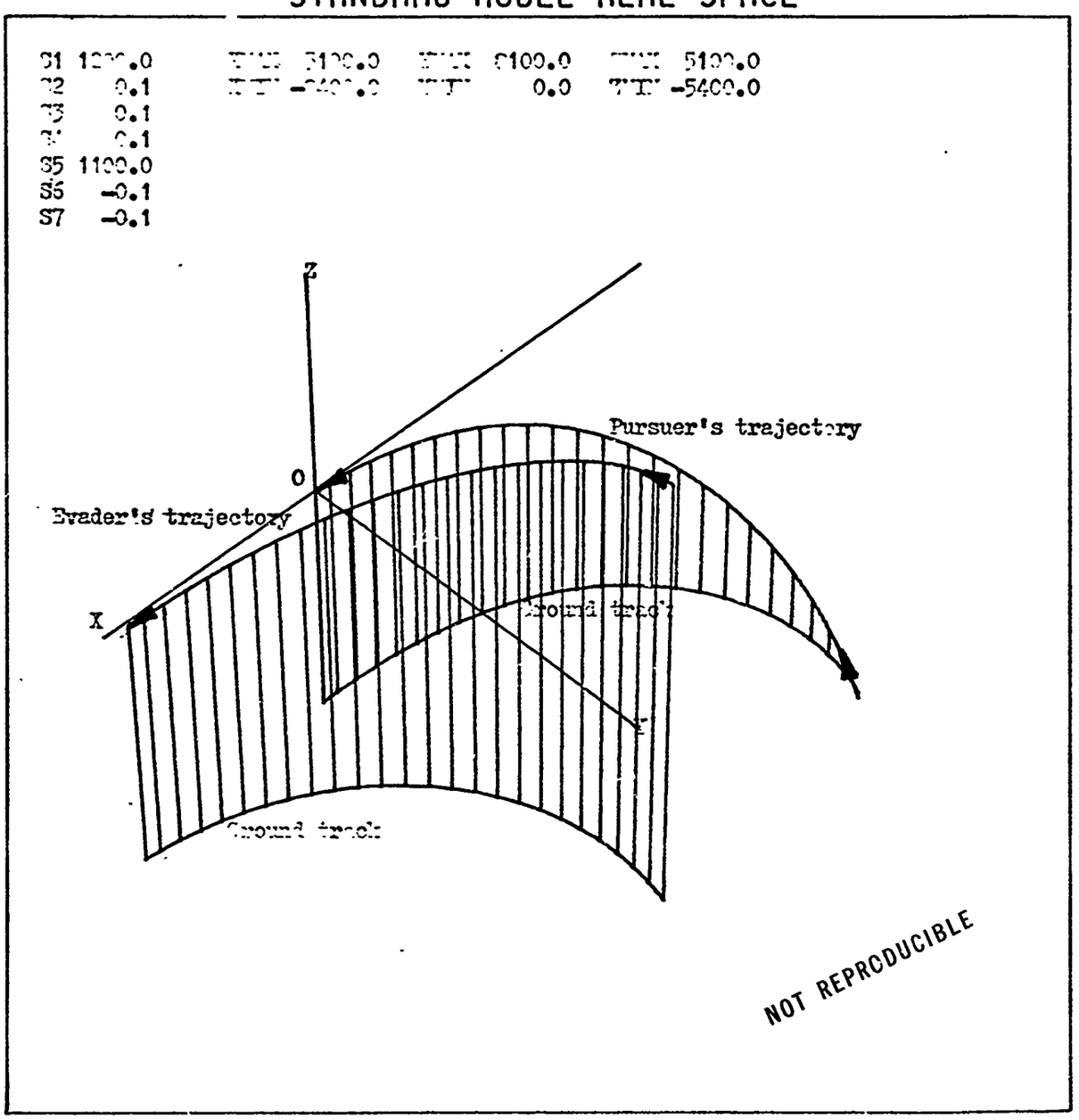

Figure 17. Standard Model, Real Space, Run 3

ZERO GRAVITY, FIXED VELOCITY MODEL-REAL SPACE

S1 1200.0 XMX 5000.0 YMX 8200.0 ZMX 6400.0
S2 0.1 YMI -7200.0 YMF 0.0 ZMI -500.0
S3 0.1
S4 0.1
S5 1100.0
S6 -0.1
S7 -0.1

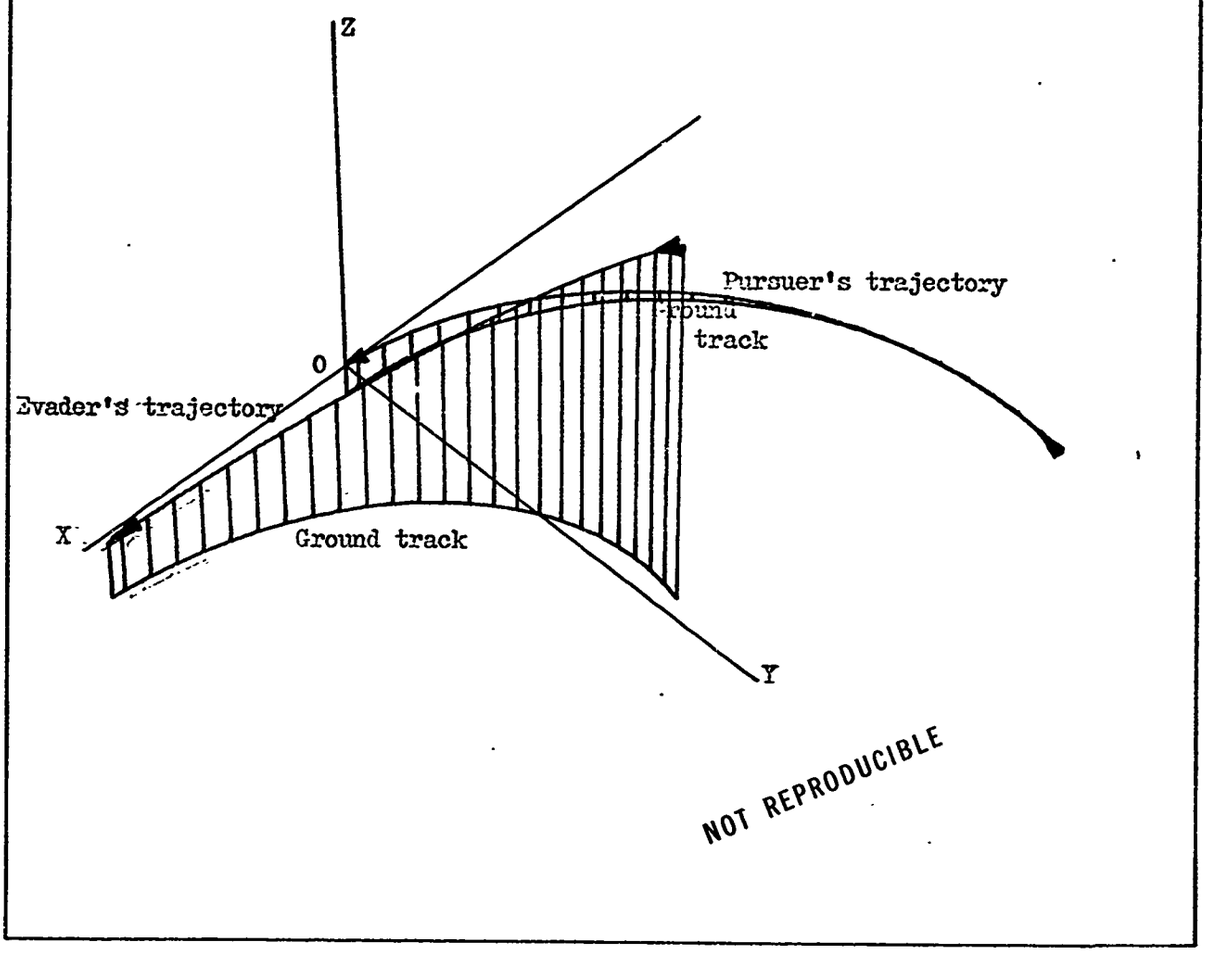

Figure 18. Zero Gravity, Fixed Velocity Model, Real Space, Run 3

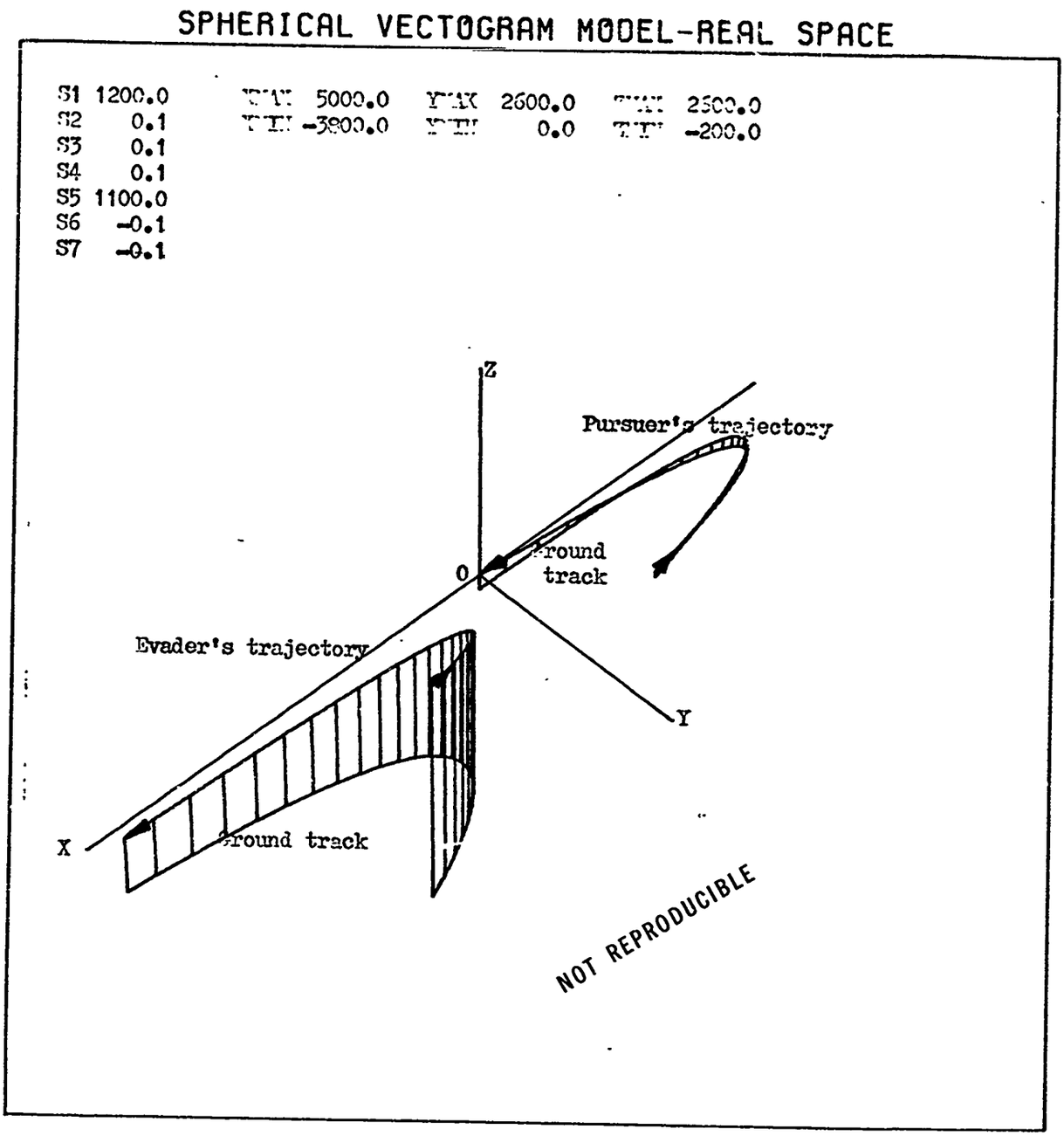

Figure 19. Spherical Vectogram Model, Real Space, Run 3

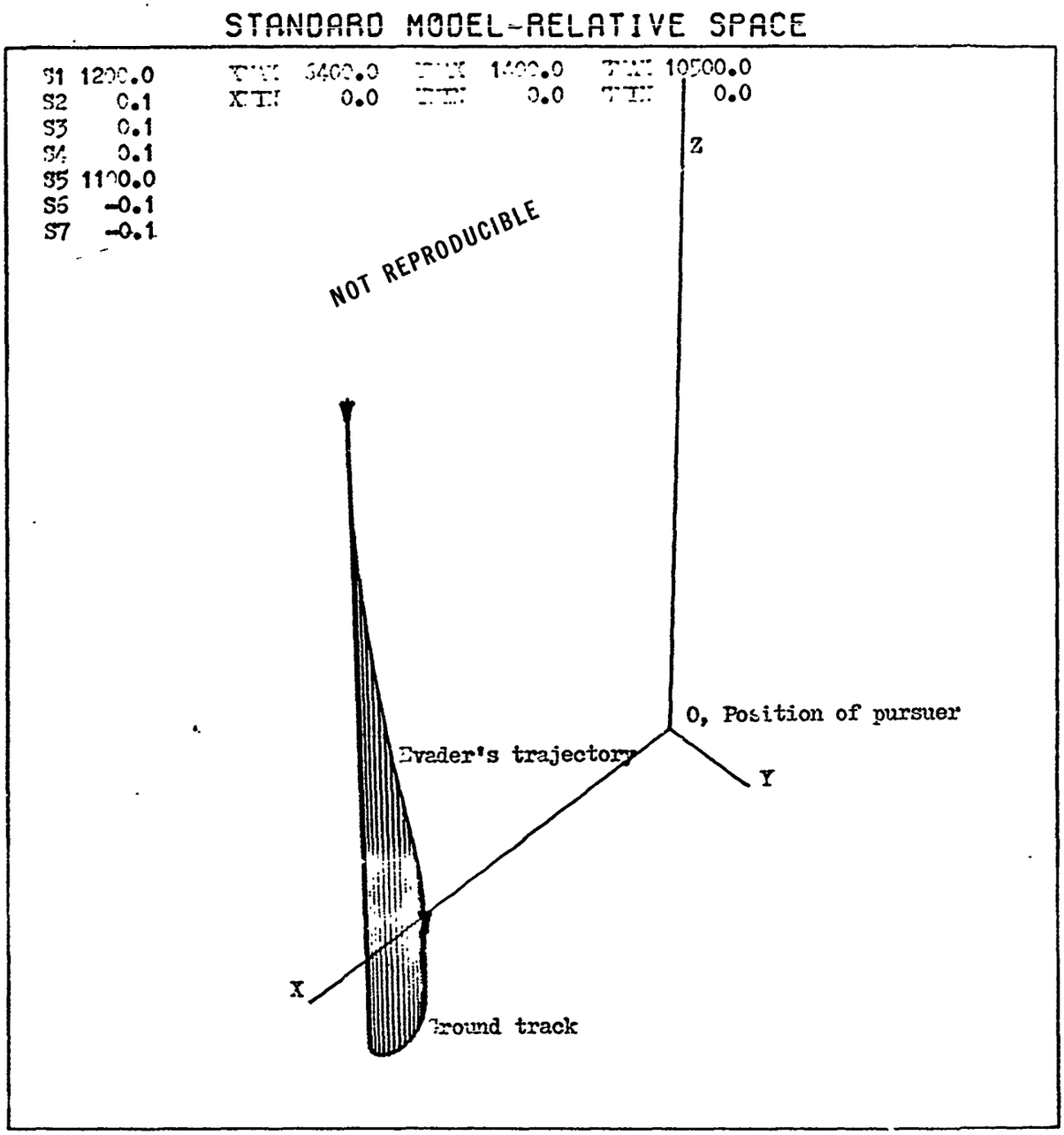

Figure 20. Standard Model, Relative Space, Run 3

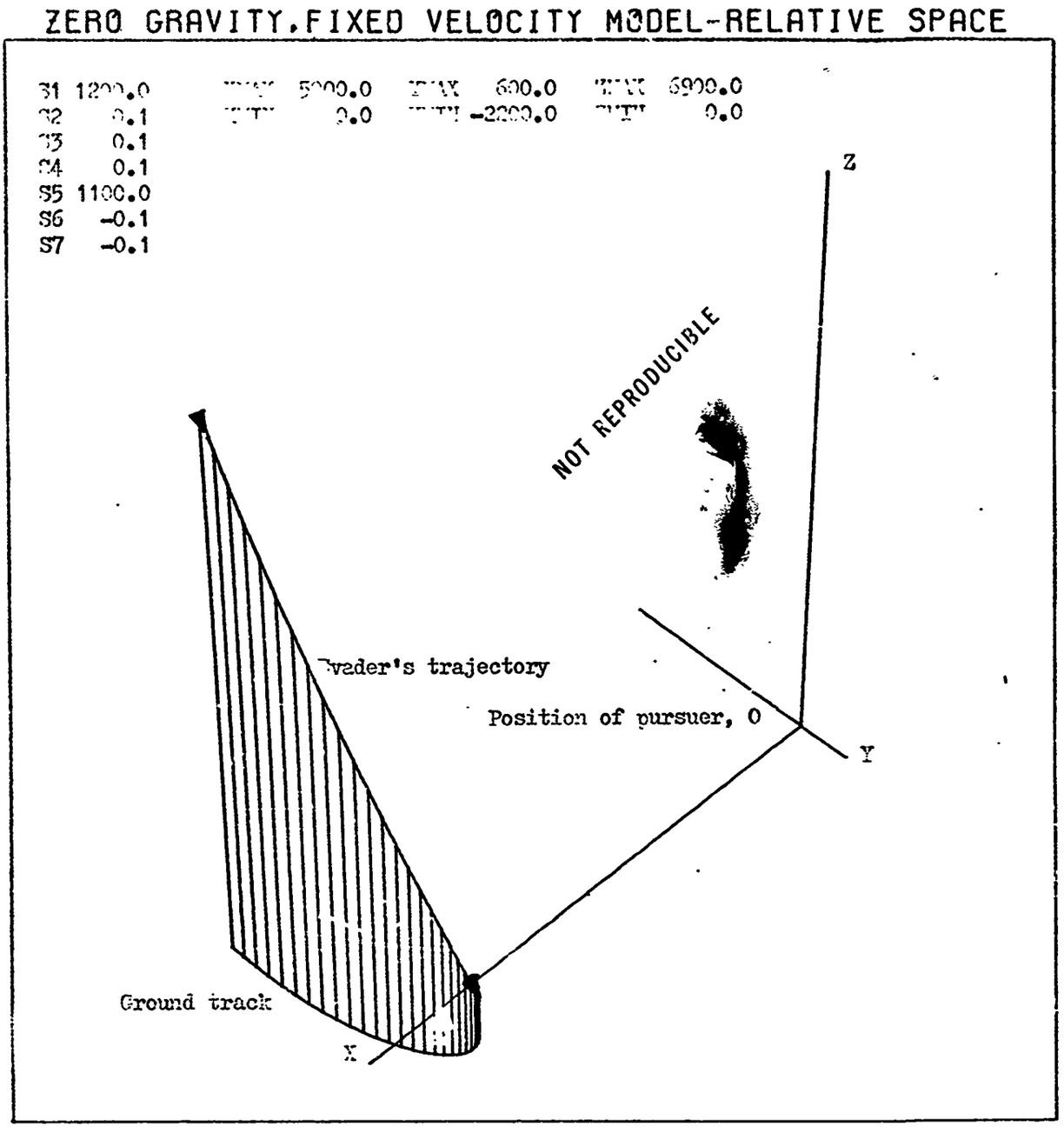

Figure 21. Zero Gravity, Fixed Velocity Model, Relative Space, Run 3

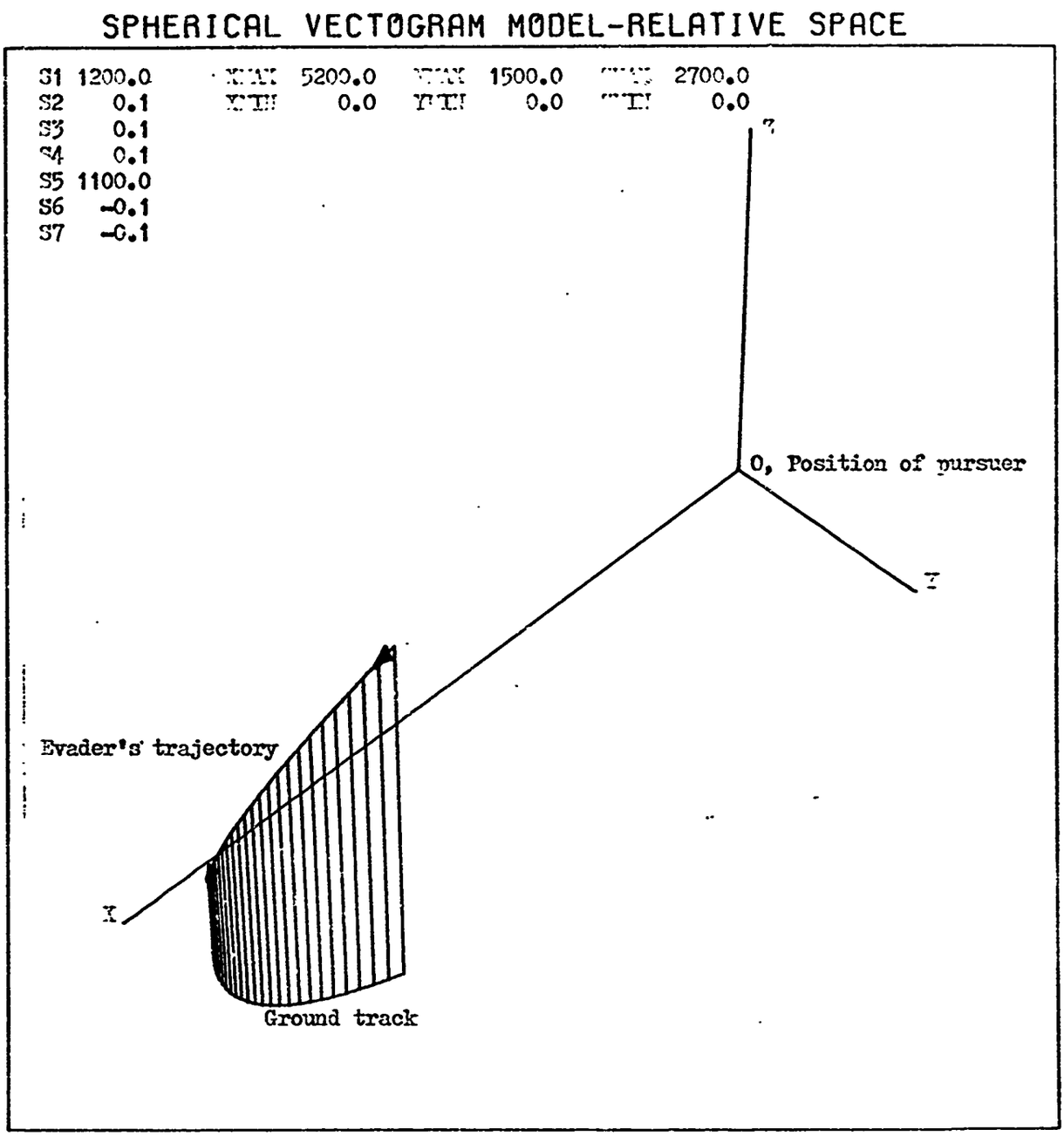

Figure 22. Spherical Vectogram Model, Relative Space, Run 3

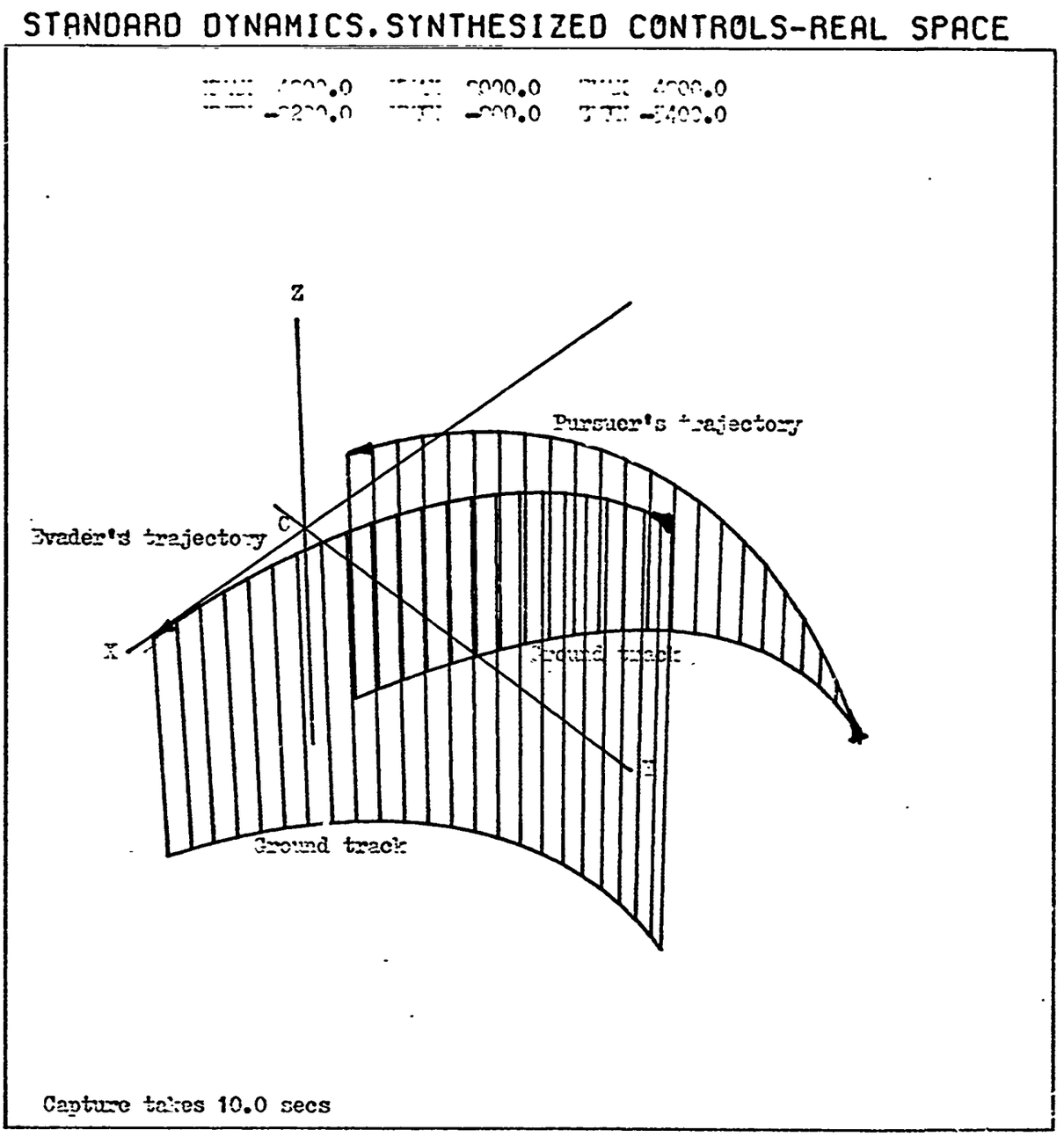

Figure 23. Pseudo Controls with Standard Dynamics, Real Space, Run 3

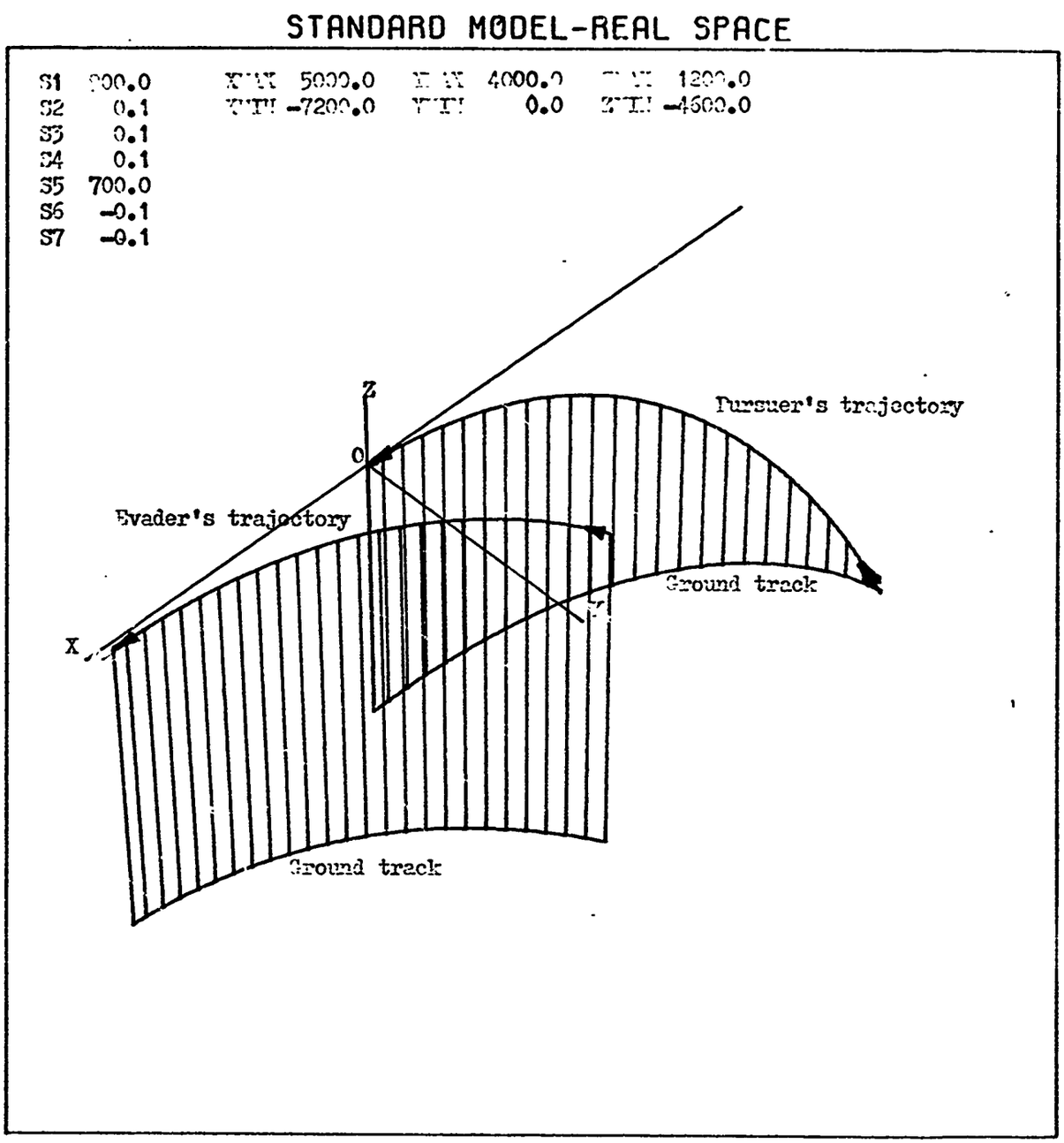

Figure 24. Standard Model, Real Space, Run 4

ZERO GRAVITY.FIXED VELOCITY MODEL-REAL SPACE

S1	00.0	[illegible]	5000.0	[illegible]	5400.0	[illegible]	3600.0
S2	0.1	[illegible]	-7000.0	[illegible]	0.0	[illegible]	-[illegible]0.0
S3	0.1						
S4	0.1						
S5	700.0						
S6	-0.1						
S7	-0.1						

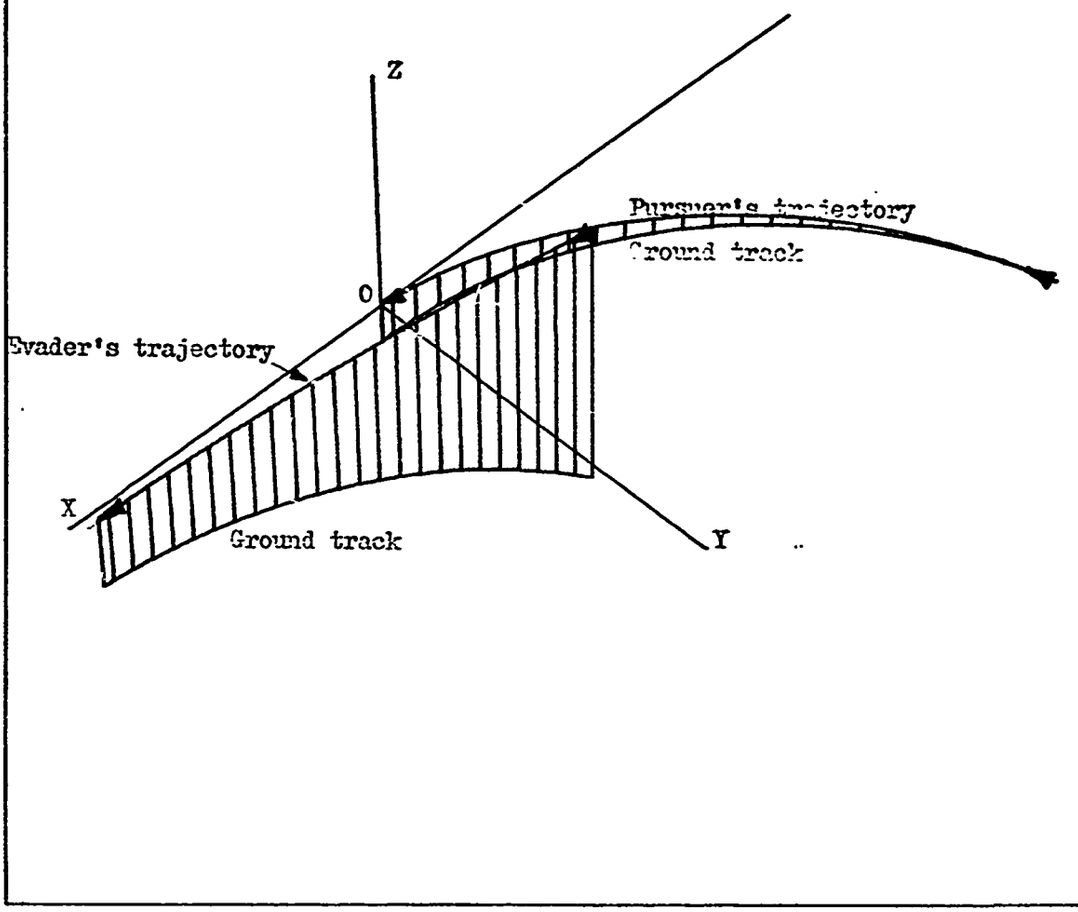

Figure 25. Zero Gravity, Fixed Velocity Model, Real Space, Run 4

SPHERICAL VECTOGRAM MODEL-REAL SPACE

S1	700.0	XTM	5000.0	YTM	1000.0	ZTM	1600.0
S2	0.1	VTM	-5000.0	PTM	0.0	GTM	-200.0
S3	0.1						
S4	0.1						
S5	700.0						
S6	-0.1						
S7	-0.1						

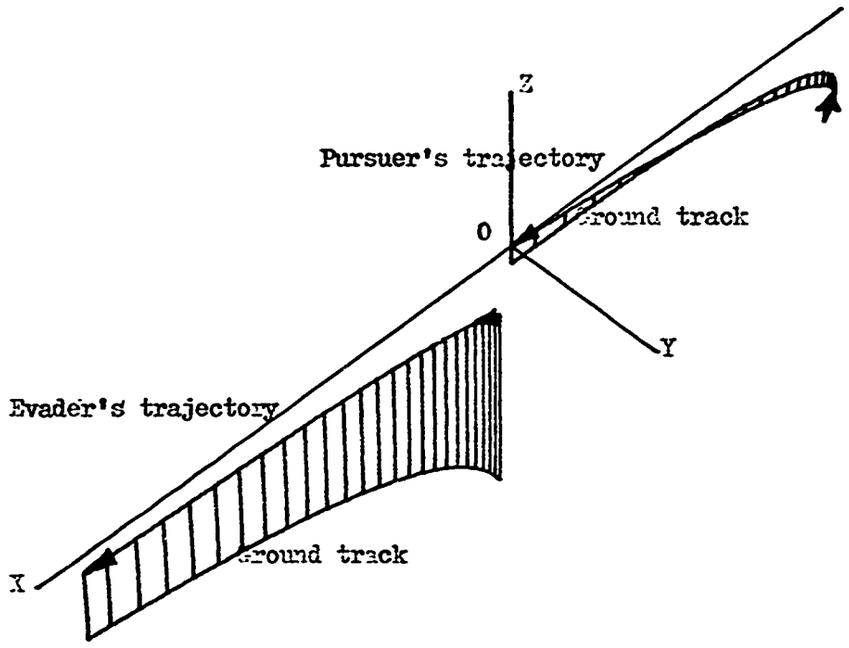

Figure 26. Spherical Vectogram Model, Real Space, Run 4

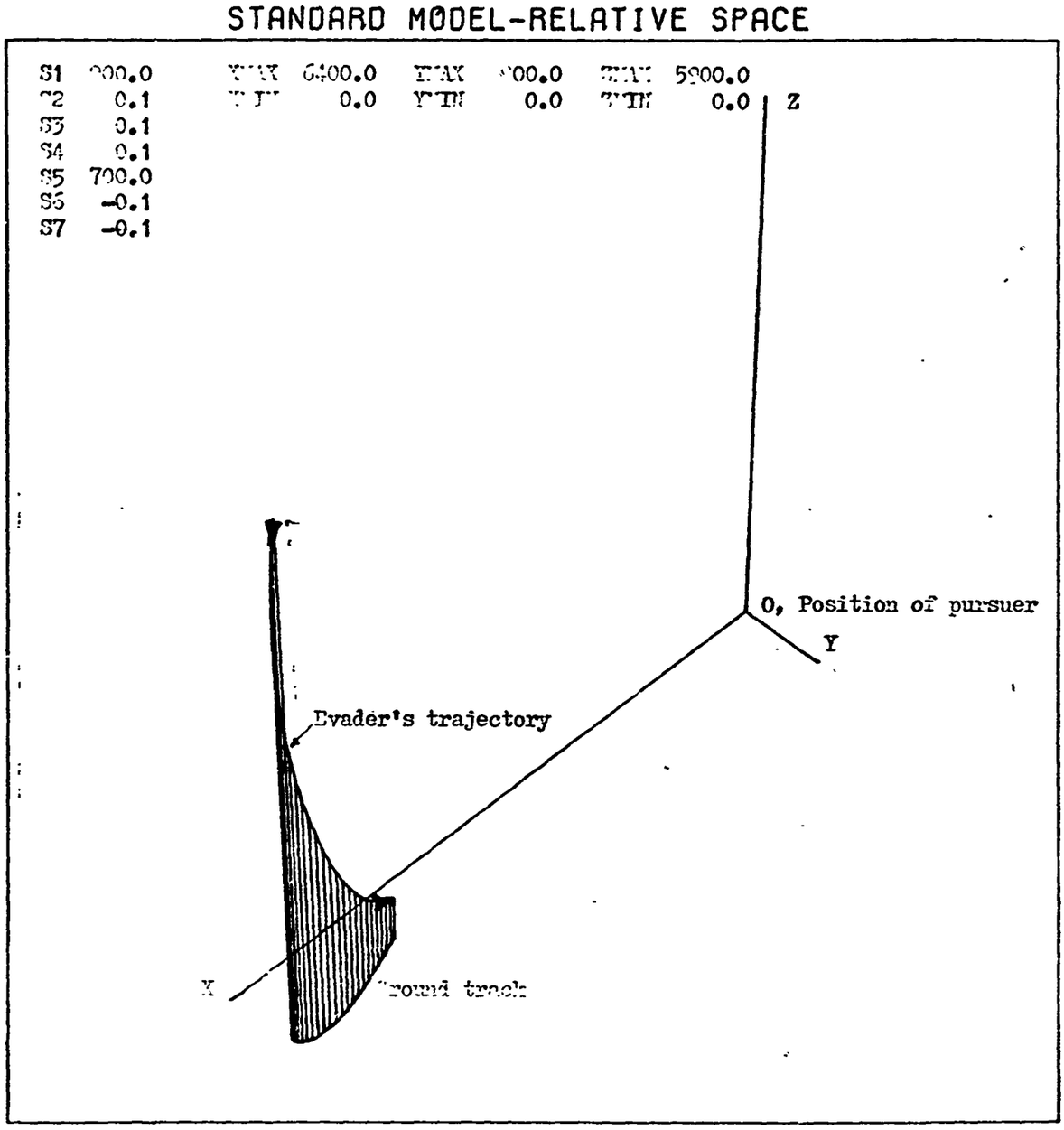

Figure 27. Standard Model, Relative Space, Run 4

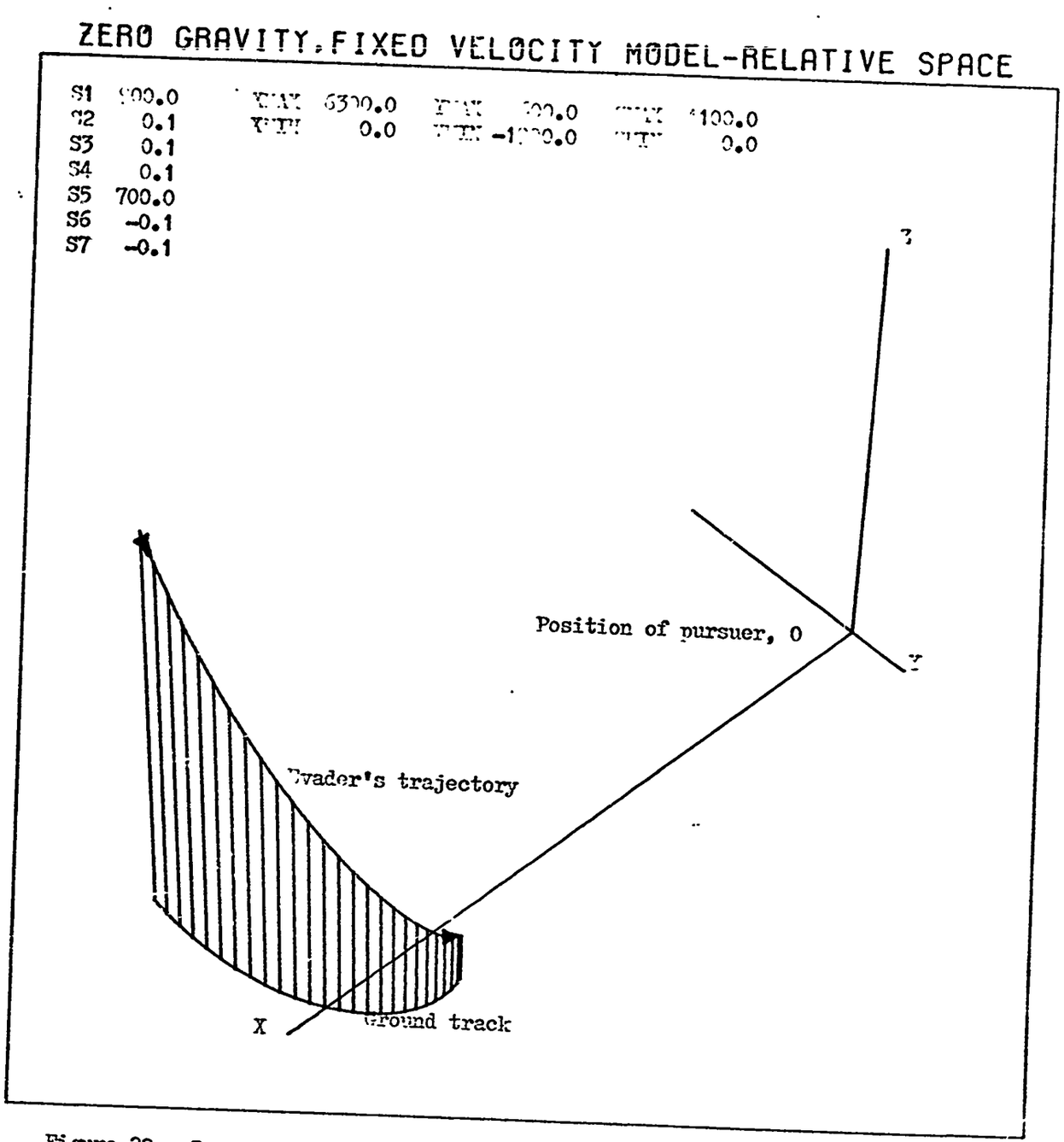

Figure 28. Zero Gravity, Fixed Velocity Model, Relative Space, Run 4

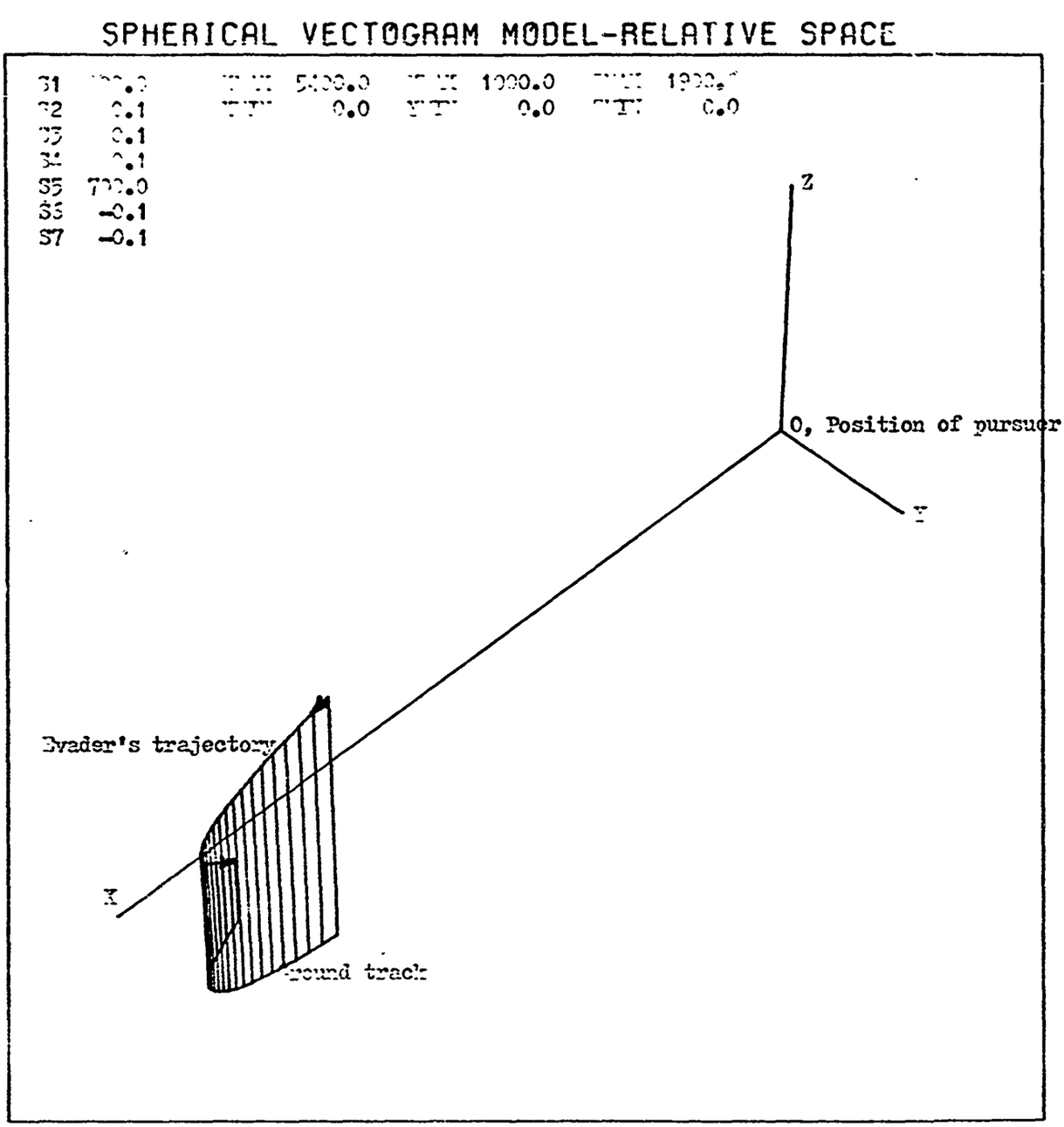

Figure 29. Spherical Vectogram Model, Relative Space, Run 4

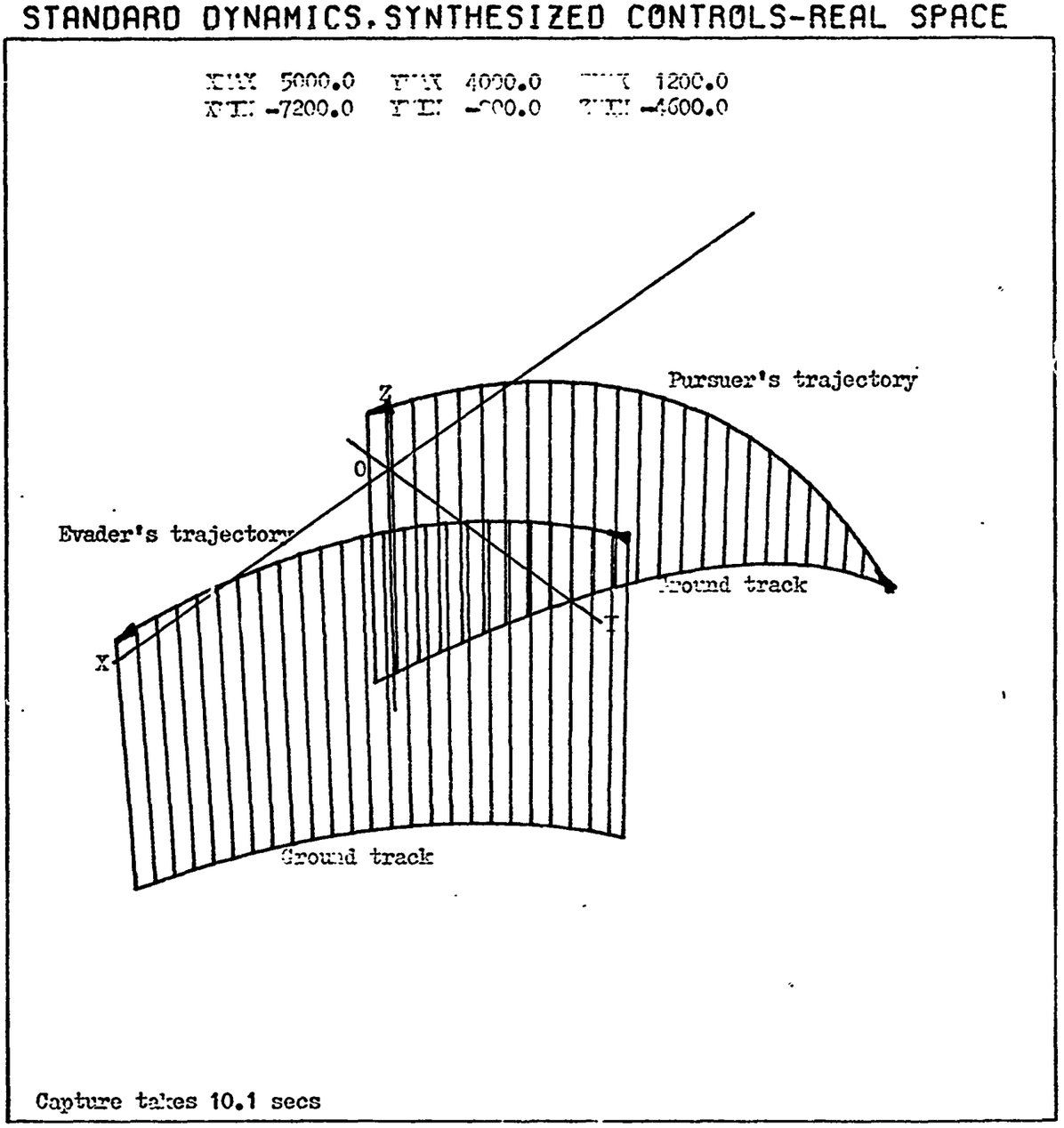

Figure 30. Pseudo Controls with Standard Dynamics, Real Space, Run 4